


U L T R A S O N I C V I S U A L I S A T I O N O F
C A R D I A C S T R U C T U R E A N D F U N C T I O N

CHARLES R. BOW B.Sc.

THESIS PRESENTED FOR THE DEGREE OF DOCTOR OF PHILOSOPHY
OF THE UNIVERSITY OF EDINBURGH, JULY 1979.



D E C L A R A R A T I O N

I hereby declare that this thesis contains
the results of my own work, and that it has
been composed by myself.

Charles R. Bow

July 1979

A B S T R A C T

Present real-time echocardiographic visualisation methods and their clinical application have been reviewed.

Ultrasonic instruments for visualising the heart were considered to have a number of limitations. Experimental and theoretical considerations of ultrasonic access and interaction with the heart and its surroundings have led to the design and development of a mechanical sector scanner. Rotating transducers within an oil filled cavity facilitates acoustic contact and vibration free operation. The small dimensions and the 90° field of view optimise visualisation of the heart avoiding bone and lung, provide a point of entry aspect allowing flexible scanning action and permit the application of two scanners simultaneously at adjacent intercostal spaces. These aspects also allow subxiphoid application of the scanner to visualise the heart and conventional T-M echograms to be obtained.

A real-time heart scanning system with grey scale display and recording facilities has been developed. This system is versatile allowing two scanners to be driven in several operating modes.

The scanner has been evaluated on a representative group of patients suffering from cardio-respiratory disease.

Visualisation of cardiac structures and their function has been successful. The possible visualisation extensions and improvements through the use of two scanners simultaneously has been investigated. Real-time compounding and biplane visualisation can be achieved. The brief clinical use of this scanner in pediatrics has indicated the potential applicability of this design philosophy in the diagnosis of congenital heart defects.

A C K N O W L E D G M E N T S

I would like to thank my supervisor, Dr. W.N. McDicken, for his continual interest and advice during the course of this work. My thanks go to colleagues in the Department of Medical Physics and Medical Engineering who have helped in aspects of this project. I am particularly indebted to Mr. T. Anderson for his constructive suggestions and electronics expertise during the design and development of the system. For his skilled assistance during mechanical construction of the scanners, I am grateful to Mr. R. Borthwick.

I wish to acknowledge Prof. J.R. Greening for his support and for making the departmental facilities available. In addition I acknowledge the provision of my Scholarship by the Faculty of Medicine and equipment grants from the University of Edinburgh.

For his significant help during clinical evaluation of the scanner I would like to thank Dr. R.E. Scorgie of the Department of Medicine and Dr. A.L. Muir of the same department for his interest. I would also like to thank Dr. M.J. Godman of the Department of Child Life and Health for his co-operation in pediatric application.

Finally I thank my parents and friends for moral support and encouragement and Miss L. Sutton for typing this script.

C O N T E N T S

CHAPTER 1	I N T R O D U C T I O N	
1.1	DEVELOPMENT OF ECHOCARDIOGRAPHY	1
1.2	OTHER DIAGNOSTIC TECHNIQUES	9
1.3	CLINICAL VALUE OF ECHOCARDIOGRAPHY	16
1.4	RESEARCH PROGRAMME	20
CHAPTER 2	P H Y S I C A L C O N S I D E R A T I O N S	
2.1	T-M ECHOCARDIOGRAPHY	21
2.2	ULTRASONIC ACCESS AND INTERACTION WITH THE HEART	24
2.2.1	THEORETICAL ASPECTS	24
2.2.2	EXPERIMENTAL ASPECTS	30
2.3	PHYSICAL CONSIDERATIONS WITH RESPECT TO REAL-TIME SCANNING	36
2.4	CONCLUSION	39
CHAPTER 3	S C A N N E R D E S I G N	
3.1	MECHANICAL METHOD	41
3.2	SCANNER DESIGN	45
3.2.1	DESIGN OUTLINE	45
3.2.2	TRANSDUCER HEAD	48
3.2.3	ELECTRICAL CONTACT	49
3.2.4	MECHANICAL DRIVE	50
3.2.5	TRANSDUCER WHEEL POSITION MONITOR	52
3.3	SCANNER PROTOTYPES	53
3.3.1	TRANSDUCER HEAD PROTOTYPE	53
3.3.2	VERTICAL SCANNER PROTOTYPE	56
3.4	FINAL SCANNER DESIGN	57

CHAPTER 4	T R A N S D U C E R H E A D A C O U S T I C S	
4.1	INTRODUCTION	60
4.2	TRANSDUCER WHEEL ACOUSTICS	63
4.2.1	TRANSDUCER CONSTRUCTION	64
4.2.2	TRANSDUCER PERFORMANCE	66
4.3	OIL AND WINDOW ACOUSTICS	71
CHAPTER 5	S Y S T E M D E S I G N	
5.1	INTRODUCTION	80
5.2	SYSTEM OPERATION	80
5.2.1	SCANNER DRIVE AND IMAGE FORMAT GENERATION	80
5.2.2	DISPLAY UNIT	87
5.2.3	CINE CAMERA	88
5.3	SYSTEM PERFORMANCE	90
5.3.1	GREY SCALE IMAGE	90
5.3.2	TEST PHANTOM	93
5.3.3	LIMITATIONS AND IMPROVEMENTS	99
5.4	ALTERNATIVE RECORDING METHODS	102
CHAPTER 6	T W I N S C A N N E R A P P L I C A T I O N S	
6.1	INTRODUCTION	104
6.2	RELATED TWIN SCANNER APPLICATION	110
6.3	UNRELATED TWIN SCANNER APPLICATION	119
6.4	CONCLUSION	130
CHAPTER 7	C L I N I C A L A P P L I C A T I O N A N D E V A L U A T I O N	
7.1	INTRODUCTION	131
7.2	EXAMINATION PROCEDURE	132
7.3	CLINICAL GROUPS	135
7.4	TABLE LAYOUT AND TABLES 7.1 - 7.6	136

7.5	THE STANDARD VIEWS	150
7.6	EVALUATION OF SCANNER IN CLINICAL APPLICATION	154
7.6.1	VALVULAR HEART DISEASE	154
7.6.2	CORONARY ARTERY DISEASE	159
7.6.3	CHRONIC OBSTRUCTIVE LUNG DISEASE	163
7.6.4	PRIMARY PULMONARY HYPERTENSION	167
7.6.5	PERICARDIAL EFFUSION	167
7.6.6	CARDIOMYOPATHY	171
7.7	GENERAL DISCUSSION	173
7.8	CONCLUSION	177
CHAPTER 8	A P P L I C A T I O N S I N P E D I A T R I C S	
8.1	INTRODUCTION	178
8.2	PATIENT GROUP	179
8.3	PEDIATRIC ECHOCARDIOGRAPHIC EXAMINATION	180
8.4	PRESENTATION OF RESULTS AND DISCUSSION	183
8.5	POSSIBLE DEVELOPMENTS	187
8.6	CONCLUSION	193
REFERENCES		195
PUBLISHED PAPERS		204

CHAPTER 1

INTRODUCTION

1.1. DEVELOPMENT OF ECHOCARDIOGRAPHY

The first application of pulsed reflected ultrasound to investigate the internal structures of the heart was conducted in Sweden by Edler and Hertz in the early 1950's. The original instrument used was a commercial ultrasonoscope which was being applied in the nondestructive testing of metals. (Edler and Hertz, 1954). Using the A scan function of this instrument, initially the posterior wall of the heart was identified and with modified equipment an echo was recorded from the anterior mitral leaflet of the mitral valve although the identification of the source of this echo was only confirmed after some autopsy investigations. Edler continued to make ultrasonic studies of the heart and was the first to identify many of the structures known today. The main clinical application to evolve from this work was the diagnosis of mitral stenosis when he noted the different pattern of movement of the anterior mitral leaflet in patients with this disorder. During the late 1950's and early 1960's Edler's work was repeated and developed by other workers and in 1961 Edler wrote a review of ultrasound cardiography which included descriptions of the detection of mitral stenosis, left

atrial tumors, aortic stenosis and anterior pericardial effusion (Edler et al., 1961).

The detection of posterior wall pericardial effusion was discovered while confirmation of Edler's work, and others was being carried out in America (Feigenbaum et al., 1965). Other investigators, while repeating this work developed interest in the left ventricle and looked at techniques to measure posterior left ventricular wall thickness, left ventricular internal dimensions and stroke volume (Feigenbaum et al., 1967). The observation by Gramiak that echoes were produced from within the heart with the use of intracardiac injections of indocyanine green dye and saline solution allowed many cardiac structures to be positively identified (Gramiak et al., 1969). The non-invasive nature of ultrasound caused greater involvement and more diverse interest to develop in the late 1960's and early 70's. Subtle variations in the echo patterns were noted and techniques were being reported to diagnose such disorders as prolapsed mitral valve, aortic insufficiency and hypertrophic subaortic stenosis.

During the 1970's many investigators duplicated and compared similar studies. Standard examination techniques have been established and many of the ambiguities of echo pattern interpretation and clinical relevance have been

clarified. The standardisation of dimensional and functional indices for normals and the development of disease related indices and the correlation of these with other diagnostic methods has been a major part of the recent development of this technique. The technique has become generally known as time-motion echocardiography or T-M echocardiography. The name developed because the received echo information is displayed graphically with the distance of the heart structures from the transducer along one axis and time on the other. The resultant graphical record shows the relative position of the heart structures against time and the name time-position scanning evolved naturally from this although the less accurate term time-motion became popular later. The scanning techniques and clinical application and interpretation of T-M echocardiograms has been described recently by Chang (1976).

Since the late 1960's various attempts have been made to produce cross-sectional or two dimensional images of the heart. The use of a conventional B scan machine to scan the heart produces a blurred picture due to heart movement, although some abnormalities and overall heart dimensions can be assessed (Kratochwil et al., 1974). Using the same equipment stop action cross-sectional images can be constructed by triggering the transmitter at a specific

phase in the heart cycle using the ECG signal (King, 1972). An image can be produced at any phase in the heart cycle by adjusting the trigger delay and by integrating the received signals over many heart cycles. Some spurious information appears in the image due to arrhythmias and patient respiration but the benefits of compounding are gained and a large field of view can be obtained by scanning from several adjacent rib spaces. The technique has been used to visualise abnormalities such as cardiac enlargement, valvular disease, atrial and ventricular septal defects and the alignment of the great arteries (King et al., 1973).

The early ECG gated technique wasted most of the information available and only constructed an image of the heart at a particular phase of its cycle during any one scan. Gramiak et al., (1973) reconstructed two dimensional images from conventional T-M arc scans, produced by sweeping the transducer from the apex to the base of the heart, and extracting the data from the resulting echogram at specific phases of the heart cycle. The number of heart beats in the arc scan determines the number of sample data in the reconstruction. This method still suffers from arrhythmic beats and respiration but wastes less information and allows images to be made at any part of the heart cycle from one arc scan. The initial images were constructed

by hand and suffered from distortion due to the arc scan data being used to construct a rectangular image. Further work based on the same principle but using a computer to store the data and a conventional B scan machine to produce the arc scan of the heart allowed automation of image reconstruction and the removal of the inherent distortion due to the use of scan orientation information from the B scan machine combined with the T-M data (Wagg and Gramiak, 1974).

The two dimensional methods described so far do not produce real-time images of the heart. To produce real-time images the ultrasonic beam has to be swept rapidly and repetitively through the section of the heart to be visualised. This accurate and rapid steering of the ultrasonic beam can be achieved by mechanical or electronic methods.

The first real-time images were reported by Åsberg and Hertz (1967) and Flaherty et al., (1967). Åsberg and Hertz oscillated an ultrasonic transducer and mirror system in a water bath to produce 6 to 7 sector images per second of the human heart. Major structures were identified such as interventricular septum, mitral valve cusps and the posterior wall of the heart. The water bath containing the

mirror system was very bulky and it was concluded that the frame rate was too low causing distortion of moving structures and image flicker (Åsberg, 1967). Flaherty and his colleagues used a standard oscillating transducer placed on the skin surface to produce images in a plane perpendicular to simultaneously produced fluoroscopic images. The interactive nature of the two techniques helped identify the structures in the ultrasonic images and the diagnosis of pericardial effusion was reported.

The design and construction of several real-time mechanical scanners for heart visualisation followed this initial investigation (Eggleton and Johnston, 1974; Griffith and Henry, 1974; McDicken et al., 1974). They are all based on the same mechanical principle of oscillating a standard transducer of known beam shape and transducer characteristics on the chest wall at an intercostal space. They all produce sector images with 30° to 60° sector angle at a frame rate of typically 30 per second, with the number of lines per frame being dependent on the pulse repetition rate of the system.

Electronic steering of the ultrasonic beam to produce real-time images is achieved by the use of transducer arrays, either linear arrays or phased arrays. Bom et al., (1971) were the first to describe a linear array designed to visualise heart dynamics. The clinical value of this

scanner, known as the multiscan system (Bom et al., 1973) has been discussed by Roelandt et al., (1974). It was found that it was possible to visualise the aorta, aortic root, left atrium, mitral valve, posterior papillary muscle and chordae, and the left and right ventricles depending on the patient. The regularity of structure recognition was investigated in a large multi-centre study (Bom et al., 1974) with an updated multiscan system and good visualisation of the aortic root, anterior mitral valve leaflet and left ventricular posterior wall was achieved in the majority of patients.

Somer (1968) has reviewed the subject of electronic beam steering and has described the construction of a 21 element phased array. Development of this system has improved the angular resolution and reduced side lobes making the original idea practical for clinical applications in echocardiography. A similar system to that of Somer has been constructed by Thurstone and von Ramm (1974) specifically for the evaluation of heart dynamics. This array has focussing on transmission and swept focussing on reception in addition to the beam steering. An updated version of this array has been described since then (Von Ramm and Thurstone, 1976) along with a report on the clinical technique and application of the array (Kisslo et

al, 1976). This array has 16 transducer elements and it measures 14mm by 24mm. It has a 60° sector view with adjustable frame rate and range, which determines the number of lines per frame. Kisslo and his colleagues described good quality images of mitral valve leaflets, aortic root and valve, left atrium and ventricle and other cardiac structures. However it has been claimed particularly useful for the deliniation of left ventricular spatial geometry by the identification of endocardium, myocardium, papillary muscles and interventricular septum, although the entire long axis of the left ventricle was often not visualised.

Although there have been no fundamental developments in real-time echocardiography since the introduction of the various approaches described here, the early work has stimulated many other investigators to research the basic systems and develop improvements and variations. Several scanners designed for cardiac application have been reported recently, for example (Skolnick and Matzuk, 1978; Pedersen and Northeved, 1977). The modification of an original oscillating scanner to include a range-gated Doppler to measure ultimately cardiac blood volume flow at known heart locations has been reported by Griffith and Henry (1978). The clinical application of some of the original and some

commercial scanners has also been described recently (Gehrke, 1976; Houston et al., 1977; Kambe et al., 1977; D.H.S.S., 1979).

It is this work which has prompted commercial companies to develop and produce scanning systems based on the various designs described. Many commercial scanners have become available recently and it is this which has enabled the active development of real-time clinical techniques and applications. At present it is this which is contributing most to the development of echocardiography as a useful non-invasive diagnostic technique.

1.2 OTHER DIAGNOSTIC TECHNIQUES

Classical methods of diagnosing cardiac malfunctions are now routinely performed by electrocardiograms, chest X-rays, serum enzyme levels and the direct measurement of intracardiac pressures. All these methods provide the physician with data which can be related reliably to previous clinical experience. Many other non-invasive methods have been investigated all of which give different indirect indications of cardiac status. These include apexcardiography, ballistocardiography, impedance plethysmography and systolic time interval analysis (Manley, 1977).

Apexcardiography is the measurement of the resultant praecordial motion due to overall heart motion at the apex

of the heart using some kind of displacement transducer. The resultant apexcardiogram (ACG) has a characteristic waveform which has been used mainly to assess the severity of ischemic heart disease. A prognostic index can be calculated from various waveform gradients. Simultaneous recording of the ACG with the carotid pulse or the phonocardiogram can be used to extract some useful cardiac event time intervals.

Ballistocardiography is the recording of whole body movements due to the heart beat. The patient lies on a floating table and the resultant motion of the body table combination is measured along the head to foot axis. Clinically, the reduction in the overall amplitude of the ballistocardiogram (BCG) after myocardial infarction can be used as an indicator of prognosis. Some specific cardiac conditions can be examined using the BCG but can equally well be diagnosed using other non-invasive techniques. It is continuing to seek diagnostic value as distinct from physiological value.

The measurement of impedance changes across the heart alone would be called impedance cardiography. However it is only practical to make impedance measurements over a complete cross section of the thorax and make the assumption that impedance changes are primarily due to blood volume changes

in the heart, and hence the name impedance plethysmography. The passage of an alternating current through the thorax by attaching electrodes to the neck and lower thorax allows the changes in potential difference to be measured between two electrodes round the thorax above and below the heart. The use of these potentials and their rate of change in equations to predict stroke volume has been attempted but there has been some conflicting evidence. Clinically the monitoring of patients qualitatively has some applications. Systolic time intervals (STI) are most commonly derived from a simultaneous record of ECG, phonocardiogram (PCG) and the carotid pulse (CP). The CP waveform is obtained by recording the wall pulsation of the carotid artery with a pressure or displacement transducer. The basic time intervals obtained from the waveforms are left ventricular ejection time (LVET) from the CP waveform, electromechanical systole (QA2) measured from the Q wave of the ECG to the A2 component of the second heart sound on the PCG and pre-ejection period (PEP) which is the difference between LVET and QA2 and represents the interval between the onset of left ventricular activation and the start of ejection. These intervals are all heart rate dependent and for the purposes of absolute measurements to be used in clinical correlations with cardiac diseased states, regression

equations were introduced to compensate for heart rate. In the late 1960's and 70's many clinical applications of STI have been reported in both ischemic and valvular heart disease.

The four non-invasive methods described are not used routinely because they offer little quantitative information for analysis or diagnosis. Because of the attraction of recovering dynamic data routinely and without trauma, much work has been done to try to clarify normal categories but the large overlap between groups meant that predictions made for individuals were not valid. However many of the methods are capable of showing trends in the cardiac status of an individual patient.

The development of atrial and venous catheterisation in the 1930's permitted the invasive, but relatively safe measurement of pressures in the heart chambers and great vessels. Direct quantification is obtained and many valvular and functional malfunctions can be diagnosed. Contrast angiography developed naturally from this as a method for visualising cardiac function and abnormalities. This technique requires dense contrast material to be injected by catheter into the left ventricle. The ventricle is visualised by the passage of X-rays through the patient and then recorded on film via an image intensifier. This

is known as cineangiography. The radiation exposure is significant and there is an associated degree of morbidity. There is also a variable mortality rate of approximately 1%.

Although the resultant images are of high resolution and quality, the injection of the dense contrast material under pressure can upset the normal ventricular rhythm. The contrast medium also has a complex reaction with the electrical stimulation of ventricular contraction. Also some alteration to the haemodynamics of the heart may be induced by the presence of the catheter. However this technique allows segmental wall abnormalities to be visualised and calculations of absolute volumes from the two dimensional images can be made if certain geometrical assumptions are taken into consideration. This technique is also very useful in the diagnosis of valvular and structural abnormalities since the contrast medium can be seen passing back through a faulty valve or through a septal defect. Biplane cineangiography can be performed using two X-ray sources and two image intensifiers at 90° to each other and imaging alternately.

The development of nuclear medicine equipment over the last decade has resulted in the application of gamma scintillation cameras in radionuclide angiography (Ashburn

et al., 1978). The gamma camera is accompanied by a dedicated computer with other processing and display equipment. There are two basic approaches to radionuclide angiography. The recording of the initial transit of an intravenously injected radioactive bolus through the cardiac chambers is called the first-pass method. This was originally used to produce serial images similar to X-ray contrast angiography. The development of interest in the measurement of ejection fraction initiated the second approach which utilizes various radioactive substances that remain evenly distributed throughout, and confined to the vascular space or blood pool as it is known. This includes the cardiac chambers and therefore once complete mixing or equilibrium has been established both ventricles can be imaged simultaneously. This second method stores the counts obtained at specific phases of the heart cycle over typically 500 cycles. This number depends on the heart rate, amount of radioactivity administered, the detector characteristics (mainly the collimator) and the desired number of counts per selected time period. Typically up to 30,000 counts in a 0.04-0.06 second gated period can be accumulated in approximately 5 minutes. The integrated counts of a specific phase can be examined in the form of a discrete image in photographic film or the stored data can be displayed later as a matrix

image. There is an inherent trade off between resolution and sensitivity in gamma cameras and modern models have a resolution of approximately 10mm.

Nuclear imaging however is relatively non-invasive only involving an intravenous injection of isotope. It is physiological rather than anatomical and therefore has scope in the assessment of myocardial infarction, for example by the use of compounds which are either actively accumulated or excluded from damaged myocardium resulting in hot or cold spots in the image. Detection of the blood pool within the chambers allows segmental dysfunction to be assessed from serial images or more recently from loops of serial images forming moving images. Direct quantification of the ejection fraction can be made from end systolic and end diastolic counts. This index is recognised as the best overall index of global left ventricular function. Absolute measurements of heart function such as cardiac output can also be calculated.

Nuclear cardiology is a technique which is capable of contributing to the management of patients suffering from a large range of heart disease. However limitations in resolution and image quality exclude the investigation of valvular disease, and repetitive studies are very limited due to the cumulative radiation dose. These limitations

and also infant radiation dose considerations restrict its usefulness in pediatric heart disease.

1.3 CLINICAL VALUE OF ECHOCARDIOGRAPHY

Traditionally the physician would decide how to manage a patient from observations made during clinical examination. The combination of these observations and previous experience were all he had as indicators of possible heart condition. The advancement of therapeutic and surgical methods requires more detailed information about cardiac status to be known before the physician can decide on patient management. The routine use of ECG, enzyme levels and chest X-ray are purely extensions of the clinical examination all providing different indirect information about the clinical condition of the heart. Similarly the other non-routinely used non-invasive techniques described in the previous section do not give direct clinical information.

Although modern clinical management is often based on invasive measurements of pressure and volume in the cardiac chambers and great vessels, these are not fundamental indices of cardiac status and are used since they can be measured directly.

What is required is a direct measurement of heart function and not the effect of heart malfunction. The heart is the

most mechanically dynamic organ in the human body and its function is to pump blood round two interlinked circuits, namely the pulmonary and systemic circuits, and hence supply the body with oxygenated blood. With heart malfunction, ultimately the haemodynamic effect is caused by a mechanical malfunction even although the mechanisms causing the mechanical malfunction may be complex and electrophysiological in nature. Therefore the measurement and recording of the mechanical dynamics of the blood/pump interface is a more fundamental index of cardiac status. This interface includes the cardiac chambers, the heart valves and the inlet and outlet vessels. This is a complex three dimensional moving surface which has been imaged by cineangiography, radionuclide angiography and two dimensional echocardiography. Cineangiography provides a shadow image and therefore the outline need not be coplaner. The same is true of radionuclide angiography. Both techniques are limited to longitudinal sections due to patient and equipment orientation and to enable differentiation between the right and left sides of the heart the two sides must not overlap causing further restriction of image plane selection. The imaging of longitudinal and transverse sections, which are coplaner, is achieved with echocardiography and there is

more plane selection flexibility. It allows the imaging of the heart valves and the inlet and outlet vessels.

Although the three techniques provide images of different quality and resolution, they all have unique built in advantages. Cineangiography offers haemodynamic information about leaking valves or septal defects by locally injecting contrast medium and following its course. Radionuclide angiography provides three dimensional information about the blood pool within the image outline by virtue of the count rate being proportional to the blood volume in a matrix of resolvable areas within the two dimensional image. Direct calculation of ejection fraction and cardiac output can therefore be made. The use of selective radionuclide compounds to image for example, infarcted myocardium, is a recent and developing feature. However echocardiography is inherently the best technique for real-time visualisation using received echo information directly from the surfaces to be imaged. It has the potential to combine good quality images with both T-M echocardiography and range-gated Doppler systems allowing high time resolution recordings and haemodynamic information to be recorded from known locations.

Although the direct or primary nature of the information gained from these imaging techniques can allow a definitive

diagnosis to be made, it is often the case that secondary data from another technique is required to make a differential diagnosis. It is only with a knowledge of all the possible heart malfunctions and a combination of measuring techniques with an understanding of their individual limitations that accurate diagnosis can be made. The ultimate goal of being able to diagnose all the known cardiac diseases with one non-invasive technique is unlikely to be achieved due to the inherent differences in the data obtained by different techniques allowing fine clinical differences to be identified when these techniques are combined.

Echocardiography is completely non-invasive and can be used for repeat studies and patients can be treated as outpatients. Equipment cost can be relatively low compared with the other techniques and the examination can be carried out by one person with the use of no expensive materials making the cost per examination negligible by comparison with cineangiography and radionuclide angiography. With the development of therapeutic methods, echocardiography could be used as a screening technique to allow the implementation of preventative therapy to reduce the incidence of cardiac disease.

1.4 RESEARCH PROGRAMME

Several methods of producing real-time ultrasonic images are now well established but there is no one real-time method which is ideal for clinical application in cardiology.

It is the aim of this investigation to examine the methods of real-time imaging in the context of the physical problems associated with heart scanning and from these findings design and develop an ultrasonic real-time scanning system with a flexible scanning action and good visualisation performance suitable for clinical application in cardiology. The scanning system is to be assessed during clinical trials on a representative group of cardiac patients. It is also intended to look into the possibility of visualising the heart with two scanners simultaneously with normal subjects.

CHAPTER 2

PHYSICAL CONSIDERATIONS

2.1 T-M ECHOCARDIOGRAPHY

T-M echocardiography is now a well established and sophisticated technique requiring a skilled operator with an understanding of what is required if an adequate echocardiogram is to be obtained. Many of the problems of access to the heart have been experienced using this technique (Feigenbaum, 1976; Chang, 1976) and therefore it is relevant to briefly review this experience in the context of real-time ultrasonic access and scanning format before considering some theoretical and experimental aspects.

The conventional ultrasonic window to the heart is just left of the sternal border and right of the left lung at the intercostal spaces situated in front of the heart.

The interference of the sternum and lung with the ultrasonic beam leaves an approximately rectangular area for transducer placement just left of the sternum which is crossed by ribs. The ribs interfere with the ultrasound beam to a lesser extent the more cartilaginous they are which is the case close to the sternum and in young patients and infants. The 2nd, 3rd and 4th intercostal spaces are commonly used for T-M examinations depending

on heart position and orientation, which can be changed slightly by alteration of patient position to bring relevant structures into the ultrasonic beam. The higher the intercostal space the greater the likelihood of lung and respiration interference. From this parasternal application of the transducer most important heart structures can be located and a characteristic echogram obtained. It is also the approach which has attracted most clinical application and experience over the period of development of T-M echocardiography.

If ultrasonic access is reduced or obscured by for example a barrel chest or inflated lungs then an alternative approach used is the subxiphoid. The transducer is placed in the epigastric area under the xiphoid process and directed towards the patient's throat and left shoulder. The problems presented in obtaining a good echogram are geometric in nature rather than those of ultrasonic access as with the parasternal approach. For example if the heart is high in the chest with a high diaphragm and horizontal heart, often associated with obesity, then angulation of the beam towards the heart almost parallel with the chest wall can be difficult. However patients with inflated lungs, where the subxiphoid approach is most applicable, also tend to have low diaphragms and

hearts lower in the chest and so closer to the transducer resulting in less acute angulation of the transducer to achieve the required orientation of the beam relative to the heart. From this approach assessment of left ventricular dimension can be made similar to the parasternal method although mitral valve echograms are not so readily obtained. The right side of the heart and the tricuspid valve and the base of the heart are more accessible.

These are the two most commonly used approaches for obtaining useful echograms and both have individual and distinct access problems.

Other transducer placements have been used with T-M echocardiography for specific applications but are of less relevance to real-time approaches. For instance the placement of the transducer in the suprasternal notch or the right supraclavicular fossa both require the use of a small transducer. The application of the transducer on the chest wall at the apex of the heart has found some clinical application in detecting the ball movements of the ball in cage type prosthetic valve and mitral ring movements due to the beam being almost normal to the base of the heart and therefore parallel to the direction of movement.

These transducer placements are in addition to the multiple locations over the chest available to the pediatric echocardiographer because of relatively free access due to the different physical conditions that apply in young infants which remove many of the restraints experienced in adult echocardiography.

2.2 ULTRASONIC ACCESS AND INTERACTION WITH THE HEART

Some basic theory and some experimentation is described in this section to help understand some of the difficulties encountered in T-M echocardiography and to predict some of the requirements and restrictions of a real-time heart scanning system.

2.2.1 THEORETICAL ASPECTS

Before the transmitted ultrasonic pulse can interact with the heart it has to interact with some or all of the biological materials in front of the heart, such as fat, chest wall muscle, breast tissue, cartilage, bone and lung tissue. The main factors affecting chest wall transmission are the attenuative properties of the individual materials and the reflective properties of their boundaries. Many measurements of attenuation and velocity in biological materials have been made but this data is not complete. Velocity measurements have been used with relevant material density measurements to calculate theoretical reflectivities

of some plane biological boundaries (Wells, 1977). Other measurements have been collected by Wells for the attenuation in biological material, which is the total propagation loss expressed in decibels per centimetre (dB/cm) and is approximately linearly dependent on frequency in the case of soft tissue and muscle. The main contribution to attenuation in a homogeneous piece of tissue is due to absorption, the transformation of ultrasonic energy into other forms through relaxation processes. It is the frequency dependence of various relaxation processes at different frequencies which is thought to result in an almost linear overall dependence in the low mega hertz range. However the complete attenuation through the chest wall is contributed to by individual structure attenuation, interstructure reflective boundaries and possible refractive boundaries causing beam dispersion and deviation.

Some relevant reflectivities of some plane biological boundaries expressed in decibels below the level from a perfect reflector are given in table 2.1. The attenuation in these materials can be expressed in terms of α/f where α is the attenuation coefficient in dB/cm and f is the frequency of ultrasound used to make the measurement in mega hertz (MHz). These figures are also presented in table 2.1 over the frequency range of interest to

T A B L E 2.1

Reflectivities expressed in decibels below the level from a perfect reflector.

Bone-muscle	5
Bone-fat	4
Lung-muscle	3
Muscle-soft tissue	30-40
Muscle-fat	19
Muscle-blood	32
Fat-blood	21

Attenuation figures expressed in terms of α/f (dB/cm MHz) for f in the range 2 to 5 MHz.

Soft tissue	0.5 - 1.0
Muscle	1.5 - 2.0
Lung	20
Skull bone	20
Ivory bone	3 - 4

Data from Wells (1977).

echocardiography namely 2 to 5 MHz.

The figures for skull bone and ivory bone are significantly different and this is thought to be due to the contribution of structure dependent wave mode conversion and scattering processes to the attenuation in these bone types. The nature of the bony structures in the chest at the area of transducer application change with age and position. The ribs are cartilaginous where they join the sternum and therefore the figures available have to be used with care in this respect. Attenuation measurements for cartilage are not available but from practical scanning experience in obstetrics it is known that the spinal canal can be visualised clearly in the fetus although some shadowing is caused by fetal ribs. Its characteristics are obviously different from bone and soft tissue but it does not interfere severely with the ultrasonic beam.

From these approximate figures of reflectivity and attenuation the overall transmission through the chest wall can be outlined. Both the reflective nature and the high attenuative properties of lung will severely impair ultrasonic propagation. The same may be said about bone from the available figures but since the state of the ribs and sternum varies as explained, these figures

should only be used as a guide to the possible hazards of calcified bone. The figures for soft tissue, fat and muscle fit with the experience of T-M echocardiography in that a thin non muscular chest wall presents no access problem and that slight attenuation is experienced with more muscular and fat patients due to muscle attenuation and more significant reverberation from muscle and fat boundaries than within soft tissue. Since T-M techniques generally involve placement of the transducer close to the sternum and within an intercostal space with minor angulation of the transducer, then the bone structures are not really a significant problem and relevant experience here will have to be gained from experimental work.

To add to the problems caused by lung and bone the velocity of ultrasound in bone is twice that of soft tissue or muscle and in lung it is about half at a frequency of 2 MHz and is frequency dependent. The absorption in lung and bone is also frequency dependent. This makes the interference by lung or bone even less desirable due to the refractive boundaries produced and the pulse shape distortions likely to result through absorption and velocity dispersion.

Interaction of ultrasound with the heart involves reflections from muscle and blood boundaries and from muscle and fat

boundaries within the heart wall and in diseased valves. Relevant reflectivity figures are presented in table 2.1. However these reflectivity figures are calculated for normal incidence at plane boundaries which is not the case in the heart. The fat muscle boundary at the rear of the heart approximates to a plane boundary but internal structures such as valves and chordae and the endocardium are far from plane surfaces and these limitations have to be recognised.

The endocardium is trabeculated but has a smooth surface which will give rise to intermittent specular reflections from parts near normal to the beam. However if surface irregularities are less than the wavelength of the ultrasound then some ultrasound can be backscattered. This scattering can be relevant and it has been shown by Reid (1966) that diseased and normal mitral valve cusps examined at the same frequency exhibit different echo amplitude variations with changing angle of incidence. The rougher surface of the diseased valve cusp gives rise to scattering. Hence the stronger echo signals received from stenosed valves are due to this and to calcification causing a greater reflectivity.

Scattering within blood is contributed to by the red cells and it has been reported that the scattered wave is 47 dB

below the incident wave at 5 MHz (Reid et al., 1969). Another more recent measurement reports this to be 74 dB (Wells, 1974). At frequencies below 5 MHz as used in echocardiography the backscatter is negligible as in the absorption in blood which is about 0.15 dB/cm. There are also no significant velocity differences within the blood filled chambers to cause distortion. However swept gain compensation is complicated by the low attenuation of the blood volumes in the heart.

So considering the interaction of ultrasound with the chest wall and heart without lung and bone or cartilage interference, it is in many ways similar in theory to abdominal scanning with soft tissue, muscle, fat and blood interfaces. As a result, if the avoidance of lung and bone structures can be satisfied, then in theory it should be possible to receive echo information over a similar dynamic range capable of producing grey scale images.

2.2.2 EXPERIMENTAL ASPECTS

It is important to assess from practical T-M echo information some of the echo amplitude ranges from specific structures throughout the heart cycle as well as their relative extreme amplitude ratios such that the total dynamic range required in a real-time imaging system can be predicted and allowed for in its design.

Hard copy T-M echograms are often made using paper sensitive to ultra-violet (UV) light. It is sometimes the case that complete uninterrupted traces of specific structures, especially valves, cannot be recorded. Although this may be due to the limited dynamic range and writing speed response of the UV paper it is the method routinely used to provide hard copy records for clinical examination. However it is not a suitable method to investigate the relative echo amplitudes outlined above.

A fast data acquisition system has been developed in the department for another research project to record ultrasonic echo signals from remote B-scanners for subsequent computer analysis. This system was used to record echo signals from the heart. The signals are digitised by a Biomation 8100 transient recorder which incorporates an 8-bit analogue to digital converter and a 2K fast buffer memory. This is interfaced to the memory of a PDP8/E minicomputer to allow the data to be transferred and stored on a disk cartridge. The disk can be removed and taken to the departmental PDP 12 computer for subsequent analysis.

The received echo signals from the heart were digitised at 20 MHz allowing a range of approximately 8 centimetres to be examined before the 2K fast buffer memory is filled.

When this happens the interface automatically initiates the transfer of the contents of the buffer memory to the minicomputer disk. When the buffer memory is cleared the cycle is repeated automatically. This was done over a few heart cycles after an optimal A scan of the mitral valve and left ventricle had been obtained. This resulted in the recording of approximately 15 waveforms per heart cycle which was adequate for the purposes of the experiment. The data was recorded over an 8 centimeter range from the right side of the interventricular septum to just beyond the posterior wall of the left ventricle. Since the echo signals are taken from the output of the swept gain amplifier it was arranged that the swept gain function was flat over the range of interest so that this did not have to be allowed for when comparing echo amplitudes. The amplification of the echo signals to this point can be considered linear for the purposes of this experiment.

The PDP 12 computer can be used to display a reconstructed waveform from the digital information, on a visual display unit. A sequence through the heart cycle can be displayed and a mental picture of the moving parts enables identification of the structures of interest. Hard copies can be made of the relevant recordings of choice on a line printer/plotter

peripheral. It was arranged when digitising the data to range the maximum clinically useful echo with full scale on the digital scale such that measurements can be made relative to this. The dynamic range can then be measured from full scale to the smallest identifiable and clinically significant echo amplitude. Figure 2.1 illustrates a hard copy of a reconstructed waveform.

Recordings were made at the 3rd intercostal space in four directions from the aortic root and valve through the mitral leaflets and down towards the chordae and apex. The recording from the mitral leaflets direction was used to measure relative dynamic ranges of echo amplitudes over the heart cycle from identifiable structures and the recordings from other directions were used to confirm these findings over the whole left ventricle in a plane most likely to be used in two dimensional real-time imaging. To investigate the effects of lung and bone the optimal standard recording of the mitral leaflets was made from sites as close as possible to the original 3rd intercostal space but in turn over sternum, rib and lung. It was found from the recordings made from the standard site that the dynamic range of echoes from mitral, endocardium and septum were 20 dB, 20 dB and 15 dB respectively. However the maxima of the endocardial and septal echoes

being the only ones significantly affected by transducer direction, fall off to 10 dB below mitral when recording towards the apex.

Although the recordings made through lung and bone necessarily require a slight change in beam direction, they were still representative since the relative echo amplitude from the septum, mitral and endocardium were similar to the standard recording, and measurements were made over a heart cycle causing in all cases relative shifts in the orientation of the heart with the beam. Recording through rib at the parasternal position causes a 3-5 dB reduction in overall amplitude. Similar results are true of sternal edge but figures for the centre of the sternum could not be used due to other significant variations due to beam direction. Through the edge of lung under normal breathing conditions produces reverberation amplitudes at the centre of the left ventricle, varying from 10-15 dB down compared with the maximum mitral echo amplitude from the original site. Inflated lung causes similar reverberations which are only 5 dB down at the left ventricle.

These figures indicate that over the whole left ventricle the major identifiable structures produce an echo amplitude range of 20-25 dB. The comparisons made between the optimal waveforms and those through bone and lung indicate

that inflated lung must be avoided only the posterior wall and parts of mitral valve being detectable with very reduced dynamic range. Deflated lung edge and bone or cartilage however have less drastic effects ultimately reducing the dynamic range of an image by overall reduction in echo amplitude accompanied by an increase in echo amplitude noise level.

However the dynamic range of potentially useful echo amplitudes in the construction of a real-time image is likely to be more than could be identified from the sequence of still waveforms because in a moving image the eye can differentiate between static noise and echo amplitudes of a similar level to the noise from regularly moving structures. The average ultrasonic noise level on the waveforms obtained from the standard transducer location was 25-30 dB below full scale and therefore at least this range should be allowed for in a real-time heart system.

2.3 PHYSICAL CONSIDERATIONS WITH RESPECT TO REAL-TIME SCANNING

In the light of the physical considerations discussed so far it is apparent that the two main access areas suitable for real-time visualisation of the heart are the parasternal and subxiphoid approach. Both have different limitations. The parasternal approach allows easy physical

access but limited ultrasonic access and with the subxiphoid approach the opposite is true where the main limitation is physical access. Assuming good ultrasonic access is achieved then it is evident that the dynamic range of the echo signals from the heart is similar to that of the abdomen. Therefore it should be possible to obtain good quality grey scale real-time images comparable to those obtained in abdominal scanning.

It is relevant here to consider the two basic real-time scanning formats available in the context of both physical and ultrasonic access to the heart. Rectilinear scan formats are produced by repetitive lateral movement of the ultrasound beam over a set distance and sector formats by regularly sweeping the beam about a point through a sector of known angle. Generally rectilinear scanning of the ultrasound beam is achieved with linear array transducers and sector scanning with phased array transducers or by rapid movement of standard transducers mechanically.

The rectilinear scanning format necessitates ultrasonic interaction with the ribs and also sternum and lung to a varying extent depending on the orientation of the long axis of the heart. For complete visualisation of the heart an array at least 10 centimetres long is required

and complete acoustic contact along the transducer length can be difficult on thin, round chested subjects. Transverse views can be partially obscured by lung. An application where interference from lung and bone would not present itself is in the subxiphoid approach but here the physical access and flexibility of scanning plane are severely limited by the transducer dimensions.

The sector format on the other hand allows a point of entry aspect suitable for parasternal applications avoiding direct interaction with lung and bone while maintaining access to structures lying under the sternum and lung. The main disadvantage is its limited near field view due to sector format plus limited sector angles. Rectilinear scanning actions do not suffer from this problem. The flexibility of scanning plane orientation is optimised by the use of a point of entry scanning format. This aspect has advantages in visualising the heart from the subxiphoid approach especially since the limited near field of view is not so critical due to the heart being further from the transducer compared with the parasternal approach.

Phased arrays have all the advantages of a point of entry scanning format but have a limited sector angle of 60° to 80° and the side lobes and less well defined beam shape

produced by increasing this angle have a degenerative effect on dynamic range and resolution. These are inherent features of the phased array design. The ultrasonic beam quality made possible by using conventional transducers is better and although phased arrays have swept focusing, this is only in one direction parallel with the plane of scan. True axial focusing either static, or swept by using annular transducers, can be incorporated in mechanical scanners. The requirement to have a scanning system with two scanners and a versatile driving system would lead to complex electronics development and expense not encountered with mechanical scanners using standard transducers which can be driven from conventional electronics. This conventional electronics allows a range of frequencies to be driven from the same unit which is not the case with phased arrays without duplication of hardware.

2.4 CONCLUSION

Based on the flexibility of scanning plane possible with a point of entry scanner and the potential grey scale image quality using standard transducers, it was decided to design a heart visualisation system using a real-time mechanical sector scanner with as wide a field of view as possible. This format of scan is also preferable because of the previously stated intention to investigate

the visualisation of the heart from the subxiphoid location and the possible advantages of simultaneous visualisation of two planes from adjacent or separate locations.

3.1 MECHANICAL METHOD

At the time when the mechanical design of the scanner was being considered all the real-time mechanical point of entry scanners which had been reported were of the oscillating type as described in Chapter 1 (Eggleton and Johnston, 1974; Griffith and Henry, 1974; McDicken et al., 1974). However two reports had just been made of mechanical real-time rotating systems in applications other than echocardiography. One device was designed specifically to visualise superficial blood vessels and incorporates a Doppler system (Barber et al., 1974). Acoustic coupling to the skin is made via a water bath attachment. The other scanner had been designed for abdominal scanning when attached to a conventional B scan machine giving the benefits of rapid searching and compounding. Acoustic coupling is made by direct contact of the transducer wheel with the oil covered skin (Holm et al., 1975). Both applications involve the searching of static structures at relatively low frame rates rather than the visualisation of rapidly moving structures.

Oscillating or rotating mechanisms could be used to produce the scanning action required to form a sector

format for heart scanning. To optimise the point of entry aspect of a rotating scanner would require the diameter of the transducer carrying wheel to be minimised while maintaining close acoustic contact with the patient at the intercostal space.

The oscillating scanners referred to above have sector angles between 30° and 60° . For small angles of oscillation coupling can be direct via some gel allowing skin movement to maintain acoustic contact. However for larger angles, especially when applied between ribs, it is desirable to couple by means of an oil and flexible membrane arrangement with the transducer face placed far enough behind the membrane to allow free oscillation within a rigid housing which supports the membrane and contains the oil. The membrane area and the dimensions of the supporting housing are dependent on the transducer diameter and the angle of oscillation of the transducer.

The average measured separation between intercostal spaces is 3 cm. As a result if two scanners are to be used at adjacent intercostal spaces and both in the same longitudinal scanning plane then the overall dimension of the scanner in that plane direction cannot exceed 3 cm if they are to fit centrally into the spaces between the ribs. This restriction could put an upper limit on the possible

sector angle in the case of an oscillating transducer due to the length of the transducer and the oscillating mechanics. In the case of a rotating transducer the maximum length of transducer would be limited.

However assuming these problems could be overcome and similar sector angles in excess of 60° were possible then the advantage of the better point of entry aspect of an oscillating scanner compared with a rotating scanner is not so applicable for larger sector angles. This is mainly due to the geometry of the design allowing the rotating type transducer to sweep down into the intercostal space due to the curved profile of the scanner whereas the oscillating scanner housing requires the scanner to sit on the adjacent ribs raising the transducer face above the ribs. The resultant relative positions of the beam and ribs at the sector edge is likely to be very similar, especially in cases where the chest wall is thick which raises the scanner above the ribs in any case. This consideration between oscillating and rotating designs is not relevant in the case of transverse and subxiphoid applications where there is no rib interference.

Vibrational forces are inherent in the operation of an oscillating scanner. For a given frame rate, the larger the angle of oscillation the greater will be the

vibrational forces caused when the transducer mass changes direction resulting in resolution degradation. The vibration also causes some patient discomfort and detracts from the general acceptability of the device.

Another consequence of this type of scanning motion is the uneven line density distribution over the sector and the structures at the off centre positions in the sector are scanned at uneven time intervals. For example structures at the centre are scanned twice every cycle at even time intervals or once every frame but at the sector edge a structure is scanned twice in close succession every cycle. Therefore frame rate and sample rate are not the same at off axis locations. Although this is not important when visualising slow moving structures, effectively the frame rate is halved at the extremes of the sector and this is important when visualising fast moving valve leaflets.

A rotational motion at constant angular velocity overcomes vibration and the line density is even over the sector. If a rotating wheel contains a number of transducers which in turn sweep through a given sector then the echo information is sampled from different locations in the sector at the same rate which is also the frame rate.

Since both the above mechanical scanning methods have non ideal point of entries then some rib interference is

inevitable if large sector angles are used when scanning the longitudinal section of the heart from the parasternal position. A preliminary experiment carried out on normals simulating the rotation of a standard transducer within the 3cm dimensions discussed above showed that significant echo information could be received from the heart over 50° to 80° sectors from various intercostal spaces. Based on this and the advantages of vibration free motion and even information retrieval, it was decided to construct a scanner based on a rotating transducer head design.

3.2 SCANNER DESIGN

This section describes some of the design and component choices made which have enabled the construction of the scanner within the restricted dimensions set due to the physical considerations previously made regarding access and flexibility of scanning plane.

3.2.1 DESIGN OUTLINE

To allow simultaneous scanning at adjacent intercostal spaces puts the basic dimensional restriction of 3cm on the transducer head external diameter. If simultaneous longitudinal and transverse scanning is to be feasible at the parasternal location then the distance from the scanning plane to one side of the transducer head must be within approximately 1.5 cm. The total dimension of the

transducer head in this direction, normal to the scanning plane, need not be restricted to 3cm if the head is made asymmetrical. Application in the subxiphoid location and scanning in the coronal plane also requires minimisation of this dimension. To maintain maximum freedom of scanning action requires the scanner body and components to be well out of the way and above the transducer head. If transducer head symmetry can also be maintained then the result is a pencil like point of entry scanner with similar scan flexibility to the traditional T-M technique.

As well as providing a suitable handle, the slim vertical body must contain a motor and drive mechanism for the transducer head and also devices to output angular position and timing information about the transducer head. This allows the scanner to be easily interfaced to a driving and display system and also synchronised with another scanner.

Having placed these restrictions on the design it remained to detail the transducer head and mechanical drive design and the choice of components compatible with the scanner body shape and dimensions. Some of the reasons for design and component choice are briefly discussed below. Figure 3.1 illustrates the final scanner component layout.

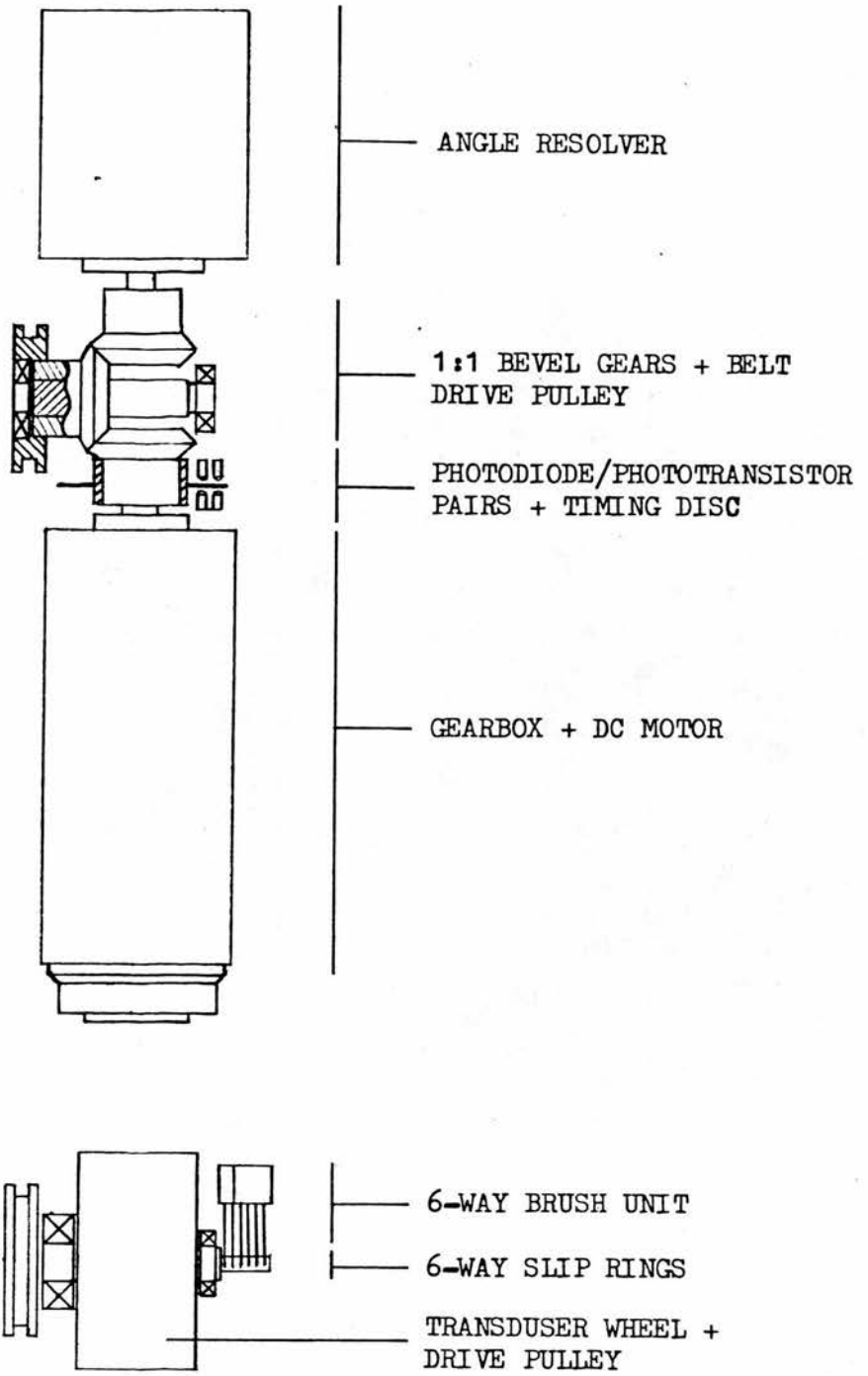


FIGURE 3.1 Schematic diagram of scanner component layout.

3.2.2 TRANSDUCER HEAD

If four individual transducers are incorporated in a wheel and the wheel is rotated about its centre then a 90° sector image can be obtained if acoustic contact is sufficient. Using standard 2.5 MHz transducers of 15 mm diameter in a wheel of less than 30 mm diameter leaves the centre of the crystal face more than 2 mm from the circumference of the wheel and therefore direct acoustic contact with the skin surface would be impractical unless the wheel was built up with a suitable material in front of the transducers. Even if this were done the depression into the skin surface to maximise acoustic contact angle would load the drive to the transducer head and wipe away the acoustic coupling and lubricating medium. This is particularly relevant in the subxiphoid application.

By surrounding the transducer wheel with a rigid acoustic window and filling this cylindrical cavity with oil then acoustic contact is assured if the window is coupled to the skin of the patient with gel. This allows depression into the skin without loading and removes the need for moving parts to contact the skin. The constant torque required to rotate the transducer wheel allows a constant angular velocity to be maintained and hence constant frame rate and frame line density. A small bonus of this design is

that the oil tends to damp any mechanical backlash.

3.2.3 ELECTRICAL CONTACT

A consequence of rotation as compared with oscillation is that there are four transducers instead of one and the electrical connection to the transducers cannot be direct in the case of rotation. An early idea was to excite all four transducers simultaneously and rely on the angle of acoustic contact with the skin to limit transmission into the body from only one transducer at a time. This would only require two electrical connections and therefore a rotating 1:1 transformer could be used. Preliminary investigations into this revealed a lack of such transformers at the required small size and in any case this operating principle limits the sector angle to 60° if only one transducer is to be in the sector at any one time. There are also problems of damping reverberations from transducers not in the sector and reduced output power per transducer. Switching the transmitter to the individual transducers requires five connections, a common earth interconnecting the front faces of the transducers and individual contacts to the back faces. The availability of miniature gold-plated slip rings and brush unit with low noise characteristics enabled this five way connection to be made. The introduction of rings with a hard gold flash

ensured good life time expectation since the original soft gold rings had been well tried. For ring surface speeds corresponding to 20 to 30 frames per second the noise level is given as $5\mu\text{V}/\text{mA}$ and so for an input and transducer termination impedance of 50 to 75 the noise is negligible. A useful consequence of separate connection is that any crystal sensitivity differences can be balanced at the transmitter source.

The five way slip ring and brush unit although miniature takes up 6mm of space in the direction along the axis of rotation. At a stage in the development when ways of reducing this dimension were being investigated it was realised that a commutator type contact could be used requiring only two rings and so reducing the space needed. This type of device was not commercially available and would need to have been developed.

3.2.4 MECHANICAL DRIVE

The simplest way to drive the transducer wheel would be directly via a drive coupling from the side and parallel to the axis of rotation. However the vertical nature of the design requires the motor to be placed above the transducer with its axis of rotation perpendicular to that of the transducer wheel. As a result some sort of drive transmission had to be designed.

Since the angle resolver and timing disc also have to be driven in synchronisation with the transducer wheel it would be ideal if a resolver with a shaft extension at the rear could be used since the motor could then drive directly through the resolver and attached timing disc via a 1:1 transmission system to the transducer wheel. Due to the slip rings attached to the resolver rotor it was not possible to obtain one with a straight through shaft.

After considering a number of transmission configurations using standard commercially available precision components the arrangement shown in figure 3.1 was used, a double level gear configuration providing 1:1 take off points for both the angle measuring device and the transducer wheel belt drive. A self centring non-slip belt was chosen since it does not need flanged pulleys allowing narrower pulleys to be used. The diameter of the pulley could have been greater to lower the belt stress but this would have restricted the amount of transducer head profiling.

The DC motor used to drive the mechanical system is of an advanced design with an ironless low inertia rotor resulting in a very high power to volume ratio and efficiency. The linear relationships between voltage, speed and torque as well as the low starting voltage make this motor suitable

for stopping and starting the scanner smoothly and if required can accurately drive the transducer wheel to a predetermined position for T-M scanning. The motor is coupled to a gearbox which increases the available torque especially at low speeds. Several motors are compatible with a range of gearboxes all with identical external dimensions and therefore motor/gearbox combinations can readily be altered for specific applications and frame rates at a later date.

3.2.5 TRANSDUCER WHEEL POSITION MONITOR

For image production and registration purposes an output is needed from the scanner related to transducer wheel position or more specifically to ultrasonic beam direction. There are various types of angle measuring device based on the principle of using an AC carrier signal of constant amplitude and producing a modulated AC output due to impedance or reluctance variation with angle. There are also direct output devices such as sine and cosine potentiometers.

The angle resolver in the scanner is a variable inductive type with a symmetrical stator and twin rotor coil configuration producing two modulated outputs from the rotor which are 90° out of phase. When full wave phase sensitive demodulated sine and cosine voltage waveforms are

obtained. This along with sector timing and transducer identification information, output from the photo-transistor located over the slotted timing disc, can be used to generate a sector sweep display format. Apart from providing this essential information the angle resolver can be used to stop the transducer wheel at known directions within the image for T-M or Doppler applications.

3.3 SCANNER PROTOTYPES

Before finalising the scanner design some experimental parts were constructed to test some of the ideas described above.

3.3.1 TRANSDUCER HEAD PROTOTYPE

To investigate the practical performance of the transducer head principle, a standard 2.5 MHz transducer was modified and incorporated in a simple horizontal scanner consisting of a transducer head and axial motor drive from the side via a drive coupling and timing disc. All the parts were contained in a perspex tubular structure of 3cm diameter with two way slip rings mounted on the opposite side of the transducer wheel from the drive. By generating a simple 180° sector format image on a variable persistence screen using the information from the timing disc photo-transistor, the general performance of the transducer head could be assessed. The angle of view possible was confirmed

to be in excess of 80° when imaging the heart. Significant reverberation echoes from the perspex window were present in the near field of the image, but the image detail beyond this was very encouraging considering the reduced rate of echo information reception due to the single transducer.

The noise level of the slip rings was negligible and did not deteriorate significantly over a cumulative scanning time of 300 hours. The hermetically sealed bearings used to contain the oil in the cylindrical cavity surrounding the transducer wheel leaked slightly causing the formation of air bubbles. This was temporarily overcome by topping up the level before use. Figure 3.2 illustrates the original prototype transducer head which was subsequently modified to incorporate the transducer in a one piece tubular perspex housing.

This simple scanner found application in the monitoring of fetal breathing movements due to its compact size allowing it to be strapped to the abdomen conveniently without disturbing the fetus. Subsequent improvements in the design of the transducer head for the vertical scanner were applied to this scanner and have resulted in the development of a versatile real-time system with a field of view up to 150° combined with pulsed Doppler and T-M facilities for fetal breathing and other obstetrical studies.

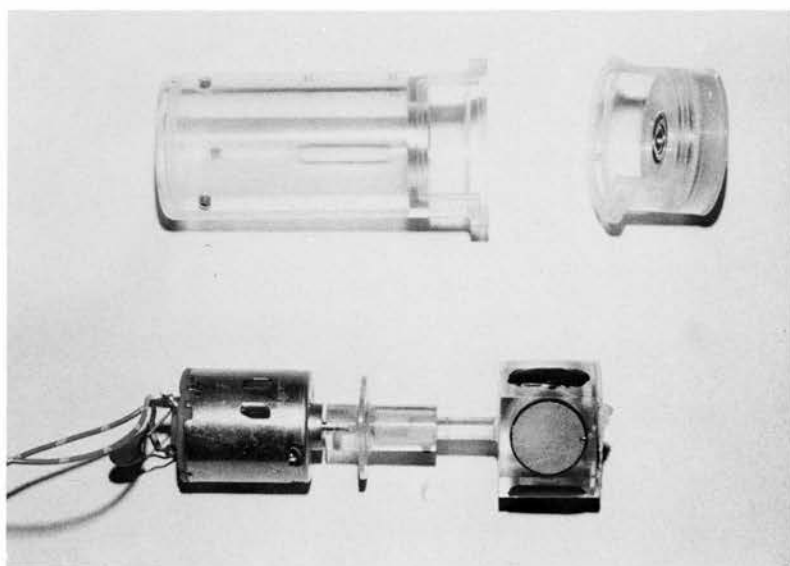


FIGURE 3.2 Original prototype transducer head - tubular scanner.

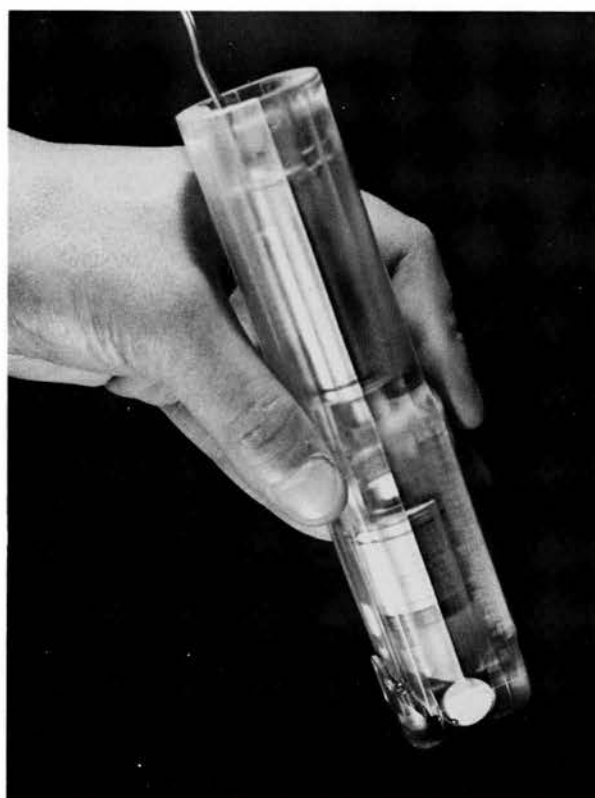


FIGURE 3.3 Perspex prototype vertical scanner.

Details of this system have been reported by McHugh et al., (1978) and McDicken et al., (1979).

3.3.2 VERTICAL SCANNER PROTOTYPE

Before designing the final aluminium scanner body to house all the components a perspex version was constructed since this was easily machined. This provided an opportunity to check thoroughly the mechanical drive system design for both construction feasibility and practical mechanical performance. This scanner is shown in figure 3.3.

Although this prototype scanner performed well mechanically running smoothly and quietly while providing output information suitable for 90° sector generation, many small design changes were implemented in the final design as a result of experience with this scanner.

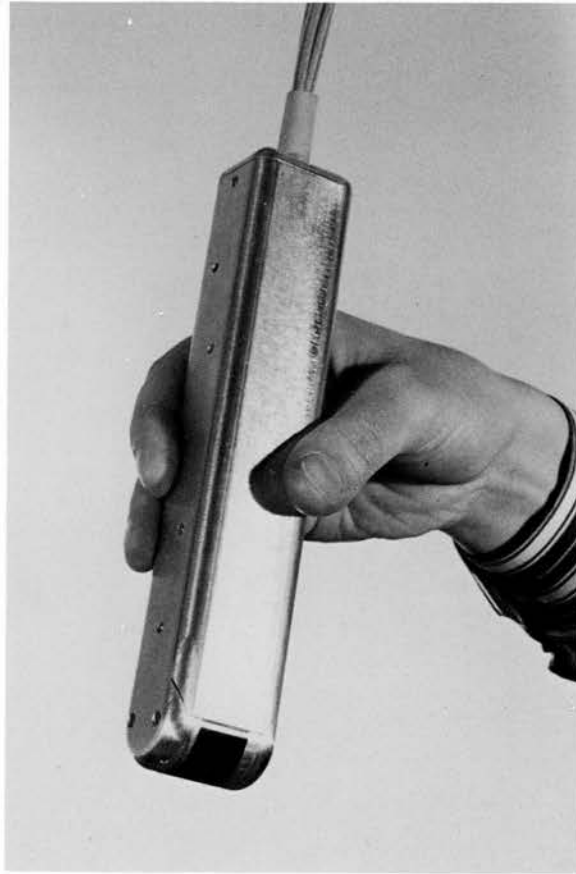
The use of a transducer wheel incorporating four 2.5 MHz crystals allowed 90° sector real-time images at an optimal frame rate and line density combination to be obtained for the first time due to echo information being received continuously. Although the heart images contained static reverberations and were of reduced dynamic range due to the transducer head construction (see Chapter 4) the dominant heart structures were visualised and the image format and line density were very stable due to the

smooth running of the scanner.

3.4 FINAL SCANNER DESIGN

The final design of the vertical scanner houses all the components in a one piece aluminium body with a separate transducer head. Figure 3.4 shows the scanner hand held and applied to the chest at a parasternal intercostal space and at the subxiphoid location. The transducer head is fixed to the main body by a central location and by side plates which also cover all the electrical leads coming to and from the scanner components. The sides of the scanner body are flat and parallel and the transducer head fits into the body without projecting beyond the body cross-section. The overall dimensions are 31 x 38 x 204mm. The flat sides allow two scanners to be clamped together easily and ensures coplanar alignment of the scanning sectors.

The transducer head consists of two aluminium sides connected by a tubular section of thin perspex which acts as an acoustic window and the transducer wheel is located in the resultant cylindrical cavity. Apart from material changes there are two basic design changes. Firstly the use of a non-sealed bearing at the slip ring side of the transducer wheel allows a thinner bearing to be used and reduces the chance of leakage. As a result the slip



PARASTERNAL



SUBXIPHOID

FIGURE 3.4 Final version of vertical scanner hand held and applied at the parasternal and subxiphoid locations.

rings have to run in oil which does not significantly increase the slip ring/brush contact noise. This reduction in dimension was made necessary to compensate for the increase due to the use of a five way slip ring and brush unit. Secondly since there is still one sealed bearing and the leakage is thought to be due to thermal expansion of the oil, a thin flexible rubber membrane has been included to reduce pressure increases within the sealed chamber. This has solved the air bubble and oil topping up problem every time the scanner is used from a cold start.

The transducer wheel is quite different from any previously used in prototypes and contains four completely independent transducers within a wheel capable of rotating within 3cm. Chapter 4 deals with the development of this transducer wheel and some acoustic aspects of the oil layer and window.

Finally the design of this scanner has been used as the basis for the commercial development of a similar scanner designed mainly for abdominal and obstetrical scanning.

CHAPTER 4

TRANSDUCER HEAD ACOUSTICS

4.1 INTRODUCTION

The first tubular prototype scanner contained a transducer wheel with one standard 2.5 MHz, 15 mm diameter transducer. This transducer was removed from its outer metal container and the backing material of aluminium loaded epoxy resin was reduced from its original length by a few millimetres. The performance of the transducer was unaffected by these modifications and by fitting it into the perspex wheel. To incorporate four such independent transducers into a wheel means reducing the original depth of backing material by about 75%. By a process of progressive removal of the backing material from the above transducer, significant reverberations from within the backing material appeared on the received signal when only 50% of the original material was removed. Further removal of material at an angle, so as to form a bevel and a non-plane reflecting surface, did not increase the reverberations.

The single transducer with a depth of backing material equal to the diameter of the wheel performed adequately and therefore if the transducer wheel could be constructed with four suitable piezoelectric crystals in a mould to

which backing material is added, then the conditions for each crystal would be similar to the original.

The backing requirements of piezoelectric crystals for short pulse production and some practical transducer construction techniques have been reported (Kossoff, 1966; Posakony, 1975; Redwood, 1963). Relatively high impedance, absorbing backing materials such as tungsten in araldite epoxy resins are generally fabricated by mixing a metal powder with epoxy resin and centrifuging the mixture onto the crystal to give a high packing ratio. The resultant impedance depends on the size of the metal particles, the rotation speed and the radius of the centrifuge arm. This results in a variation of impedance through the transducer length with it being greatest at the back face of the transducer crystal. It is the impedance of the backing material at this interface which controls the matching of the transducer to the backing and the consequent increase in bandwidth. Kossoff (1966) has reported a variation of impedance from 6 to $16 \times 10^6 \text{ Kg/m}^2\text{s}$ for a tungsten loaded araldite epoxy resin centrifuged at 3000 rpm at a radius of 8 inches. The packing density increases with decreasing particle size and the impedance increase for higher densities is less than expected due to the lower velocity of sound. The acoustic impedance of lead

zirconate titanate (PZT) ceramic crystals used in medical applications varies from 29 to 35 x 10⁶ Kg/m²s.

Using a 2.5 MHz, 15 mm diameter PZT 5A ceramic disc backed with araldite epoxy resin loaded with 1 micron tungsten powder and following the reported centrifuge procedure, a successful technique was established for producing standard transducers with similar pulse shape and sensitivity to the commercial transducer used in the above prototype.

The problem then arose of how to centrifuge a tungsten/araldite mixture onto four crystals in a small transducer wheel mould. This was done by rotating the transducer wheel mould in a horizontal plane in a specifically built rig at approximately 12000 rpm with the liquid backing material sealed in the mould. This rotational speed was chosen because it corresponds to the same centrifugal force on a particle at the back face of the transducer. However as a result of the small dimensions, a different packing density distribution within the transducer will be produced.

The resulting transducers in the wheel had slightly longer pulse shapes than the transducer constructed by conventional methods but a fundamental drawback was the significant reverberations which corresponded to reflections

from the transducer crystal directly opposite. Although the depth of backing material is approximately the same as the single transducer in the prototype, the density distribution is different and the surface at the back of the single transducer is not flat and parallel to the crystal.

The commercial introduction of small compact transducers at this time, with better performance characteristics than the previously available transducers, opened up new possibilities for the use of individual transducers as originally planned. The reduced amount of backing is due to the use of loaded absorptive materials which when centrifuged give the required combination of acoustic impedance matching and absorption. Due to the expense and the fact that these transducers would still require some backing material to be removed with an associated risk of permanent damage it was decided initially to construct a batch of transducers using conventional methods with absorptive backing materials. Four cut down versions of these transducers could then be fitted to a small transducer wheel.

4.2 TRANSDUCER WHEEL ACOUSTICS

The main desired characteristics of a transducer are a wide bandwidth which gives short echoes and a low

transmission loss which gives good sensitivity. The bandwidth can be increased by backing which also reduces sensitivity. However the bandwidth and sensitivity can be increased by quarter-wave matching the transducer to the load. Inductive tuning of the transducer also results in bandwidth and sensitivity improvements (Kossoff, 1966). The transducers in the scanner wheel have both quarter-wave matching and inductive tuning.

4.2.1 TRANSDUCER CONSTRUCTION

A silthane rubber (Flexane 84) which has high absorption characteristics was loaded 1:1 by weight with 1 micron tungsten powder and evacuated before being centrifuged onto the back of a PZT 5A, 2.5 MHz, 15 mm ceramic disc at 3000 rpm and 8 inches radius. A low viscosity primer was used on the face of the crystal to improve bonding. The standardisation of this bond is most important for consistent performance (Posakony, 1975).

Often quarter-wave plates are made from araldite resins. However the acoustic impedance of araldite resins varies from 2.5 to $3.0 \times 10^6 \text{ Kg/m}^2\text{s}$ which although between that of the load and the ceramic disc, is not the ideal geometric mean. Assuming a load of impedance $1.5 \times 10^6 \text{ Kg/m}^2\text{s}$ then the quarter-wave plate material should have an impedance of about $7 \times 10^6 \text{ Kg/m}^2\text{s}$ since the impedance of PZT 5A is

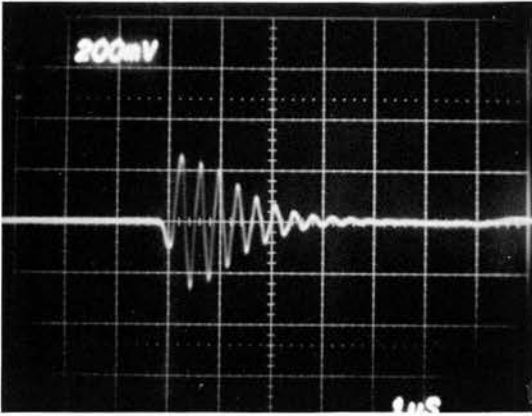
$29.3 \times 10^6 \text{ Kg/m}^2 \text{ s}$. To get closer to this geometric mean figure araldite resin loaded 1:1 by weight was centrifuged at 1000 rpm onto the front face of the crystal. This centrifuging speed was chosen since it results in a packing density at the crystal face which could be machined to a high surface quality and was likely to result in about the desired impedance based on the acoustic impedance values detailed earlier of Kossoff (1966). The required thickness of the loaded araldite plate depends on the velocity of sound in the plate and the frequency of the sound. The velocity of sound in 1:1 loaded araldite is 2000 m/s and for an assumed resonant frequency of 2.5 MHz the quarter wavelength is 0.2 mm. Since both the velocity and the frequency are not known accurately at this stage in the construction the plate was initially machined to a thickness 20% large. The plate was then ground very gradually and the reflected pulse from an aluminium block in water, at a range of 10 cm was monitored for optimum shape and amplitude. The optimum has to be recognised before the plate is ground too thin. This is relatively easy since both the amplitude of the first cycle increases and the out of phase components decrease as the optimum thickness is approached. If it is exceeded slightly, the pulse shape is still good with

just a small reduction in amplitude. The optimum amplitude and pulse shape was reached when the plate thickness was $0.2 \text{ mm} \pm 5\%$.

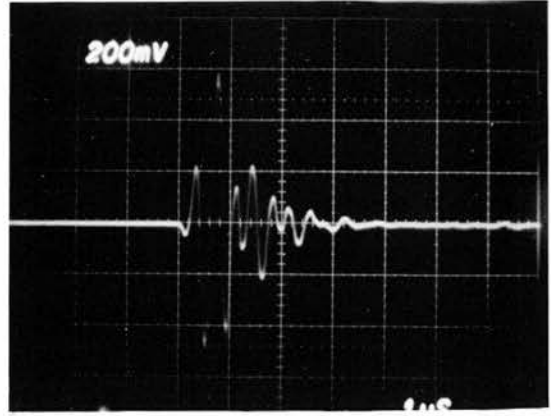
4.2.2 TRANSDUCER PERFORMANCE

In this section the performance of the flexane/tungsten backed transducer with and without both quarter-wave plate and tuning are compared and the final result compared with a good commercial transducer. In order to standardise results the transducer was always placed in a water load 10 cm from an aluminium block and the maximum reflection of the transmission pulse was recorded on an oscilloscope before entering the RF amplifiers of the A scan. The A scan transmission pulse amplitude was kept constant to avoid transmission amplitude dependent effects.

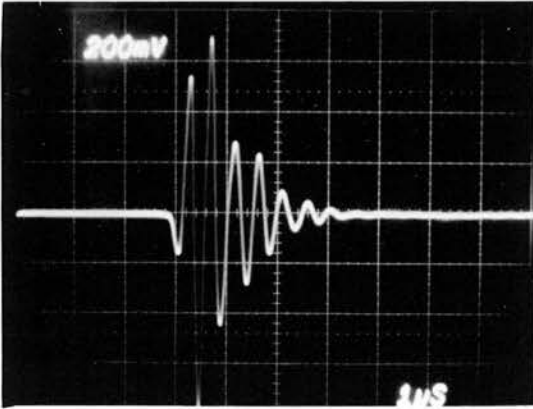
Figure 4.1 shows some reproductions of recordings all taken at the sensitivity and time base settings as indicated on the oscilloscope screen. Figure 4.1A shows the pulse shape obtained from a flexane/tungsten backed transducer made as described earlier and when inductively tuned changes the shape to that of 4.1B. Another transducer made in the same way but with an araldite/tungsten quarter-wave plate optimally ground to $0.2 \text{ mm} \pm 5\%$ is shown in 4.1C and the resultant pulse shape when this transducer is tuned with a $3.3 \mu\text{H}$ shunt inductor is



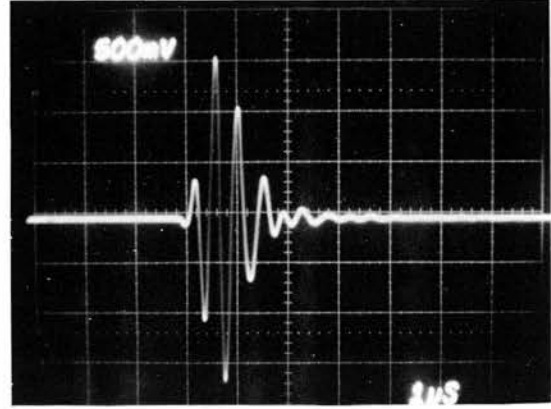
A. Flexane/tungsten backed



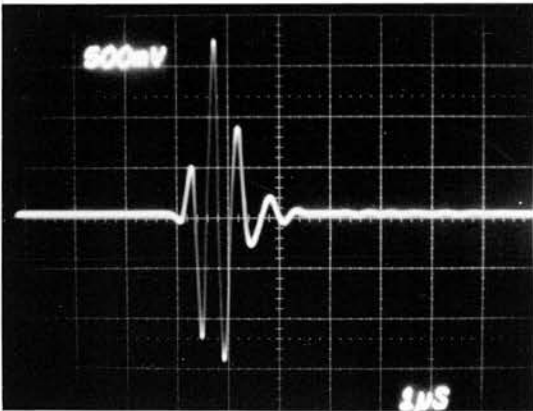
B. Flexane/tungsten backed and tuned



C. Flexane/tungsten backed with quarter-wave plate



D. Flexane/tungsten backed with quarter-wave plate and tuned



E. Aerotech transducer

FIGURE 4.1 Transducer pulse shape waveforms

illustrated in 4.1D. This can be compared with the recording from a commercial 2.25MHz, 13 mm Aerotech transducer in 4.1E which also has a quarter-wave plate and inductive tuning. This pulse amplitude has been normalised to that of 4.1D for easy comparison, by increasing the transmission pulse amplitude and after making allowance for the different transducer diameters the flexane/tungsten transducer is 4 to 5dB more sensitive. As can be seen the pulse shapes are very similar and a frequency analysis of the reflected pulses over a signal dynamic range of 20dB showed the frequency spectrum of both to be similar. Both had symmetrical peaks with the -10dB bandwidth of the flexane/tungsten transducer being 1.2 MHz and the Aerotech 1.5 MHz. The narrower bandwidth of the flexane/tungsten transducer is consistent with its higher sensitivity.

For the purposes of standardisation all the above measurements were made using a transducer with 15 mm depth of backing material which is the constant depth used during fabrication to conform tungsten powder packing density. However the reduction of the dimensions required to accommodate four within the 3 cm limit does not change the pulse shape or frequency spectrum and no reverberations are received by the transducer from the backing material.

The ultrasonic beam profile of the cut down transducer was plotted from 2cm to 15cm range at 1cm intervals using a high precision test tank which was specially built for this purpose. A 1cm diameter steel ball target was used. Apart from the irregular peaks in the first few centimetres range as expected, the profile is smooth with no evidence of side lobes over a range of 40dB. Each plot is symmetrical about its maximum within 0.8 mm and the maxima lie within 0.5 mm of each other along the length of the beam. Having checked the symmetry at suitable intervals the detailed plots were only made on one side of the beam and therefore the complete plots presented in figure 4.2 appear exactly symmetrical. Plots at 5, 10 and 15 cm range are representative of the whole beam and are plotted relative to the centre axis maximum which occurs at a range of 9cm. Figure 4.2 also shows the profile of the Aerotech transducer at a range of 10cm indicating the more consistent beam width of the Aerotech over a 30dB range, although the flexane/tungsten transducer is narrower over the first 15dB.

Every effort was made to keep construction methods identical for each transducer which would be fitted to the same scanner. A batch of six were made simultaneously including evacuation and centrifuging, the largest variable

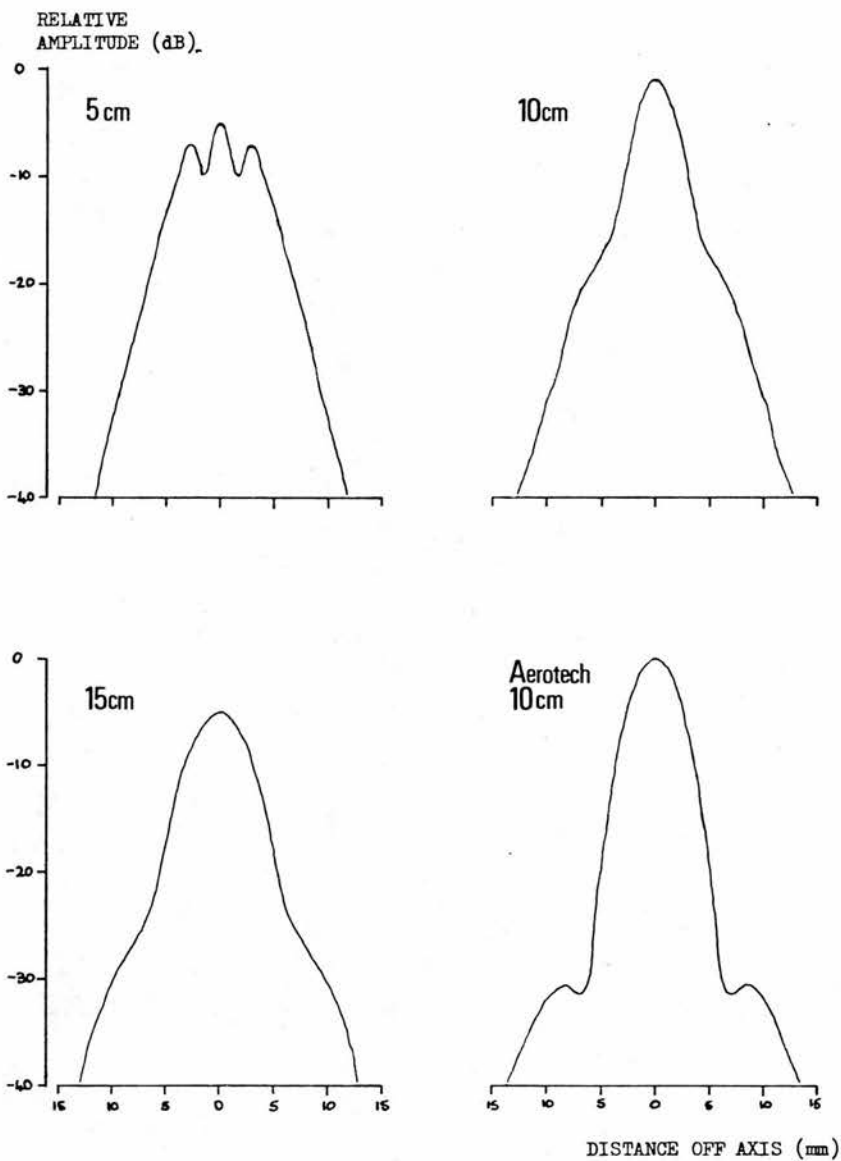


FIGURE 4.2 Beam profiles of cut down transducer at 5, 10 and 15cm range and Aerotech transducer at 10cm.

during fabrication being the hand grinding of the wave plate. This resulted in very consistent pulse shapes. The maximum sensitivity varied by up to 5dB but out of any one batch, four were selected within 2dB. This mismatch was allowed for in the scanner by using attenuators in the transducer switching system and therefore the close matching of the original transducers is important to minimise lost sensitivity. Measurement of the transducer beam profiles at a 10cm range indicated a maximum variation in total beam width of 3mm with the resultant beam profile generally lying within that of figure 4.2.

Four transducers were fitted into a perspex housing specially designed to take the 5 way slip ring unit and allow space for the tuning inductors while still having enough mechanical strength to allow machining down to a width of 16mm. The performance of the transducers is unaffected by mounting due to their acoustic isolation and the tufnol insulating layer between the transducer crystal and the wheel housing. Figure 4.3 shows the cut down transducers and the completed transducer wheel with slip rings.

4.3 OIL AND WINDOW ACOUSTICS

A problem identified with the prototype scanners is the significant reverberation echoes which appear in the near field of the image due to a component of the transmission

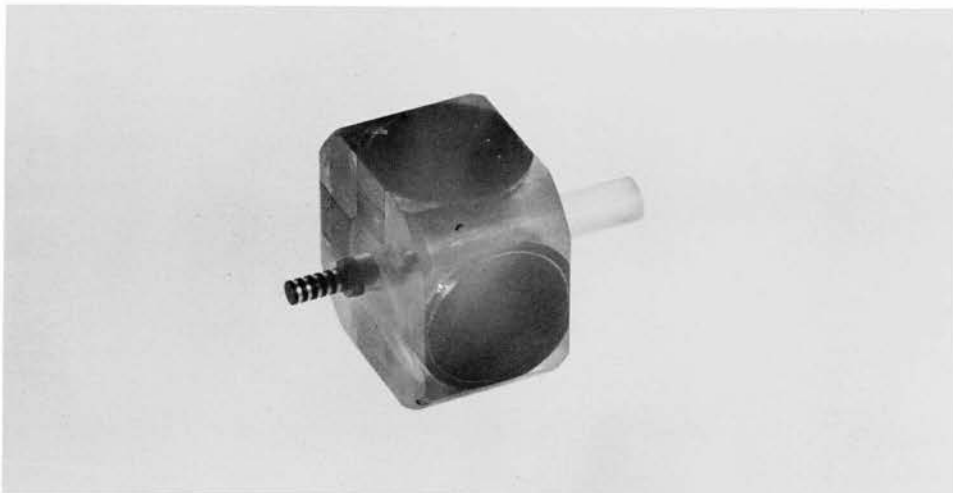
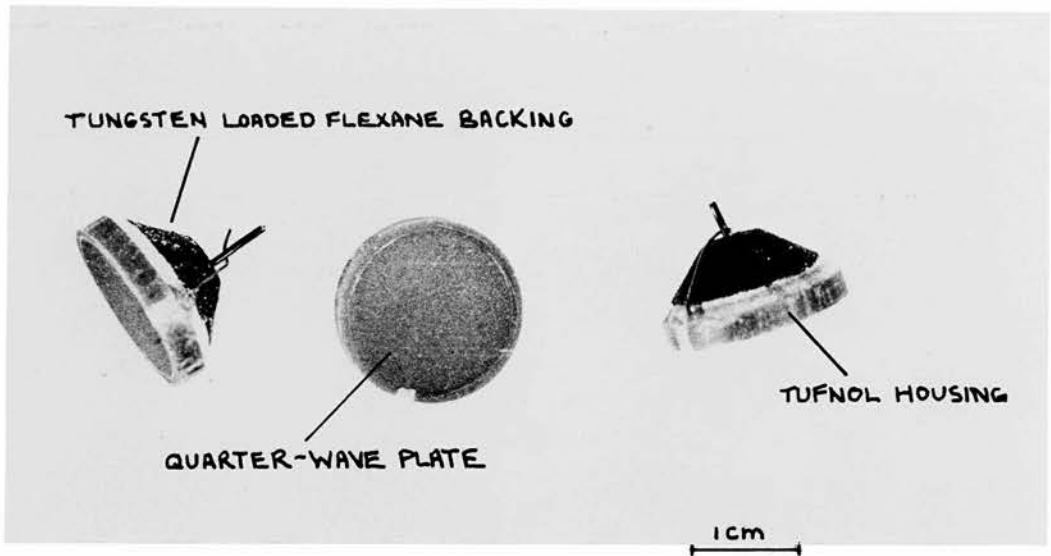


FIGURE 4.3 Cut down transducers and transducer wheel with gold slip rings.

pulse being reflected back into the oil gap between the transducer and the window material. Almost total transmission through the window is required to solve this problem.

The theory of transmission through three media can be used to predict some special cases where 100% or high transmission can be achieved (Kinsler and Frey, 1962). The oils used in the scanner are of a low acoustic impedance and similar to tissue and by necessity the window being rigid, has a larger but moderate acoustic impedance. In this situation if the window is very thin transmission can be independent of the window material depending only on the acoustic impedances of the other two media, which when similar, results in high transmission. However for this to apply, $Z \sin kl \ll 1$ must be satisfied for the highest frequency to be transmitted where Z is the acoustic impedance of the window material of thickness l and $k = 2\pi/\lambda$, the wavelength constant. There are no commonly available materials which could be made thin enough and maintain the required mechanical strength. The above transmission conditions also apply for a window of half a wavelength thickness but in this case the degree of transmission is dependent on frequency and is only totally applicable for the centre frequency of the pulse. The

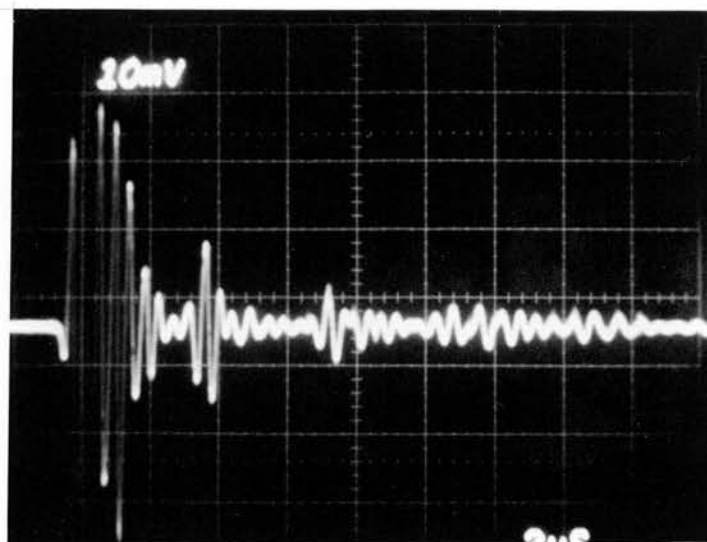
only other special case is when the window is quarter wavelength thick. This also results in frequency dependent transmission and the impedance of the window material would have to be the geometric mean of the other two impedances which is not possible using practical window materials. In any case these are special cases of the transmission formula which is derived from theoretical considerations at normal incidence. This is not the case in the scanner due to the curved window and therefore the theoretical situation is complex.

The window thickness of a tubular prototype was progressively reduced from 0.75 to 0.3mm which was the minimum practical thickness. This resulted in a steady decrease in the reverberation level with no evidence of an increase in transmission at the half wavelength of just over 0.5mm for perspex (polymethyl methacrylate) at 2.5 MHz. A test rig was built with a cut down transducer and a 0.3mm perspex window to make measurements of the changes in reverberation level due to the use of different oils. Originally the prototype oil had been selected from samples of refined mineral oils obtained from an oil company. An oil was chosen which had a low and relatively stable viscosity with temperature increase. This minimised the variation in required driving torque with temperature.

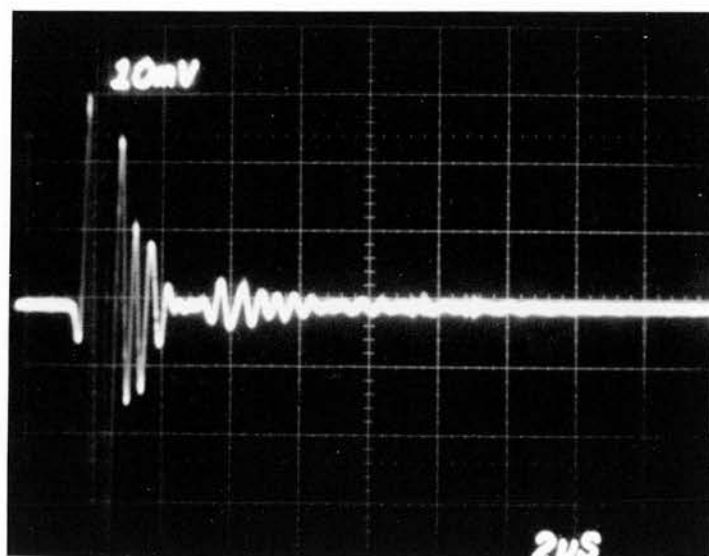
The velocity of sound in the oil was also similar to that of tissue to avoid beam divergence since oils can have velocities greater than tissue.

In looking at the properties of various samples it was apparent that since the density and the velocity of sound of most suitable oils is very similar then so are their characteristic impedances, at about $1.5 \times 10^6 \text{ Kg/m}^2 \text{ s}$, and therefore the degree of reverberation cannot be reduced by better matching. However since every reverberation has to traverse the oil layer in both directions then multiple reverberations could be significantly reduced by using an absorptive oil.

A less refined mineral oil with long chain hydrocarbons with suitable physical properties and an unusually high attenuation coefficient 3 to 5 times that of the other medium refined oils was used in the test rig. Its measured attenuation coefficient at 2.5MHz pulsed sound is 7.9 dB/cm. The reverberation levels after the transmission pulse and the resultant reverberation echoes after a received echo from the aluminium block were recorded as before. Figure 4.4 shows the reflected pulse for both the typical medium refined and the attenuative oil. The amplitudes have been normalised by increasing the transmitter output by 5dB in the case of the attenuative oil. The reduction in multiple



Typical oil



Attenuative oil

FIGURE 4.4 Reverberation comparison

reverberations is clearly illustrated and since the original reflected pulse amplitude is 140 mV in both cases then the first reverberation is 25-30 dB below for the attenuative oil. The third reverberation is still above this level for the typical oil. The reduction in the near field reverberation is best assessed using the scanner in a practical situation with swept gain since the swept gain in the near field increases the reverberation level due to no swept gain delay being used in heart imaging. The depth of reverberation in the near field was reduced from about 4 to 2cm for typical settings of swept gain. These changes to window thickness and oil improved the near field reverberation problem but did not cure it. However the problem was no longer significantly affecting performance when imaging adult hearts.

Since thin membranes are used successfully in many applications of ultrasound transmission the problem could be solved by using a suitable material with a high velocity of sound to maximise the wavelength for a given frequency and so allow a practical thickness of window to satisfy the special case mentioned earlier where the transmission is independent of frequency and the window material impedance. Possibly the use of injection moulding techniques using modern plastics could produce

a suitable window.

Finally a consequence of this oil in the transducer to window gap is a beam divergence in the scanning plane direction, the perpendicular direction being unaltered. The overall effect is a 10% increase in beam width. This was first thought to be due to the velocity of sound in the attenuative oil being 1570 m/s. However since the beam width increase is not uniform it could be a combination of pulse shape variation, due to dispersive absorption in the oil, and divergence. The amount of absorption varies over the transducer face.

Frequency spectrum analysis of the reflected pulses using a transducer alone and then in the test rig with oil, confirmed the presence of dispersive absorption and the resultant frequency spectra are illustrated in figure 4.5. The -10dB bandwidth is unaltered but the frequency of the peak amplitude of the spectrum is reduced.

It was originally intended to include weak focussing in the transducer head. The velocity of sound in a silicone rubber (Dow Corning RTV silicone rubber) was found to be $917 \text{ m/s} \pm 10\%$ and so convex lenses can be moulded onto the transducer to produce focussing. A 3cm radius of curvature lens produced a sharp focus from 3 to 5cm range producing a beam width of under 0.5cm at the -20dB level.

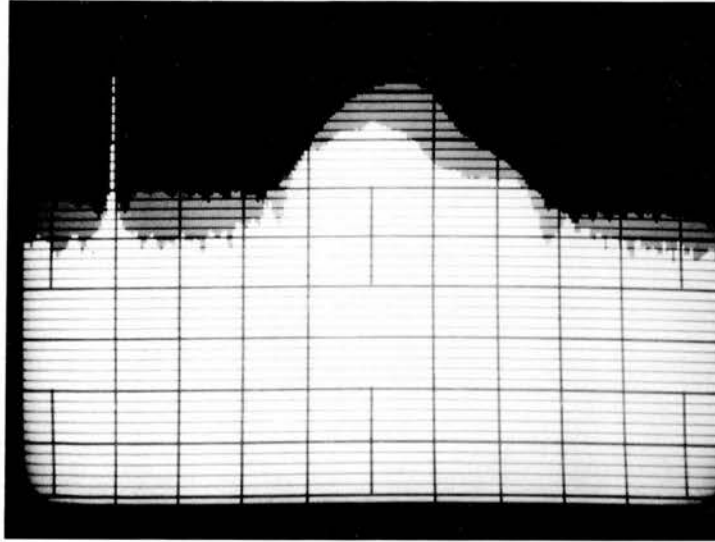


FIGURE 4.5 Frequency spectra of reflected pulses illustrating the change in the frequency spectrum due to the attenuative oil. The horizontal graticule intervals are 0.5 MHz and the centre of the screen is 2 MHz with the vertical intervals being 10dB. The darker spectrum is that of the transducer alone.

Very thin layers would have to be used for weak focussing. The application of such layers to an isolated transducer was possible but due to the complications which would be caused in the construction of the transducer wheel and head, lenses were not fitted.

C H A P T E R 5

S Y S T E M D E S I G N

5.1 INTRODUCTION

The mechanical real-time scanner requires both ultrasonic and electronic drive. The received ultrasonic information has to be suitably processed to be displayed in the form of a real-time grey tone image. The image format has to be generated in synchronisation with the scanner to register the image on a display which can be observed by the scanner operator and also can be photographed using a 16mm cine camera to produce permanent real-time and still frame recordings. The image format generation has to be flexible to allow the display of double images for various twin scanner applications. The real-time system is shown schematically in figure 5.1

5.2 SYSTEM OPERATION

Figure 5.2 shows a block diagram of the real-time system which is explained in this section.

5.2.1 SCANNER DRIVE AND IMAGE FORMAT GENERATION

The basic timing signal that both the scanner and the image sector generation are synchronised to is supplied from an oscillator or from the camera when filming. Both supply twenty pulses per second. The scanner produces four pulses every revolution of the transducer wheel at

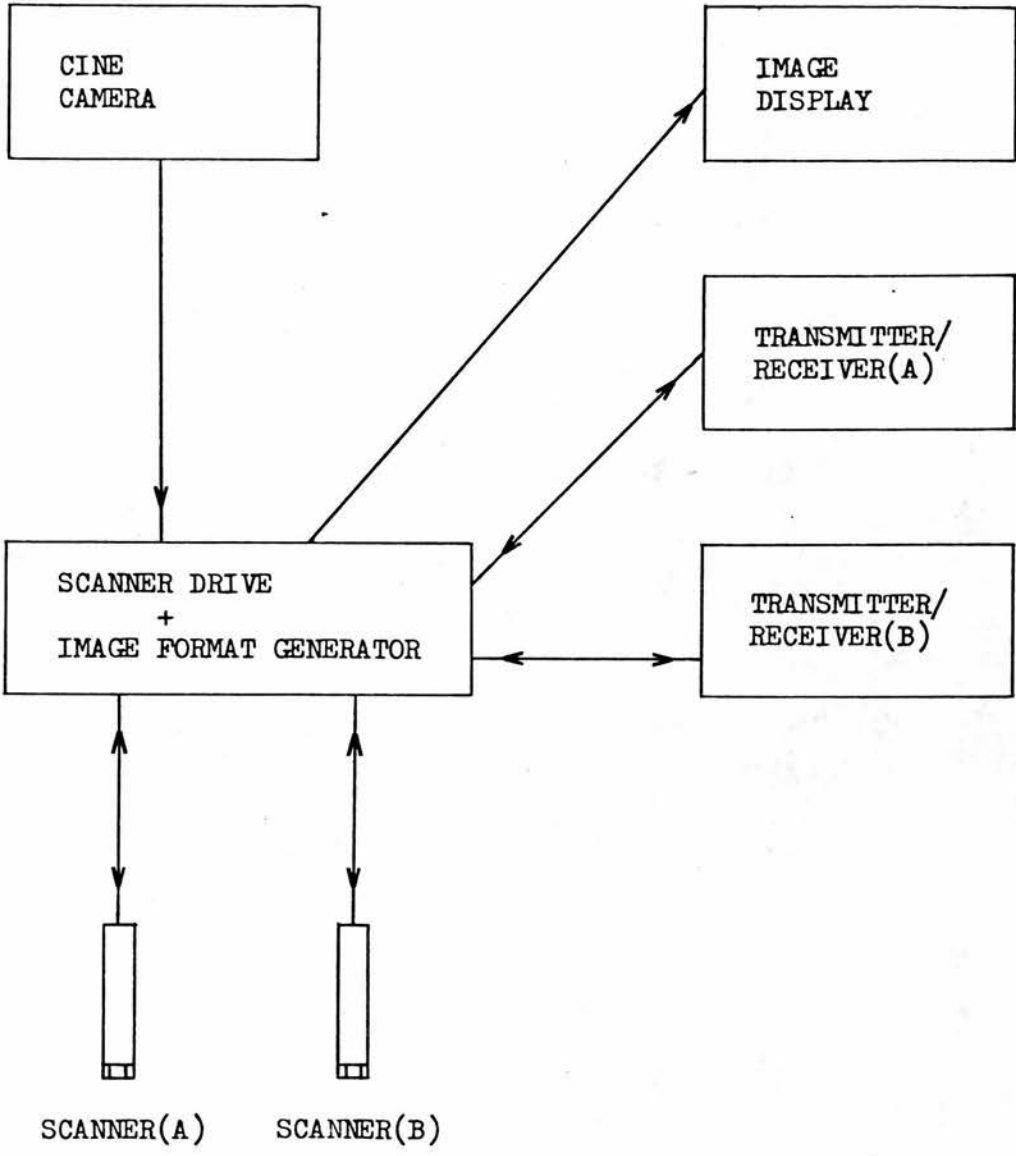


FIGURE 5.1 Real-time system.

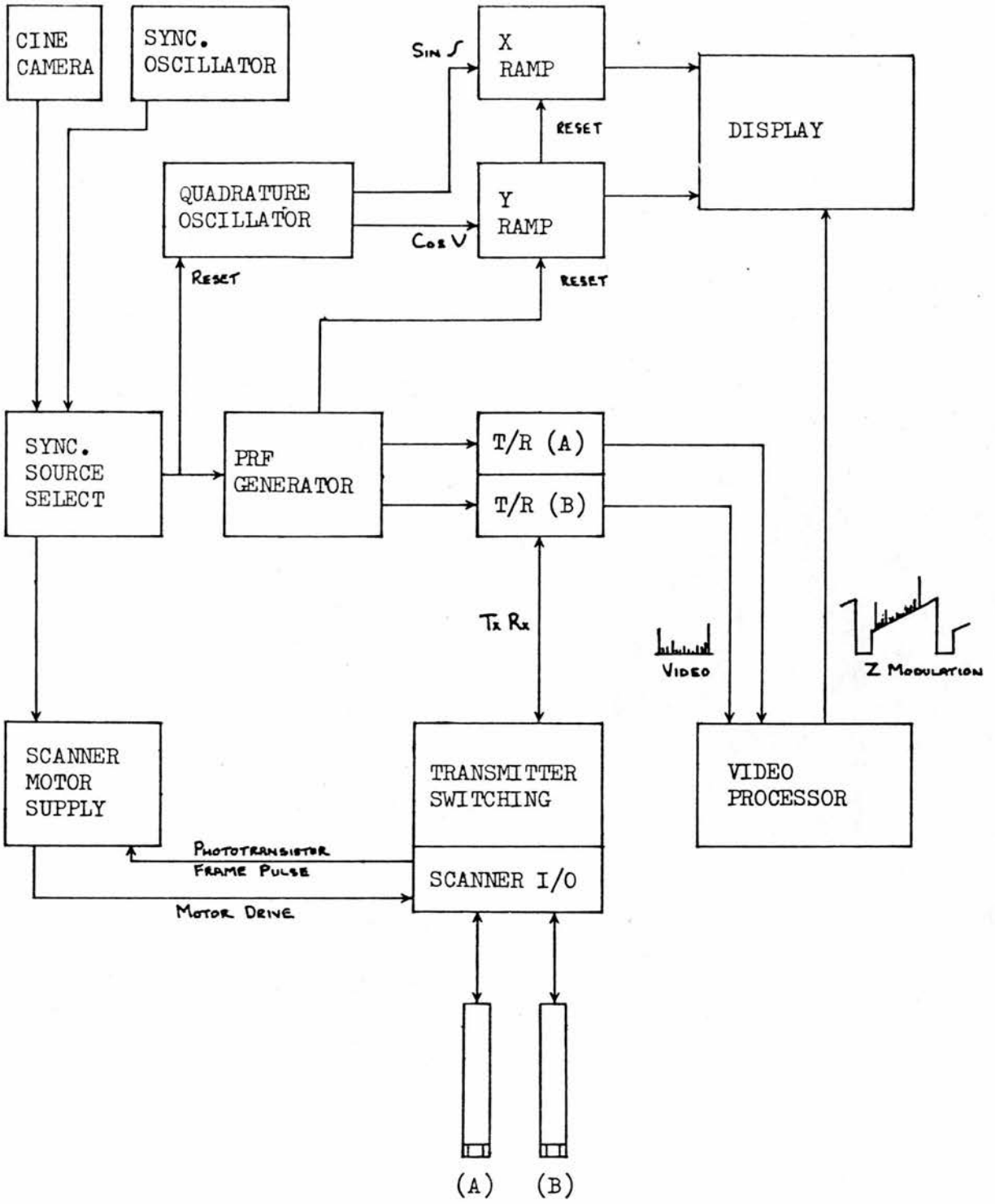


FIGURE 5.2 Block diagram of real-time system.

the start of each 90° sector from the timing disc and one of the photo-transistors. These two signals are used by the scanner motor supply which consists of a phase detector, the output of which is integrated and added to a DC level which is used to drive the scanner. To lock the signals in phase requires the output of the phase sensitive detector to be amplified and added to the above driving signal resulting in small voltage impulses superimposed on the slowly varying driving voltage.

Once synchronised the scanner produces twenty frame pulses per second and from another photo-transistor a pulse once every four frames for transducer identification. This enables the transmission switching circuit to synchronise its switching sequence to excite the transducers in turn and only when they pass through the sector which is directed out of the front of the scanner. This switching is done using reed relay switches. The PRF generator outputs a transmitter trigger pulse to the A scan transmitter/receiver unit (NE 4121) and therefore determines the transmission PRF which is 3000 Hz. It also interrupts transmission during relay switching using the frame pulse from the synchronisation source. The PRF generator also produces a signal which divides the PRF interval into a live and dead time. During the live time the integrators

in the X and Y ramp generators and the video processor are active, resulting in a line of ultrasonic echo information being written on the screen. During the dead time the display is blanked and the X and Y integrators are reset along with the video processing integrators and the A scan receiver swept gain.

Registration of the lines of echo information on the display to correspond with the ultrasound beam direction is done using the sine and cosine outputs from a quadrature oscillator. The outputs from the scanner resolver were not used as originally planned and this is discussed later. The angular frequency of the oscillator outputs are preset so that they correspond to the transducer wheel angular velocity when the scanner is synchronised with the synchronisation source. The quadrature oscillator integrators are reset at the start of every new frame to preset values corresponding to the sine and cosine of the angular position of the beam at the start of a sector sweep. The resultant outputs are proportional to the sine and cosine of the angular position of the transducer through the sector and are used to set the rate of integration in the X and Y ramp generators. They produce sets of ramps at PRF intervals whose amplitudes are modulated by the sine and cosine outputs. Since the PRF

is 3000 Hz and the frame rate is 20 per second then this results in each sector image being composed of 150 individual lines.

The sector is generated from a point corresponding to the centre of rotation of the transducer wheel. To allow for the transducer face being 12mm from the centre of rotation the PRF generator transmitter trigger output to the A scan has a time delay equivalent to 12mm depth in the image. The live time is such that 16cm tissue depth is displayed in the sector image.

The video processor modifies the video signal from the A scan to make it suitable for Z modulation of the display and to output the video and blanking signals to the display at a time synchronised with the X and Y ramp generators. To facilitate video signal blanking during flyback and the transfer of the video signal to the display over the correct range and at the appropriate level, the video signal is added to an adjustable DC level in the form of a pedestal, the video signal amplitude being adjustable. The pedestal starts simultaneously with the transmitter trigger and ends at the start of the dead time in the PRF interval.

Another modification to the video signal is necessary due to the merging of the lines in the near field of the image

causing an increase in screen intensity for a constant video input signal. This is a complex effect which will be discussed later in connection with cine photography. However the corrective processing consists of an adjustable linear ramp which is added to the pedestal. By adjusting the amplitude of the pedestal, the video signal and the slope of the ramp, a more even image can be obtained over the full intensity range of the screen.

Finally there are two system operating modes when using two scanners simultaneously. The two scanners are synchronised to the system synchronisation source and the transmission switching is simply duplicated as is the A scan unit. When the scanners are clamped together and in the same scanning plane then it is relatively easy to register the two sectors on the display since the scanner centres of rotation are a known distance apart. The second format, when the sector images are independent on the display, can be used when the scanners are not locked together allowing any two planes to be visualised simultaneously. In both cases the PRF generator triggers the two A scan units alternately and the resultant alternate video signals are input to the video processor which operates as before but producing a sequence of alternate video signals on identical pedestals and ramps.

The registration of this video on the appropriate sector is done by adding an alternate DC shift to the X ramp generator in the case of the clamped scanners and to the X and Y ramp generators in the case of the independent mode where the sector images are diagonally positioned on the screen to maximise the sector size. Examples of these image formats are illustrated in Chapter 6.

5.2.2 DISPLAY UNIT

The display unit (Lan 420) is a large screen oscilloscope (38 x 29cm) with a P4 phosphor giving a white light output suitable for photography and for displaying grey scale images to the direct observer. The small signal 3dB bandwidth in the X and Y plane are DC to 15 and 45 KHz respectively and the response to a step input over the X and Y shifts involved in sector flyback are limited by the X response of approximately 100 μ S. The Z modulation 3dB frequency response is DC to 4.5 MHz over the full dynamic range of the screen and is therefore adequate. The screen has a medium-short persistence of 60 μ S which is the time for the intensity to fall to 10% of original and is suitable for real-time imaging. The beam spot size relative to the screen size is as good as some expensive high definition small deflection displays and there is no distortion over the majority of the screen for the

writing speeds encountered in sector format image production. The display and the rest of the real-time heart system is shown in figure 5.3.

5.2.3 CINE CAMERA

The 16mm cine camera used (Bolex H 16 EBM Electric) has an open shutter angle of 170° which allows 85° of the 90° sector to be recorded. Standard frame rates are 10, 18, 24, 25 and 50 f.p.s. The camera is driven from its own rechargeable 12V power pack and produces synchronisation pulses for the scanner drive system via a slotted disc and electro-optical device mounted to a 1:1 take off from the shutter. During every second image frame the shutter is closed when the cine film is being transported, known as the pull down time. This results in every second image frame being recorded. Cine cameras with fast pull down times of about 1ms are available but are very expensive and specialised and often use 35mm film. Suitable 8mm cine cameras are available but the choice of professional film developed for phosphor screen photography is limited. Also the availability of a conventional overhead screen viewer routinely used for replaying 16mm cineangiograms supports the 16mm choice. The 16mm film used (Agfa-Gevaert Scopix RPl) is a low contrast film specially developed for cine-radiography and therefore image intensifier

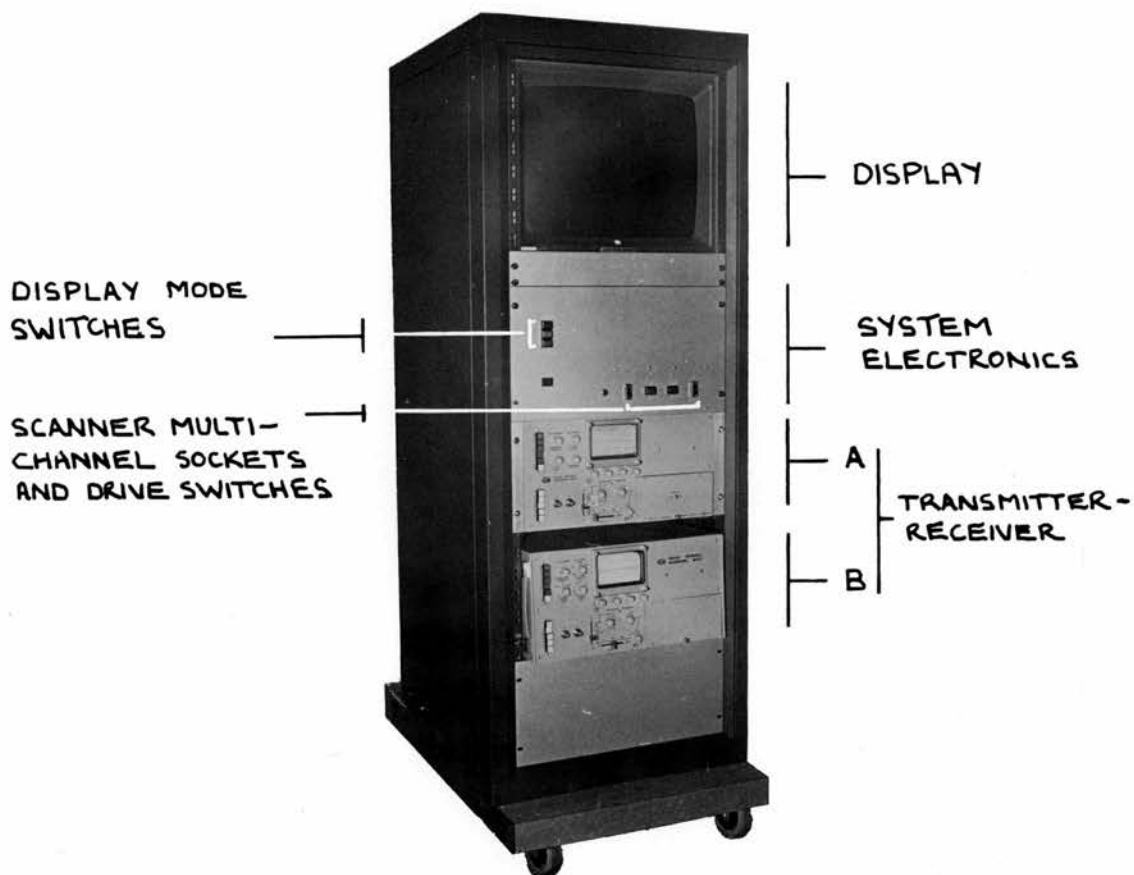


FIGURE 5.3 Real-time heart system.

screen phosphors. The emulsion is panchromatic and suitable for rapid machine processing which is routinely used in radiology departments.

5.3 SYSTEM PERFORMANCE

5.3.1 GREY SCALE IMAGE

The dynamic range of the A scan receiver is $40\pm$ 1dB and to optimise the dynamic range of the observed image requires the useful range of received echo signals to be set in amplitude and DC level such that they use the full dynamic range of the display. Ideally the large display should be used for observation and a separate P11 blue phosphor should be used for photographic recording since it has the highest photographic efficiency of all the medium-short persistence phosphors. This combined with gamma correction would result in maximising the photographic dynamic range. However an adequate compromise between observed image and photographic record was obtained using the large P4 phosphor display.

To set the system up a grey bar generator was constructed which consists of a 2.5 MHz oscillator and a step function generator. The step generator is triggered by the frame start pulse and has a time constant such that eight steps of equal duration are produced during one frame time interval. The step amplitudes are evenly spaced and

modulate the 2.5 MHz signal which is then transferred via an attenuator to the receiver of the A scan such that the eighth level is almost saturated. The result is a set of small sectors of increasing video amplitude through the 90° sector.

The input/output signal transfer characteristic of the A scan receiver amplifier is sigmoid in shape. However this sigmoid response is asymmetrical with the low amplitude tail only compressing signals in the first few decibels of the 40dB range while the large signal compression affects the top 20dB of range. The range from -30dB to saturation has a logarithmic characteristic. The pedestal height and the video amplifier were set in the video processor such that this range of the A scan receiver corresponded to the just visible to saturation level of the display. When scanning the heart the smallest significant echoes can then be made just visible by adjusting the transmitter output. The video input to the display therefore is logarithmically compressed which is desirable.

The ramp rate in the video processor is set to produce the most visually even intensity distribution over any one grey shade. The distance from the sector apex at which lines merge varies with intensity since the line width

is intensity dependent. As a result a compromise has to be set where the most intense shade merges in the near field and the least intense fades in the far field.

The final adjustments are made such that the photographic result is optimal for the grey scale and then for heart images over the required dynamic range to include all significant structures. Due to the sigmoid characteristic of the phosphor-film combination the film density produced by some small endocardium echoes is not high enough. However the further increase in large amplitude compression does not create a problem. To take the small endocardium echoes out of the influence of the low amplitude tail of this characteristic the video signal is compressed and the overall DC level increased. The result is an improved film result with a reduced dynamic range image on the display.

Without gamma compensation and a separate P11 recording scope and complete A scan logarithmic response an optimal photographic result cannot be obtained. The compromise achieved here allows at least eight grey tones to be recorded on film and to be appreciated by direct observation, the latter only being possible due to the latitude of human vision and perception (Stockham, 1972).

Figure 5.4A illustrates a single frame reproduction of

the grey scale image of the longitudinal scan of the heart. This is a frame taken from the series of successive frames shown in figure 5.4B.

5.3.2 TEST PHANTOM

To measure the image distortion and registration of both the single and double scanner a test phantom was constructed with two parallel side plates and nylon filaments threaded perpendicularly between the side plates. The scanner is located at the top centre of the phantom with the scanning plane parallel to the perspex sides. The nylon filaments are at radii of 5, 10 and 15cm from the transducer faces and at known angles from the centre line of the scanning sector.

A feature built into the scanning system which has not been mentioned so far is a reference grid of markers which can be superimposed on the image to indicate relative movements within the image or to give easy calibration. This is done by adding a series of pulses to the video signal which are triggered by the transmitter trigger and repeated along a line of image information at time intervals equivalent to 2cm tissue depth. Such marked lines are repeated at regular intervals through the sector image. The time-base of the video is set for an assumed velocity of sound in tissue of 1560 m/s since

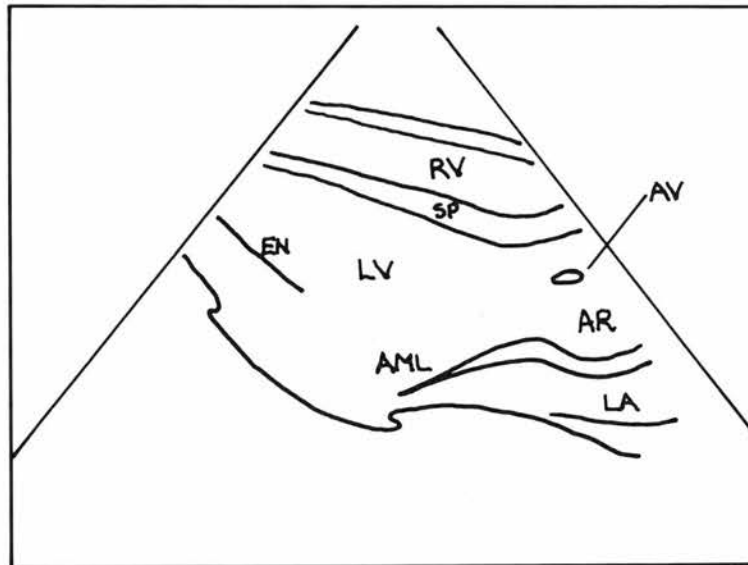
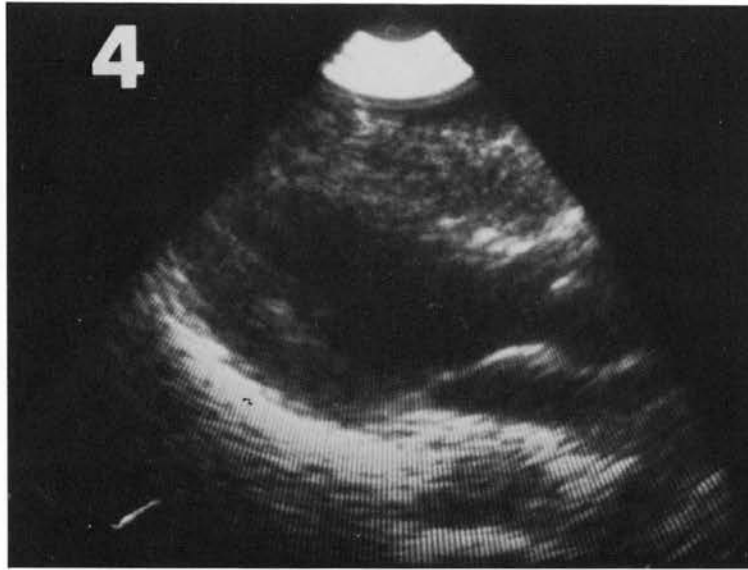


FIGURE 5.4A Grey scale image of the longitudinal section of the heart corresponding to frame four of Fig. 5.4B showing left ventricle (LV), right ventricle (RV), left atrium (LA), aortic root (AR), aortic valve (AV), anterior mitral leaflet (AML), septum (SP) and endocardium (EN).

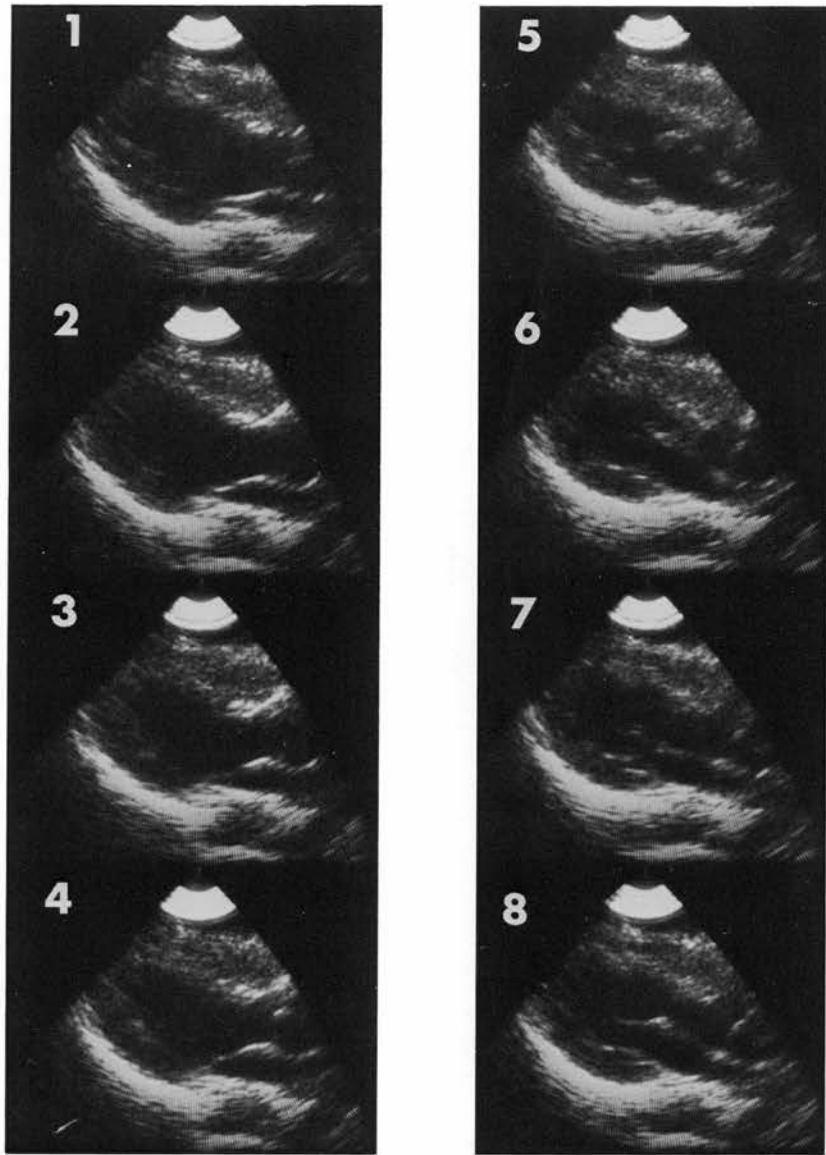
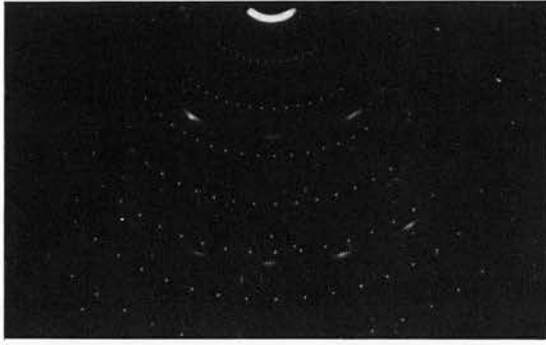


FIGURE 5.4B Series of eight successive 16mm cine frames at 1/10th second intervals showing the action of the longitudinal section of the heart through systole.

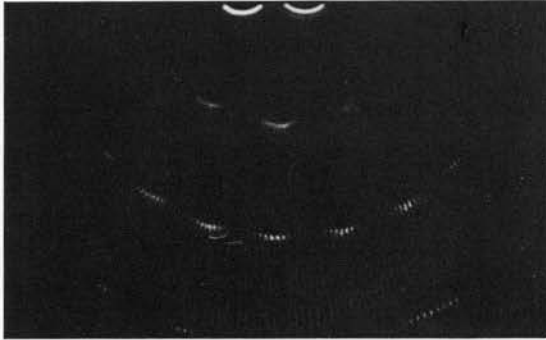
this is the value for blood.

A scanner placed at the top centre of the phantom and immersed in water at room temperature produces an image of the nylon filaments as shown in figure 5.5A. This shows that the echoes from the filament radii run parallel to the marker radii and that the echoes from the two outer filaments at the 10cm range are at the edge of the sector as they should be since they are both 45° from the centre line. The echo pattern moves relative to the marker grid by less than 2 lines or just over 1 degree. This is due to small variations between the preset quadrature oscillator angular velocity and that of the transducer wheel due mainly to belt stiffness variations. The noncoincidence of the 10cm filaments and markers is due to the velocity of sound in water at room temperature causing a 5% error in calibration. This does not affect the tests being performed.

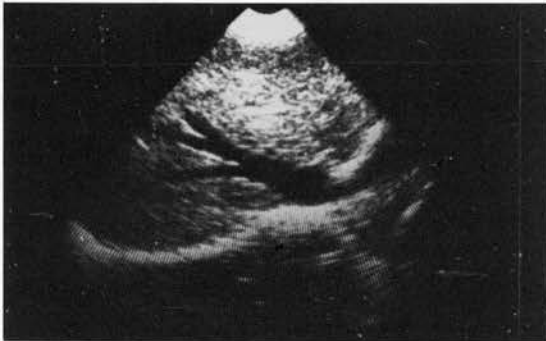
Having checked the alignment of two scanners the phantom can be used to set up and check the registration of the twin scanner mode when they are clamped together. For the purposes of setting up the display X shift voltage the system time-base has to be adjusted to match the velocity for the water in the phantom. Figure 5.5B shows the pattern resulting from the central placement



A. Test phantom and marker grid



B. Test phantom - twin scanners



C. Liver scan showing intrahepatic vessels



D. Right kidney



FIGURE 5.5 Scanner registration, distortion, resolution and grey scale results.

of the twin scanners over the phantom. The registration variations again are within 1 degree per scanner and therefore within 2 degrees maximum.

The phantom was also originally designed to give some measure of scanner resolution by the inclusion of groups of filaments spaced at 1,2,3,4 and 5 mm intervals. The variation in echo amplitude due to slight changes in filament alignment and the artificially low transmission level and swept gain settings can lead to misleading results. Using this technique two filaments could be resolved when separated by 2 and 3mm at 5 and 10cm range respectively. The divergence of the lines in the sector image contributes to a degradation in lateral resolution with depth. However the line separation is only about 1mm at 10cm range and since there are usually relative movements of at least 1mm in real-time images between frames whether scanning through static structures, due to physiological movement, or scanning dynamic structures, the resolution is not reduced as much as expected due to visual integration. It is in this sense that resolution in real-time scanning differs from static B-scanning.

Garrett and Kossoff (1975) have suggested a realistic resolution test using the fetus as a test target and measuring the minimum detectable rib or vertebra spacing.

The real-time scanner has been used to visualise fetuses at an early stage of development and in the mid range of the sector image resolution is between 2 and 3mm laterally. However axial resolution is better allowing small moving heart structures to be visualised. This is a good example of the situation where the presentation of a reproduced static single frame taken from the real-time recording does not allow the same discrimination between small moving intracardiac structures and similar static echoes. Images of the liver and kidney enabled the resolution to be assessed in the far field. Both lateral and axial resolution is reduced to 3 to 4mm and 2 to 3 mm respectively. Small ducts can be resolved and figure 5.5C illustrates some bifurcations in the intrahepatic vessels and figure 5.5D shows the right kidney outline and collecting system. Allowing for the fact that these illustrations are reproductions of bromide prints made from single 16mm cine frames, the grey tone range can be appreciated.

5.3.3 LIMITATIONS AND IMPROVEMENTS

The use of a quadrature oscillator to produce the image format means that there is no angular position information output when the transducer head is stationary. As a result the facility of stopping the transducer wheel at a known angular position cannot be utilised to obtain

T-M recordings of high PRF at selected directions in the image. This is a facility which if combined in the one point of entry device would be very useful in the examination and diagnosis of valve disease.

The resolver originally used in the scanner had to be driven with a carrier frequency large enough to allow distortion free filtering of the desired sinusoidal waveforms from the demodulator. For this frequency of carrier the load impedance varies across the stator with changing rotor angle. The resultant demodulated sine and cosine outputs are distorted. This small distortion would be acceptable if only one quadrant of the outputs is used as with the quadrature oscillator. However since the resolver produces continuous outputs which cannot be reset the four quadrants of the sine and cosine waveforms have to be alternately switched between X and Y deflection and in three of the quadrants one or both of the waveforms has to be inverted. The net effort is to produce the same repeat quadrant but with random distortion which repeats every four frames. The relative movement of echo information on the screen causes a loss of both axial and lateral resolution greater than the lateral loss due to the use of the quadrature oscillator.

With the development of modern plastic resistive materials

low noise sine/cosine potentiometers are now available with suitable performance characteristics to allow them to be driven constantly at 5 cycles per second for long periods. This provides a sine and cosine output directly in both dynamic and static operations.

A direct influence on picture quality and resolution is the number of lines in the sector image. The PRF is 3000 and is limited by the display X step response during flyback. Increasing the rate introduces distortion in the near field of the sector. Assuming the system reset times and scope response are fast enough then the limiting factor on PRF is the appearance of reverberations in the image. This will vary depending on the size of heart being examined and examination of an average sized normal heart allowed a rate of 4000 to be used without introducing reverberation noise. Rates up to 5000 over a 15cm range have been reported by Eggleton (1974) but no comment is made regarding reverberation. The ideal would be a variable rate so that the line density can be maximised for the scanning situation. The presence of reverberations locally may not be detrimental to specific diagnosis.

Genuine interlacing could be achieved by introducing half a PRF time interval delay to the transmitter and the X and Y ramp generators during alternate frames while

leaving the quadrature oscillator frame reset unaltered.

The introduction of a variable swept gain function generator into one of the prototype systems proved to be of no advantage since invariably the best overall image is obtained with a smooth function which can be produced with a conventional swept gain. A variable swept gain along a particular line of echo information such as T-M can be advantageous but different parts of the sector image require different functions. Ultimately an automatic swept gain control would solve this problem.

Finally the inclusion of separate variable delays between the system synchronisation and the scanners drive and display system would enable the direction of the sector in both scanners to be varied relative to the scanner body. When used in the twin clamped mode this would allow variable sector overlap and hence the advantages of compounding to be optimised over a chosen area.

5.4 ALTERNATIVE RECORDING METHODS

An alternative method of recording the real-time image from the display is to use a TV camera and video tape recorder. This allows simultaneous recording and display via a TV monitor and therefore a small high definition display can be used with the TV camera. The available systems would require the scanner to run at 25 f.p.s. to synchronise with

the full line density video frame rate. This is a convenient recording method with instant playback and a reuseable recording medium. However the still frame replay often introduces distortion and consists of only one raster scan resulting in half the line density of the real-time frame. A hard copy of a single frame produced by photographing this image is therefore of significantly reduced quality.

Cine film provides good still frame recordings although at half the original frame rate. Sequences of still frames can be examined repeatedly and conveniently and unless the cine frame rate is exactly synchronised with the heart rate then the recording of many cycles of any one view should render still frames at any desired part of the heart cycle.

The recent introduction of real-time scan converters provides a versatile display, recording and replay system which could be interfaced with this type of scanning system. Although more expensive, it overcomes most of the above disadvantages. The contrast and brilliance of the recorded images can be adjusted during playback and the data is stored in a way suitable for interfacing to a computer for on line image processing or subsequent image quantification and analysis.

C H A P T E R 6

T W I N S C A N N E R A P P L I C A T I O N S

6.1 INTRODUCTION

The most recent literature regarding echocardiography still contains a great deal on T-M echocardiography. The sensitivity and specificity of diagnostic criteria have been thoroughly investigated and some of the limitations of the techniques have been reported (Kotler et al., 1977). Many quantifiable indices of heart function are now well established for valve action and left ventricular function (Feigenbaum, 1976; Chang, 1976). Left ventricular internal dimensions have been used to calculate ventricular volume and correlate well with cineangiographic techniques. These dimensions have therefore been used to calculate ejection fraction and stroke volume as well as velocity of circumferential fibre shortening and ventricular mass, all of which have been used as indices of ventricular performance. These correlations only apply when the left ventricle contracts coherently which is generally not true during ventricular malfunction. The high time resolution of T-M echocardiography allows convenient computer analysis of digitised echograms. This time resolution is essential in the study of left ventricle and posterior wall dimensional rates of change and in the

construction of pressure and apexcardiogram - dimension loops. This work has been described recently in the context of left ventricular function mechanisms (Upton and Gibson, 1978).

Real-time visualisation reports have not yet concentrated on quantification mainly due to the initial interest in technique and general visualisation performance. More recently reports have described the application of real-time techniques applied to the diagnosis of specific clinical conditions. For example, in the diagnosis of complex congenital heart disease (Sahn et al., 1977; Henry et al., 1977), atrial septal defect (Lieppe et al., 1977) and in the study of abnormal septal motion due to mitral stenosis (Weyman et al., 1977) or right ventricular overload (Weyman et al., 1976) and left ventricular asynergy (Kisslo et al., 1977). In these and other studies successful diagnosis has been possible through structure identification and visualisation of structure movement. Two-dimensional pattern recognition and deductive reasoning allow accurate qualitative assessments to be made. There are aspects of two-dimensional images which could yield useful quantitative information such as the area and degree of curvature of the valve leaflet in stenosed valves or the area and shape index of the

ventricle in ventricular function assessment.

However real-time echocardiography is primarily a visualisation technique even although it can reveal some unique quantitative information. It is the spatial resolution of real-time echocardiography and the time resolution of T-M echocardiography which make the two techniques complementary. Statements have appeared in the literature which clearly point to the misunderstanding of the different and complementary nature of the techniques.

In the real-time applications referred to above the parasternal approach is used with both linear and phased arrays. In every case visualisation information from the subxiphoid would be useful and could be achieved using a phased array. However no reports of this application in adult echocardiography have been made. A similar approach has been reported where a phased array is applied to the chest at the apex of the heart (Schiller and Silverman, 1977). The visualisation possibilities revealed through initial scanning experience on normals using the rotating head scanner prompted the routine application of this approach during clinical evaluation of the scanner and this is described in the next chapter. The potential expansion of real-time heart visualisation and the visualisation benefits gained through the use of

twin scanners was investigated on normal subjects. Two distinct applications were examined. Firstly the use of two scanners locked in contact such that their scanning planes are coplanar and their sector images are related and overlap. Figure 6.1 shows the scanners applied on the chest at adjacent intercostal spaces and scanning along the longitudinal axis of the heart. The second application is with the scanners unrelated either coplanar or in completely independent scanning planes. In this case the sector images are both displayed separately on the display screen. Figure 6.1 also shows the scanners unrelated but clamped such that they are both scanning the left ventricle longitudinally from the parasternal and subxiphoid locations.

This work is described at this stage since it will help to familiarise the reader with the standard sections visualised on normal subjects before describing more specific views related to clinical conditions in the next chapter. There are four standard scanning planes used to describe the application of twin scanners in related and unrelated scanning planes. From the parasternal location the longitudinal axis of the heart generally points towards the right shoulder and from the same location the transverse or short axis of the heart lies

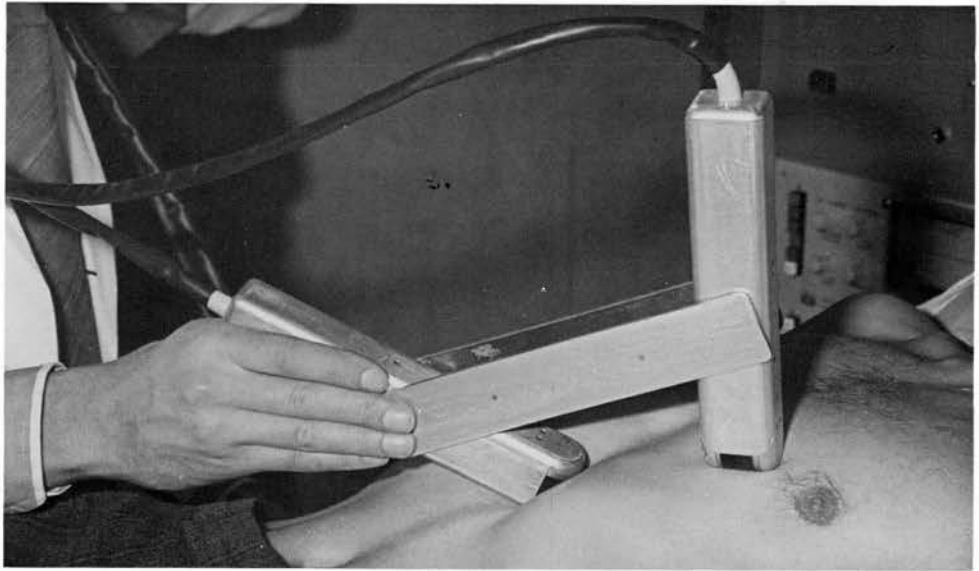
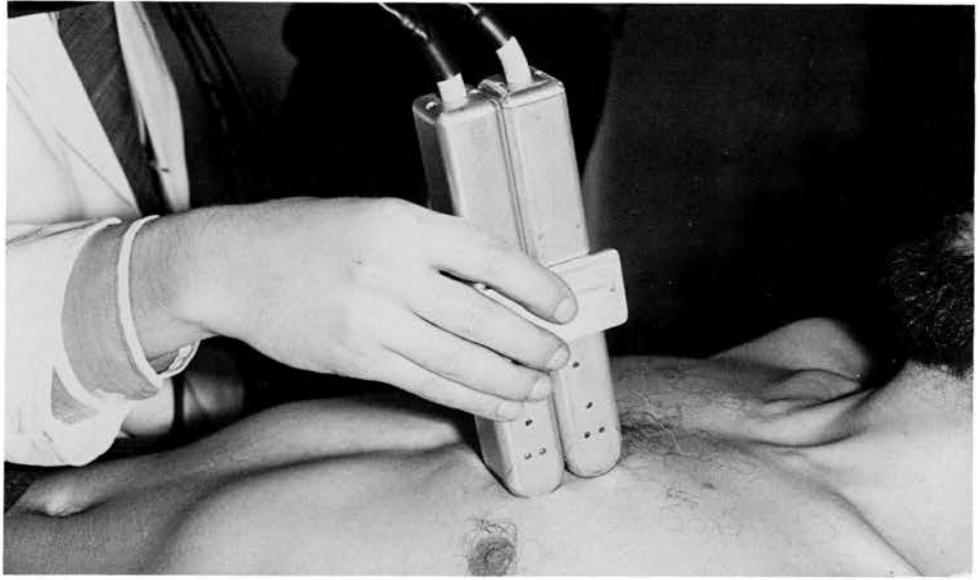


FIGURE 6.1 Twin scanners applied at adjacent intercostal spaces and unrelated at the parasternal and subxiphoid locations.

perpendicular to this direction. These two scanning planes yield longitudinal and transverse sections of the heart. A longitudinal four chamber section of the heart is obtained from the subxiphoid approach scanning in a plane mutually perpendicular to the above planes. This is approximately parallel to the coronal plane of the body. The fourth standard plane direction is a transverse section of the heart from the subxiphoid location which is parallel to the parasternal transverse plane and is often referred to as the sagittal subxiphoid approach. Hence the standard four scanning planes all lie in one of three mutually orthogonal reference planes, namely the longitudinal, transverse and coronal planes.

Images are presented where possible to comply with the American Institute of Ultrasound in Medicine interim standards for the presentation of echocardiographic images (AIUM, 1976) where the longitudinal and transverse images are presented as if viewed from the left side and the subject's feet respectively. The time increases from left to right in the image. The subxiphoid coronal or longitudinal views are presented as if viewed from the front of the subject but are inverted relative to the standard with the inferior structures at the top of the image to standardise sector image format in this scanning

system. If any images are presented differently then reference directions are included in the figure.

6.2 RELATED TWIN SCANNER APPLICATION

When used in this mode the scanning system offers a larger field of view and the introduction of some compounding in the area of sector overlap. The original reason for introducing the increased field of view was to improve parasternal visualisation of the anterior right heart structures and to visualise the complete left ventricle. However the 90° sector successfully visualises the whole left ventricle and even with enlarged hearts, the ventricle appears in the wider part of the sector image. Also the subxiphoid approach is often best for right side visualisation and therefore the increased anterior field of view is not a major advantage. Although subxiphoid visualisation could always be adequately covered with one scanner with normal subjects, clinical experience has shown that the increased field of view could be advantageous in cases where the heart is horizontal and low in the chest or if the heart is enlarged.

The advantages gained through the simple form of compounding can be assessed by rapidly switching image format. While both scanners are running the single sector format image of either scanner or the composite

double sector can be displayed by front panel switches. This allows direct comparisons to be made conveniently. An area most obviously improved is the visualisation of heart valves. Due to the changing angle between the leaflet and the ultrasound beam direction during the heart cycle, there is often a lack of visualisation continuity during the cycle. The continuity of valve visualisation is improved and visualisation from different interspace combinations can contribute to the visualisation of the aortic and mitral valve at different parts of the heart cycle.

The improvements made to septal and endocardial visualisation are less obvious and difficult to assess due to the comparison here being more dependent on image quality rather than the detection of movements within the image in the case of valves. Since the single sector image of either scanner alone has twice the line density of either sector in the compound image then the comparison is not easily made especially since it is the low intensity grey levels which are relevant. The overlap area also suffers from complex interference patterns at areas of line crossing due to writing intensity enhancement on the screen at these points. This is similar to the effect of sector line convergence mentioned in the previous

chapter but here it also varied through the overlap area of the image since the angle of intersection between lines varies. It was found that the most pleasing image in the area of overlap was obtained at a lower transmission level and this also produced the best recordings to try to illustrate the differences. As a result the video levels in the areas beyond the overlap area are not optimally recorded. It is also very difficult to illustrate some of the cycle dependent improvements in valvular visualisation using still frame reproductions. At the end of this section figures 6.2 show compound images and single sector images both taken sequentially at the same location, of a transverse section of the liver showing vessel bifurcation and a longitudinal section of the heart from the parasternal position. A transverse section of the heart is also shown from the parasternal position along with a coronal scan of the heart from the subxiphoid location.

Making allowance for the reduced image quality of the compound images the vessel boundaries in the liver were more readily delineated and the variation of echo amplitude from heart structures through the heart cycle was reduced. This results in better visualisation continuity. The transverse compound section of the heart

at the level of the mitral valve leaflets and the subxiphoid section illustrate the softer compound image containing the same structures as the single sector.

The subxiphoid approach is limited to coronal plane visualisation using twin scanners locked together. Access under the left costal margin is similar to a single scanner but variation of scanner direction parallel to the scanning plane is restricted. Access from the parasternal position was unrestricted both longitudinally and transversely in the case of the normal subjects examined. Transverse access however could be restricted in some patients due to the restricted lateral width of the echocardiographic window by overlying lung. During clinical evaluation of the scanner parasternal access was often good from two or three adjacent intercostal spaces and therefore there should be no restriction in access to the longitudinal plane.

Compensation for the video enhancement effects in the overlap area of the image would be complex and impractical using a conventional display. However a real-time scan converter would enable even grey scale compound images to be displayed just as scan converters solve the problems of overwriting and integration with conventional compound B scanning. If one sector image contains spurious echo

information at the edge of the sector in the overlap area then this overwrites the genuine information from the other scanner. This spurious noise may be due to lung or rib interference or lack of complete acoustic contact. This could easily be allowed for by incorporating a variable duration pedestal in the video processor such that interfering portions of the sector edge can be blanked. A significant reduction in resolution and image quality results while using the scanners simultaneously due to the PRF per sector being halved through alternate scanner transmission. To investigate the degree of interference caused when simultaneous scanner excitation is adopted one scanner was operated in normal single mode and displayed with the second scanner synchronised to it and arranged to transmit only when desired. The influence of the sound from the second scanner received by the first could be assessed and the composite effect on the double sector image predicted by repeating this with the scanner positions reversed. Although interference was present, causing in some cases significant overwriting, this tended to be very localised and dependent on scanner location. Interference from valves is transient and therefore may not deter from the imaging of certain less dynamic structures. The lack of strong interference and its often

localised nature indicates that simultaneous transmission of twin scanners would improve the visualisation of certain parts of the heart. Since its applicability is dependent on heart structure then it would be a useful alternative operating mode. Display of the simultaneous information would require a real-time scan converter with dual input memory and memory processing. This processing would define the upper limit of the combined PRF.

F I G U R E S 6.2

Figures 6.2 show related twin scanner compound images and single sector images from one of the scanners taken at the same location sequentially. The sections visualised are as follows:-

- A. Transverse liver scan of intrahepatic vessels
- B. Parasternal longitudinal heart scan
- C. Parasternal transverse heart scan
- D. Coronal subxiphoid scan of heart

Abbreviations used in the diagrams are listed below.

LV	Left ventricle
LA	Left atrium
RV	Right ventricle
RA	Right atrium
AML	Anterior mitral leaflet
AV	Aortic valve
CH	Chordae
TV	Tricuspid valve
PW	Posterior wall

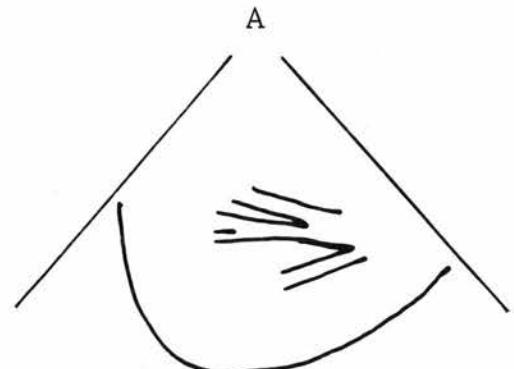
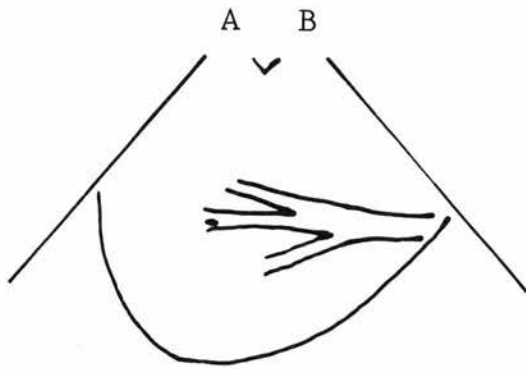
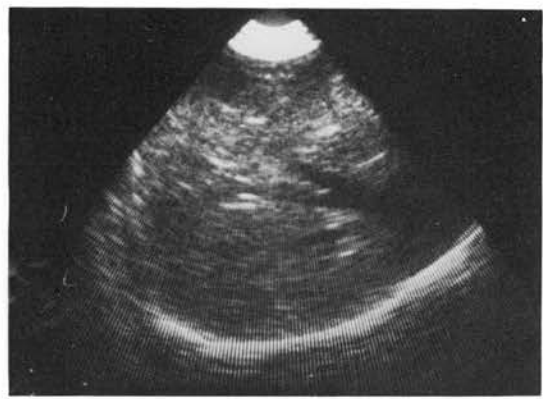
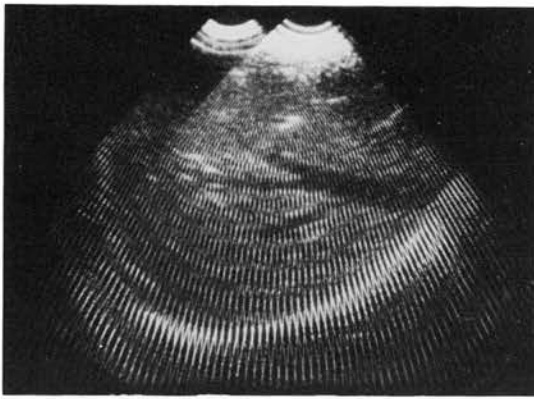


FIGURE 6.2A

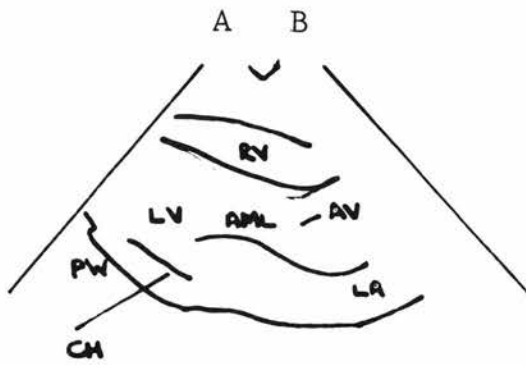
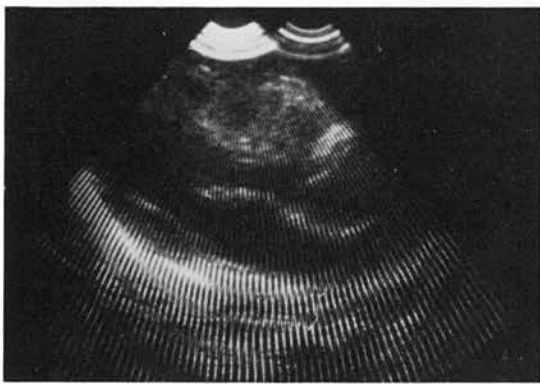


FIGURE 6.2B

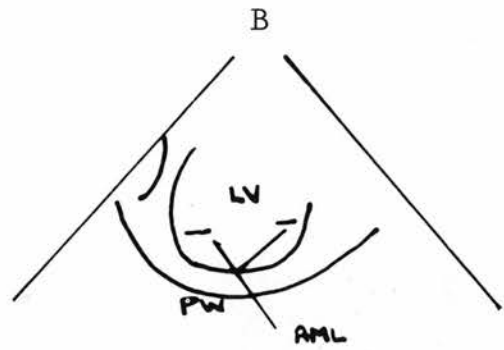
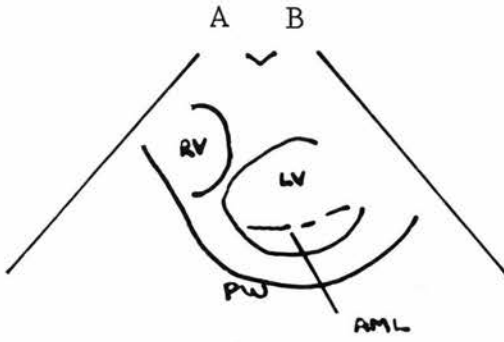
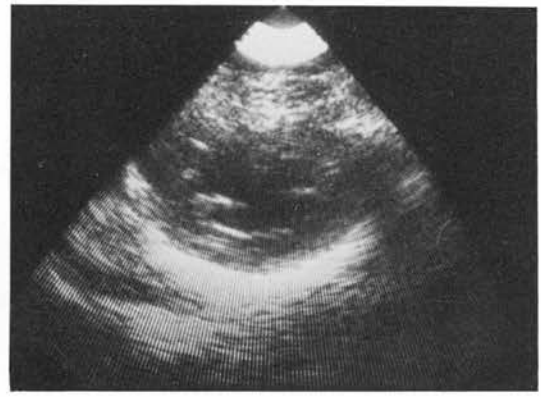
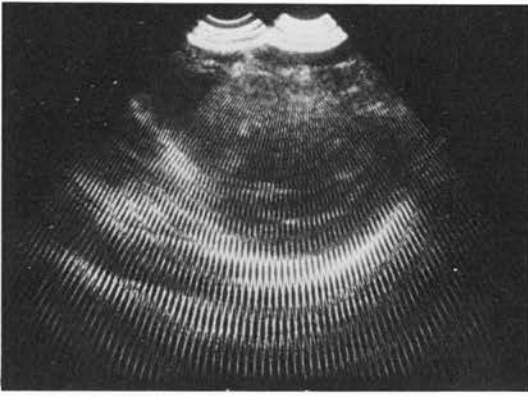


FIGURE 6.2C

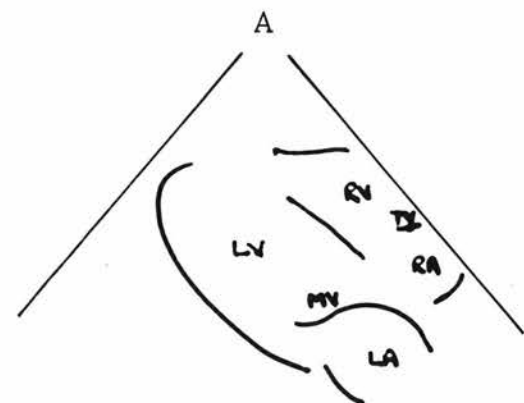
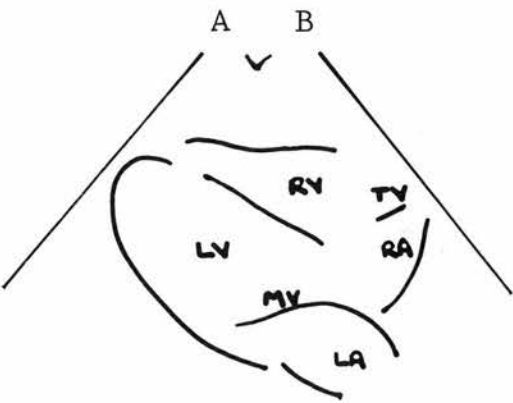
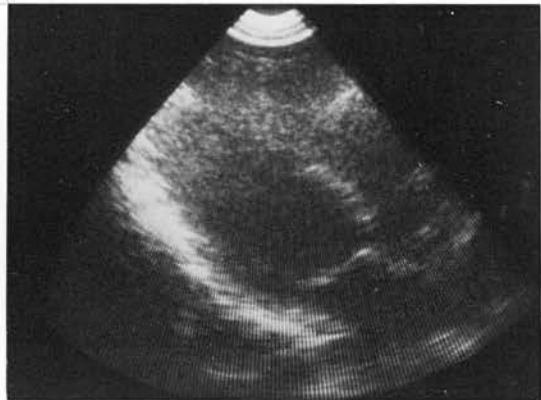
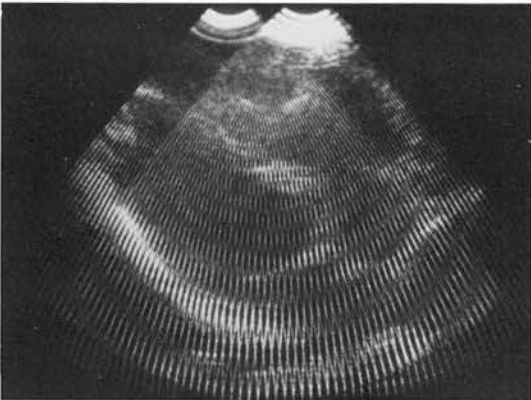


FIGURE 6.2D

6.3 UNRELATED TWIN SCANNER APPLICATION

The use of two scanners unrelated but constrained to scan in the same plane is an extension of the previous related application which has the potential to optimise visualisation in any one plane by allowing an increased freedom of scanner orientation. The possible scanning applications are as described for the related scanners with the one addition of coplanar transverse sections from the parasternal and subxiphoid approach. These transverse images would produce a good compound image if the sectors were registered by connecting the scanners via a scanning framework. However the negligible access advantages gained in practice through extra scanner freedom in the other applications combined with only one unique application negates the viability of such a complex system. This is particularly true if the related scanners are driven by a system which allows sector steering to be achieved as described in Chapter 5.

However truly unrelated scanners with unrestricted scanning action and individual separate sector images displayed simultaneously facilitates many unique visualisation applications which are outlined below and discussed in the context of their feasibility and clinical relevance. In terms of the four standard imaging sections described in

section 6.1 the basic combinations possible are grouped together in table 6.1. Some illustrative images are presented at the end of this section in figures 6.3.

Combinations 1, 2 and 3 are all relatively easy to obtain if parasternal access is possible with a single scanner from two or three intercostal spaces. Combination 1 allows the optimal view of aortic root and valve, left atrium and mitral valve in one sector while the other visualises the apical half of the left ventricle. The optimal planes for visualising these areas are generally not exactly coplanar and therefore improved visualisation of the complete left side of the heart is possible using this combination. Although a similar view can be obtained with one scanner the visualisation of endocardial contraction towards the apex requires some anti-clockwise rotation and lateral angulation of the sector plane. This is in keeping with T-M techniques.

A longitudinal view at the mitral valve level and a transverse view from the lower intercostal space, or in some cases from the same space but lateral to the other scanner, can be obtained using combination 2. Depending on the level of the transverse section, simultaneous visualisation of the mitral valve or the left ventricle, in two planes, allows more detailed examination of

T A B L E 6.1

UNRELATED SCANNING COMBINATIONS

SCANNER LOCATIONS	APPROXIMATE SCANNING PLANES	COMBINATION REFERENCE
BOTH PARASTERNAL	Long + Long	1
	Long + Trans	2
	Trans + Trans	3
BOTH SUBXIPHOID	Long + Long	4
	Long + Trans	5
	Trans + Trans	6
PARASTERNAL + SUBXIPHOID	Long + Long	7
	Trans + Trans	8
	Trans + Long	9
	Long + Trans	10

Where Long = Longitudinal

Trans = Transverse

Note: 1 Longitudinal Reference Plane

4 Coronal Reference Plane

8 Transverse Reference Plane

their function. Application 3 is potentially useful in left ventricular function assessment since simultaneous transverse visualisation at two levels in the ventricle allows disketic and akinetic areas to be found by comparison of relative wall movements in, and between the images. A large volume of ventricular wall can therefore be examined. Overall ventricular movement relative to the scanner can be related between images and used to investigate ventricular rotation and tilting during contractions. The relative movement of the centres of contraction in two transverse images were observed in a normal subject confirming heart rotation.

The use of both scanners at the subxiphoid location offers the same three possibilities from a different position relative to the heart. For optimal left ventricular visualisation in application 5 the longitudinal scanner is placed lateral to the transverse scanner along the costal margin. The transverse view is optimal at the parts of the ventricular wall which were not best seen in application 2. A feature of the subxiphoid longitudinal view of the left ventricle is its visualisation of the ventricular apex, especially when viewed from a more lateral position. Using combination 6 the ventricular rotation can be assessed about an axis which is perpendicular

to that in combination 3.

The optimal views from the parasternal position are more closely defined than the subxiphoid due to the greater restriction on the possible point of entry locations. Generally a large portion of the left costal margin is suitable for subxiphoid scanner location and therefore the possible combinations are increased. Single plane visualisation from the subxiphoid can produce images of structure combinations which cannot be obtained otherwise. For example the simultaneous visualisation of the aortic and pulmonary valves from a lateral position looking towards the base of the heart has been achieved on a normal subject. Both the tricuspid and mitral valves can be visualised together. Although many structures are accessible from this approach the optimal visualisation of heart chambers simultaneously, is often not possible in the same plane. For example the optimal visualisation of the left ventricle does not include the left atrium or the complete right ventricle. Scanner combination 4 allows optimal imaging of right and left sides of the heart simultaneously or atrium and ventricle combinations on one side of the heart. This allows the relative magnitude and phases of contractions to be examined on the left and right side of the heart.

Combined subxiphoid and parasternal visualisation offers useful left ventricular functional assessment using applications 7 and 8. These combinations are ideally suited for segmental wall function assessment. Set ups 9 and 10 also permit unique areas of heart wall to be visualised simultaneously and are potentially useful for valve function examination or structure identification. Combination 9 could be used to visualise the extent of pericardial effusion especially in the lateral wall.

The acquisition of subxiphoid and parasternal views simultaneously requires careful positioning of the subject and their co-operation and ability to control their breathing is necessary. In general inhalation improves subxiphoid access by raising the rib cage above the abdominal muscles. However the opposite is true in the case of parasternal access where inflated lungs can interfere. With normal subjects moderate inhalation combined with shallow breathing allowed good access. Although subxiphoid and parasternal access was possible during clinical trials of the single scanner, the application of both together may not have the same success due to the compromise patient position.

Although some of the combinations described may not be practical for general clinical use the system is capable

of providing sufficient spatial information to allow the three-dimensional movements of the heart within its surroundings, and its internal contractions to be examined. This enables the most applicable single plane or T-M techniques to be predicted. The potential subxiphoid combinations are numerous and indeed could prove very useful in the identification and interpretation of single scanner subxiphoid applications if this approach is adopted generally in clinical application.

The relative angle between the ultrasound beam and the direction of blood flow in the heart when scanning from a lateral position at the subxiphoid location is most appropriate for range-gated Doppler applications. Blood flow could be measured in the aorta on both sides of the aortic valve and in some cases on either side of the pulmonary valve. Likewise measurements could be made on either side of both the mitral and tricuspid valves. The design of the scanner allows it to be easily interfaced with a pulsed Doppler system.

Finally the interference between scanners when transmitting simultaneously is less than the related twin scanner application interference. This is due to the non-coplanar nature of the scanning planes in most of the unrelated combinations. Therefore if a suitable scan converter and

display is used the line density of the simultaneous sector images could be doubled.

FIGURES 6.3

Figures 6.3 show unrelated twin scanner images taken at the following location combinations simultaneously:-

- A. Parasternal - Trans + Long
- B. Subxiphoid - Long + Long
- C. Parasternal - Long + Long
- D. Parasternal - Long + Subxiphoid - Long
- E. Subxiphoid - Trans + Trans

Figure 6.3F illustrates a single sector image from the lateral subxiphoid location, directed towards the base of the heart, in a plane which includes both the aortic and pulmonary valves.

Abbreviations used in the diagrams are as figures 6.2 with the addition of those listed below.

MV	Mitral Valve
PV	Pulmonary Valve
AR	Aortic Root
EN	Endocardium
IVS	Interventricular septum
RVO	Right ventricular outflow
ANT	Anterior
POST	Posterior

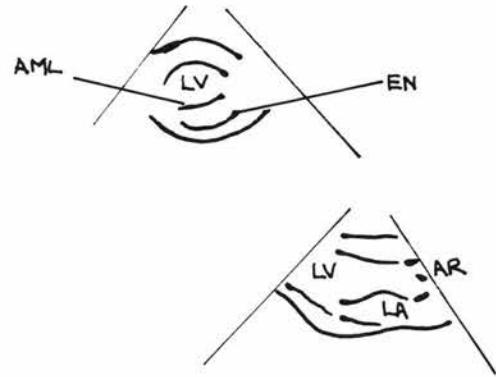
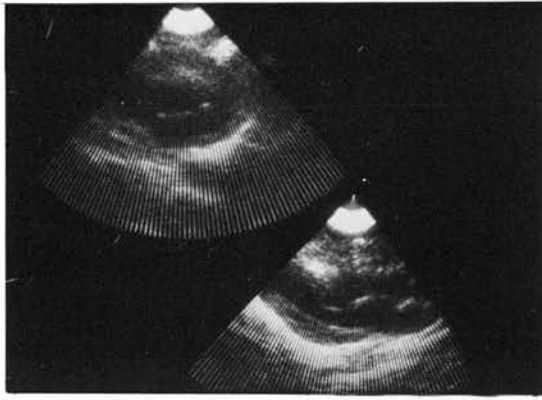


FIGURE 6.3A

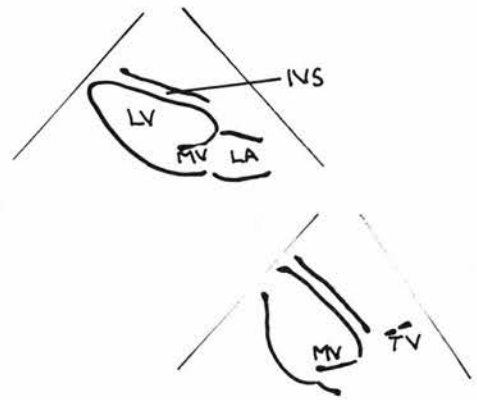
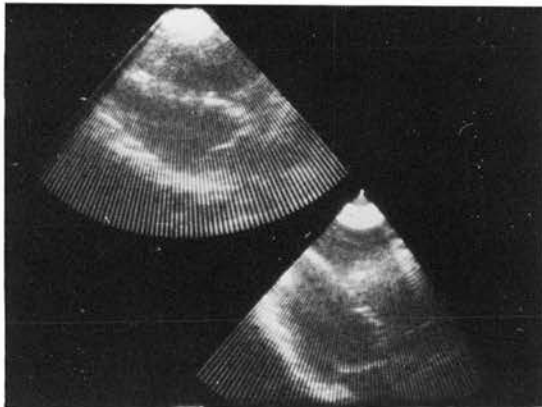


FIGURE 6.3B

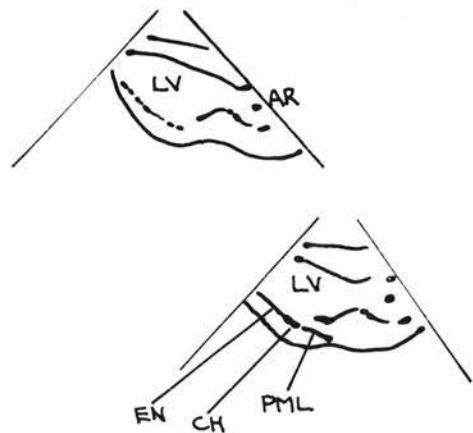
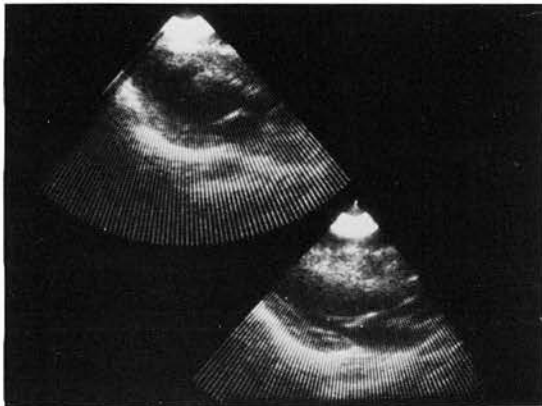


FIGURE 6.3C

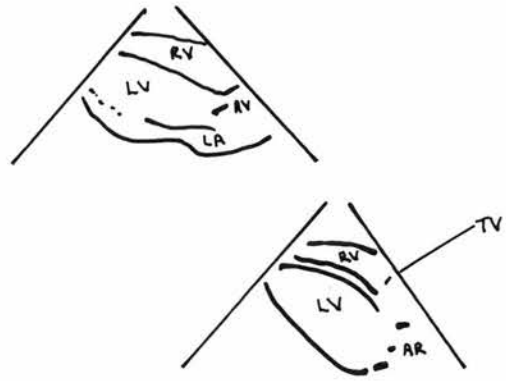
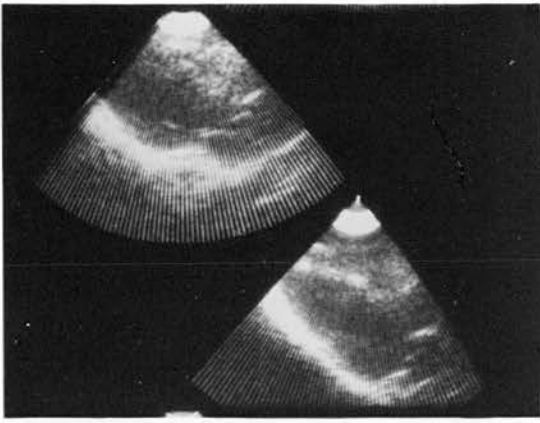


FIGURE 6.3D

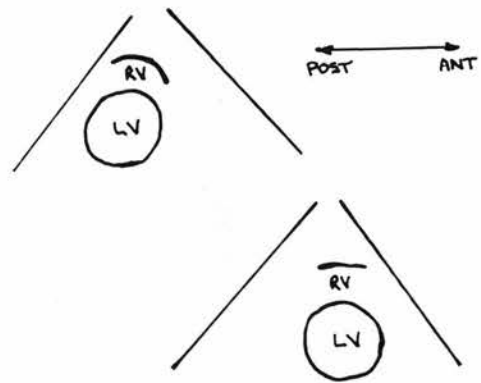
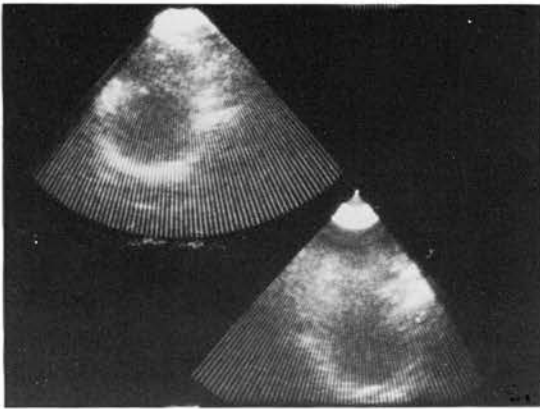


FIGURE 6.3E

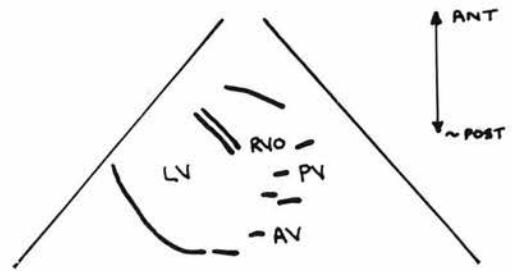
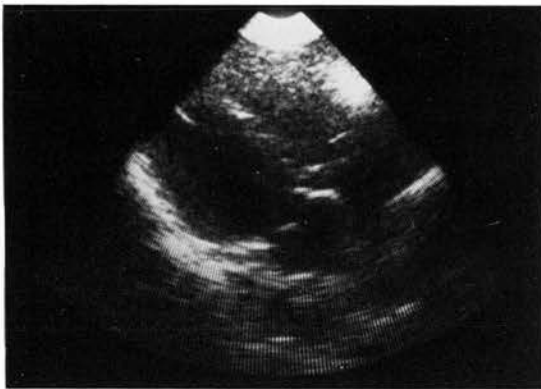


FIGURE 6.3F

6.4 CONCLUSION

Both related and unrelated twin scanner applications are feasible and expand the visualisation capability of the scanning system in different ways. Real-time compounding significantly improves visualisation continuity of heart valves and with improved video processing would contribute to endocardial delineation. The increased field of view contributes most to the subxiphoid view.

The visualisation of many heart section combinations simultaneously is feasible which contributes another dimension to heart visualisation making it possible to investigate heart function mechanisms more accurately. Some of the combinations are directly applicable to specific clinical heart conditions.

CHAPTER 7

CLINICAL APPLICATION AND EVALUATION

7.1 INTRODUCTION

The scanner design is based on experimental and theoretical predictions about the interaction of ultrasound with the heart and its surroundings. Cardiac disease can change the physical conditions within the heart and its surroundings. For example the heart can be displaced due to enlarged chambers or partially contained by fluid trapped between the pericardial layers. Parts of heart structure can be calcified or the lungs can be hyperinflated over the anterior wall of the heart. It is therefore important to assess the visualisation performance of the scanner in a real clinical situation on a representative group of patients suffering from cardio-respiratory disease.

The development and experimental work on the application of twin scanners to visualise the heart was carried out on normals in parallel with the clinical trials. The clinical experience therefore provided guidance on the possible scanner combinations most likely to be practical and diagnostically useful.

Tables containing a summary of visualisation results for 50 patients are presented in this chapter. The results

are discussed under the various clinical conditions examined and this is followed by a general discussion of the clinical performance of the scanner.

7.2 EXAMINATION PROCEDURE

The standard position of the patient for parasternal examination is supine with a 30° head-up tilt from the waist. In some cases, particularly obese patients and women with large pendulous breasts, this position has to be modified by turning the patient into a half left lateral position. A complete supine position is best for subxiphoid examination as this gives relaxation of the abdominal wall muscles, allowing the transducer to be introduced comfortably into the hollow below the xiphoid process. This relaxation of the abdominal wall muscles also helps to allow the transducer head to be moved laterally along the lower border of the costal margin.

Figure 7.1 shows schematically the scan directions of the four parasternal views which are used in the examination. The longitudinal section or view 1 is the first to be found. Initially the transducer is placed in the 4th intercostal space just to the left of the sternal border with the plane of the sector along the expected longitudinal axis of the heart. This axis may vary depending on the patient's build or the degree of inflation of the lungs.

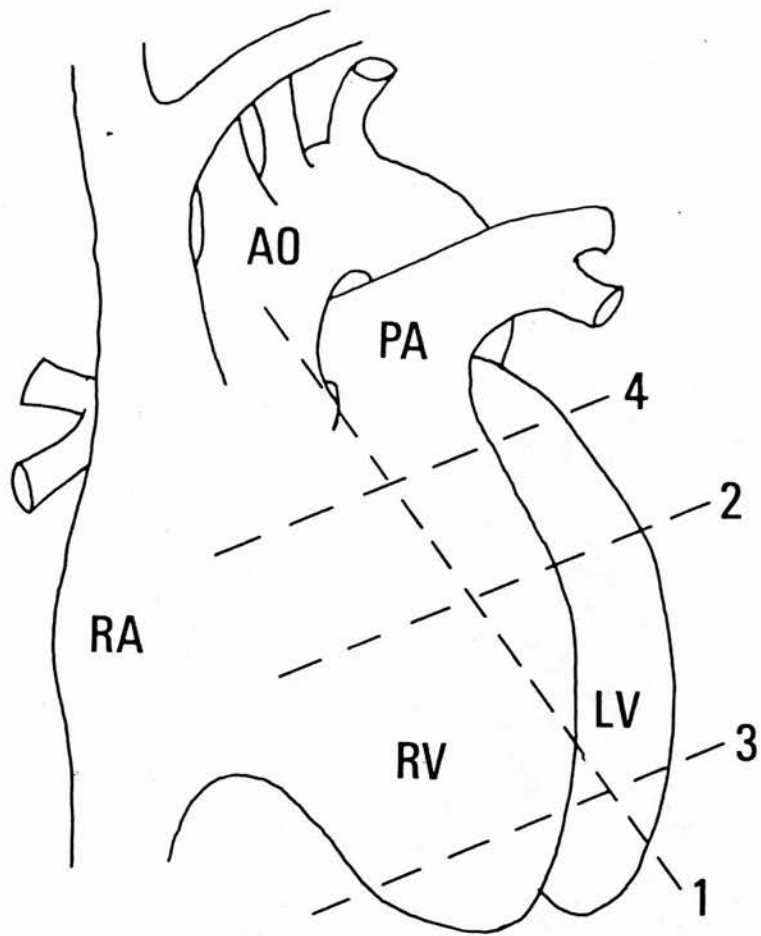


FIGURE 7.1 A schematic diagram of the heart showing the approximate scan directions of the four parasternal views. Aorta (AO), pulmonary artery (PA), left ventricle (LV), right ventricle (RV) and right atrium (RA).

Also the heart may be displaced to the left by conditions such as pectus excavatum. The long axis of the heart can be approximately assessed by inspection of the patient and by assessing the position of the apex beat by palpation. In a few patients the longitudinal view is obtained better from the 3rd, 5th or even occasionally the 2nd intercostal space. Once obtained, the precise orientation of this view provides guidance to obtaining subsequent views during the examination. A modification of this view is obtained by rotating the scanner clockwise until the pulmonary artery root and pulmonary valve are visualised. The scanner is then rotated through 90° such that the plane of the sector is perpendicular to the longitudinal axis of the heart. This gives a transverse view of the heart. Transverse sections can be obtained at various levels through the heart and with the transducer adjacent to the sternum, in the intercostal space giving the optimum longitudinal view, a transverse section at the roots of the atrioventricular valves is obtained (view 4). Moving the scanner laterally along this space gives a view through the atrioventricular valve cusps (view 2). Further lateral movement of the scanner with usually movement to the intercostal space below allows visualisation of a transverse section through the distal portion of the left

ventricle.

Finally, the subxiphoid view is obtained by placing the scanner in the patient's epigastrium. The sector plane is positioned approximately parallel to the coronal plane of the body and the sector is directed upwards towards the region of the patient's left shoulder. This view is enhanced by gently pushing the scanner head under the costal margin but only so far as not to cause patient discomfort.

7.3 CLINICAL GROUPS

The 50 examined patients have been divided into 6 clinical groups. The clinical groups are listed below with the number of patients in each group indicated in brackets.

1. Coronary artery disease (16)
2. Valvular heart disease (14)
3. Chronic obstructive lung disease (6)
4. Prosthetic heart valves (4)
5. Pericardial effusion (3)
6. Others (7)

Coronary artery disease is the most common cause of death in men over 45 years of age in the western world and is becoming increasingly common in younger men and all women. Patients in group 2 above are becoming less common as a result of penicillin therapy for rheumatic fever. Chronic

obstructive lung disease is the most common chronic illness causing loss of work in the United Kingdom. Group 4 is linked with group 2 and group 5 is not very common.

Group 6 includes cases such as cardiomyopathy, primary pulmonary hypertension and post myocardial infarction syndrome, which are all relatively uncommon. Systemic hypertension is included in group 6 and is very common but few examples were seen because the majority of patients with this condition are managed as out patients and hypertensive patients tend to be admitted to hospital only with complications of the disease such as stroke or myocardial infarction. Because of the general nature of the unit referring the patients, there has been no opportunity during the period of study to examine patients with certain conditions which would have been of interest. Examples of these conditions are cardiac tumours and adult congenital heart disease.

7.4 TABLE LAYOUT AND TABLES 7.1 - 7.6

Visualisation results and clinical information about the examined patients are presented in tables 7.1 - 7.6 corresponding to the six clinical groups detailed above. Every patient has a number between 1 and 50, these numbers being in chronological order of examination. These numbers appear in the left hand column of the table.

To the right of each patient number there is a row containing a results summary and below this the clinical condition before examination and the real-time echocardiographic findings during the examination are detailed. If relevant this is followed by a comment.

The results summary row is in three main sections as indicated by the headings, patient, views and structures at the top of the table. The numbers which appear under the headings, views required and views obtained, correspond to the four views illustrated in figure 7.1. The fifth view is the subxiphoid approach and is denoted by the letter 'S'.

The listed 'views required' are those most likely to give the best diagnostic information about the condition being examined. During the examination all views are looked for and those found are listed under 'views obtained'. These two columns show quickly how well the heart is visualised and also how different clinical conditions affect visualisation and therefore examination technique. The subxiphoid approach was not used routinely until half way through the clinical assessment and therefore view 'S' only appears in the views obtained column after patient number 25. However it is included in the views required column for all patients when appropriate and allowance

should be made for this with the first 25 patients in the tables.

The third section of the results summary row is a more detailed breakdown of the structures visualised with broad quantification. There are nine heart structures recorded in this section and they are abbreviated as follows:-

(MV) mitral valve, (AV) aortic valve, (TV) tricuspid valve, (PV) pulmonary valve, (LA) left atrium, (LV) left ventricle (EN) endocardium, (SP) septum, (RV) right ventricle.

The symbol which appears in the column below the structure title is a subjective measure of how well it has been visualised. The symbol ++ indicates that the structure is well visualised allowing easy identification and assessment of function. The symbol + indicates adequate visualisation to allow identification but limited functional assessment. For example, incomplete visualisation of a well identified ventricle or valve. The identification could be good due to good visualisation of surrounding structures. Finally if the structure is not seen the symbol 0 appears.

Abbreviations used in the clinical and echocardiographic details section of the table are listed below.

LV	Left ventricle
RV	Right ventricle
LA	Left atrium

MI	Myocardial infarction
SOB	Shortness of breath
X/7	X days
X/52	X weeks
X/12	X months
?	Query

TABLES 7.1 — 7.6

7.1 CORONARY ARTERY DISEASE

PATIENT				VIEWS		STRUCTURES								
Number	Age	Sex	Init ¹	Required	Obtained	MV	AV	TV	PV	LA	LV	EN	SP	RV
4	74	F	TML	12	123	++	++	++	++	+	+	+	++	+
Clinical	SOB on exertion - MI 4/52 before - systolic murmur													
Echo	Aortic valve calcification													
Comment														
6	65	M	DMEL	123	12	++	o	o	o	+	++	++	+	o
Clinical	Anterior and inferior MI 1/12 before													
Echo	Normal													
Comment	Access to base of heart restricted by lung interference													
7	69	M	JW	123	123	++	++	o	+	++	++	++	+	o
Clinical	Anterior MI 1/52 before													
Echo	Normal													
Comment														
26	59	M	BE	123 S	12 S	++	++	++	o	++	++	++	++	++
Clinical	Anterior MI 3/12 before - LV aneurism demonstrated on nuclear angiography													
Echo	Saccular anterior aneurism with calcification in wall													
Comment														
27	72	M	AI	123 S	1 S	++	++	o	o	+	++	++	++	o
Clinical	Inferior MI 2/52 before with two extensions subsequently													
Echo	Diffuse hypokinesia													
Comment														

PATIENT				VIEWS		STRUCTURES									
Number	Age	Sex	Init!	Required	Obtained	MV	AV	TV	PV	LA	LV	EN	SP	RV	
31	48	M	AC	123 S	12 4S	++	++	o	o	+	++	++	++	o	
Clinical	Inferior MI 2/52 before - Persistent fever														
Echo	Moderate LV function but no segmental myocardial abnormality														
Comment	Sagittal subxiphoid plane only														
32	53	M	JH	123 S	1 S	+	+	o	o	+	+	++	+	o	
Clinical	Inferior MI 10/7 before - Persistent fever														
Echo	Apical segment of akinesia														
Comment	Image quality reduced by thick chest wall ++														
34	84	M	JD	123 S	12	+	o	o	o	+	+	+	+	o	
Clinical	Left ventricular failure - ? ventricular aneurism														
Echo	Gross LV dilatation and hypokinesia - no evidence of ventricular aneurism														
Comment	Obese ++														
35	68	M	CS	123 S	1234	++	++	++	o	+	++	++	++	+	
Clinical	Inferolateral MI 3/7 before														
Echo	Apical and posterior wall akinesia - examinations 7/7 and 10/7 post MI showed improved wall movement														
Comment	Thin with rigid abdominal wall - no subxiphoid access														
36	62	M	JB	123 S	1 S	+	+	+	o	+	+	+	++	+	
Clinical	Inferoposterior MI 1/52 before														
Echo	Mild generalised left ventricular hypokinesia - examination 10/7 showed posterior infarct-no change														
Comment	Visualisation best from subxiphoid - narrow vertical heart														
37	49	M	WM	123 S	12	++	++	++	o	++	++	++	++	++	
Clinical	SOB - atrial fibrillation														
Echo	Posterolateral segmental hypokinesia														
Comment	No subxiphoid due to pectus excavatum														

PATIENT				VIEWS		STRUCTURES								
Number	Age	Sex	Init!	Required	Obtained	MV	AV	TV	PV	LA	LV	EN	SP	RV
39	66	M	JB	1234S	1	++	++	++	++	+	++	++	++	+
Clinical	Paroxysmal atrial fibrillation - apical systolic murmur - ? mitral regurgitation													
Echo	Abnormal echoes deep in LV cavity - ? chordal													
Comment	High horizontal heart - no subxiphoid													
41	48	M	JC	123 S	12	++	++	o	o	+	+	++	+	+
Clinical	Inferolateral MI 8/7 before													
Echo	Posterior wall akinesis - small pericardial effusion													
Comment	Thick chest wall and muscular abdomen													
42	39	M	AMM	123 S	12 4	++	++	o	o	+	++	++	++	o
Clinical	MI 4/12 before - recurrent chest pain													
Echo	Apical dyskinetic segment													
Comment														
47	61	M	JA	123 S	123 S	++	++	++	o	++	++	++	++	++
Clinical	Ischemic heart disease - LV aneurism in nuclear angiography													
Echo	Globular grossly hypokinetic LV with apical aneurism													
Comment														
50	57	M	TL	123 S	12 S	++	++	+	o	+	++	+	++	+
Clinical	Inferolateral MI 10/7 before - pericardial friction													
Echo	Globular LV with posterior wall hypokinesis													
Comment	Lung interference during inhalation													

7.2 VALVULAR HEART DISEASE

PATIENT				VIEWS		STRUCTURES								
Number	Age	Sex	Init ¹	Required	Obtained	MV	AV	TV	PV	LA	LV	EN	SP	RV
2	77	F	MD	12	123	++	++	++	++	+	+	o	++	+
Clinical	Mitral regurgitation - systolic murmur - fever - ?													
Echo	infective endocarditis													
Comment	Mitral valve calcification - normal aortic valve													
3	53	M	AD	123	123	++	++	+	o	+	++	++	+	o
Clinical	SOB - systolic murmur - mitral regurgitation													
Echo	Mitral valve calcification													
Comment														
12	36	M	MT	12	1	++	++	o	o	+	++	++	++	o
Clinical	? Mitral valve prolapse - systolic click													
Echo	Normal													
Comment	Lung interference													
13	43	M	GB	12	12	++	++	o	++	++	++	++	++	o
Clinical	Mitral stenosis - mitral valvotomy 3/12 before -													
Echo	subsequent arrhythmias													
Comment	Immobile thickened mitral valve													
14	63	M	JM	12 4	12	++	++	o	o	++	++	++	++	+
Clinical	Mitral stenosis - mitral regurgitation - aortic													
Echo	valve disease													
Comment	Mitral valve calcified and immobile - aortic valve													
	calcified - generalised LV hypokinesia													

PATIENT				VIEWS		STRUCTURES									
Number	Age	Sex	Init!	Required	Obtained	MV	AV	TV	PV	LA	LV	EN	SP	RV	
16	19	M	AG	12	1234	++	++	o	o	++	++	+	+	o	
Clinical	Systolic murmur														
Echo	Asymmetrical aortic valve - ? bicuspid														
Comment															
17	71	F	MG	123	12	++	++	o	o	++	++	+	+	o	
Clinical	Biventricular failure - systolic murmur - mitral regurgitation														
Echo	Enlarged LA - generalised LV hypokinesia - no definite valve abnormality														
Comment															
18	71	F	CS	12 4	12	+	++	o	o	+	+	+	+	o	
Clinical	Malaise systolic murmur - ? mitral regurgitation														
Echo	Enlarged LA - no other abnormality														
Comment															
19	81	F	AV	12 4	123	++	++	++	o	++	+	+	+	+	
Clinical	? Mitral stenosis														
Echo	Calcified mobile mitral valve - marked enlargement of LA														
Comment															
21	61	M	CD	12 4	12	++	++	o	++	+	+	++	o	o	
Clinical	SOB - apical systolic murmur - ? mitral regurgitation														
Echo	Rigid thickened mitral valve														
Comment															
22	57	F	MG	12	1	++	+	o	o	+	+	o	o	+	
Clinical	Mitral systolic and diastolic murmur - mitral stenosis														
Echo	Rigid mitral valve - enlarged LA														
Comment															

PATIENT				VIEWS		STRUCTURES								
Number	Age	Sex	Init!	Required	Obtained	MV	AV	TV	PV	LA	LV	EN	SP	RV
28	39	F	HF	12 4	123	++	++	o	o	++	++	++	++	o
Clinical	Chest pain - aortic systolic murmur													
Echo	Normal													
Comment														
29	59	F	CA	12 4S	1 S	++	++	o	o	+	o	o	o	o
Clinical	SOB ++ - atrial fibrillation - signs of mitral stenosis													
Echo	Thickened mitral valve with restricted movement - enlarged LA													
Comment	Small high access window and obesity													
33	78	M	JT	12 4	12	++	++	o	o	+	+	+	+	o
Clinical	Biventricular failure - atrial fibrillation - systolic murmur													
Echo	Calcified stenosed aortic valve with aortic dilatation													
Comment	Thin flat rib cage - no subxiphoid													

7.3 CHRONIC OBSTRUCTIVE LUNG DISEASE

5	23	M	MD	1 S	123	++	++	++	++	++	++	++	++	++
Clinical	Bronchial asthma													
Echo	Normal													
Comment														
8	34	M	VK	1234S	123	++	++	++	o	+	++	++	++	++
Clinical	SOB - cause unknown													
Echo	No definite abnormality													
Comment														

PATIENT				VIEWS		STRUCTURES										
Number	Age	Sex	Init!	Required	Obtained	MV	AV	TV	PV	LA	LV	EN	SP	RV		
30	67	M	TG	123	S	1	S	++	o	++	o	+	++	++	++	++
Clinical	Chronic bronchitis - unwell 18/12 before - single probe T-M showed dilated LA, LV and RV.															
Echo	Normal															
Comment	Main visualisation from subxiphoid															
38	79	M	DM	12	S		S	++	o	++	o	++	++	++	++	++
Clinical	Chronic bronchitis ++															
Echo	Active RV contraction - no other abnormality															
Comment	No parasternal access due to hyperinflated lungs															
48	62	M	TF	12	S		S	++	o	++	o	++	++	++	++	++
Clinical	Chronic bronchitis															
Echo	Good RV contraction															
Comment	Inflated lungs															
49	59	M	CS	12	S		S	++	o	++	o	+	++	++	++	++
Clinical	Chronic bronchitis with cor pulmonale															
Echo	Variation in LV size with respiration															
Comment	Inflated lungs															

7.4 PROSTHETIC HEART VALVES

1	18	M	KD	12		12		++	++	+	o	+	++	++	o	o
Clinical	Starr-Edwards aortic prosthesis inserted 1973 - increasingly loud systolic murmur															
Echo	Thickening around valve cage - good LV function															
Comment																

PATIENT				VIEWS		STRUCTURES									
Number	Age	Sex	Init!	Required	Obtained	MV	AV	TV	PV	LA	LV	EN	SP	RV	
9	70	M	GS	123	12	++	++	+	o	+	++	+	+	o	
Clinical	Bjork-Shiley aortic prosthesis fitted 1/12 before - right heart failure														
Echo	Prosthesis apparently functioning normally - generalised LV hypokinesia														
Comment															
40	34	M	TW	12 4S	1234	++	++	o	o	++	++	++	++	++	
Clinical	Hancock aortic prosthesis inserted 11/7 before for infective endocarditis														
Echo	Prosthesis visualised - heart otherwise normal														
Comment	Subxiphoid not attempted due to recent sternal repair														
46	67	F	JL	12 4S	1	+	++	o	o	+	+	+	+	o	
Clinical	Bjork-Shiley aortic prosthesis inserted 1/12 before anaemia recurrent - early diastolic murmur														
Echo	Prosthetic valve seen - LA enlarged														
Comment	Wires in sternum limited access														

7.5 PERICARDIAL EFFUSION

20	22	M	MW	1234S	123	++	++	o	o	++	++	++	++	o
Clinical	Pericarditic pain - ? effusion													
Echo	Small pericardial effusion - normal heart													
Comment														
23	56	M	JW	123 S	1	++	++	++	++	+	+	+	+	+
Clinical	Diabetic with nephropathy and chronic renal failure - pericardial friction rub													
Echo	No pericardial fluid - no cardiac abnormality													
Comment														

PATIENT				VIEWS		STRUCTURES									
Number	Age	Sex	Init!	Required	Obtained	MV	AV	TV	PV	LA	LV	EN	SP	RV	
44	28	M	KW	123 S	1234	++	++	++	o	++	++	++	++	++	
Clinical	Viral pericarditis 3/12 before - slow to improve														
Echo	Normal														
Comment	Thin muscular abdomen - no subxiphoid														

7.6 OTHERS

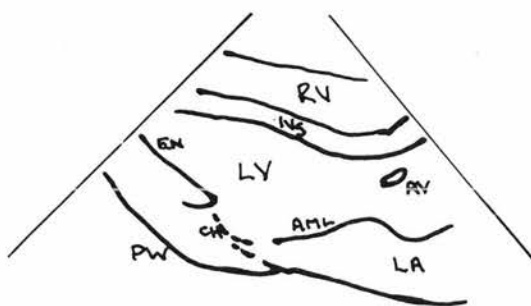
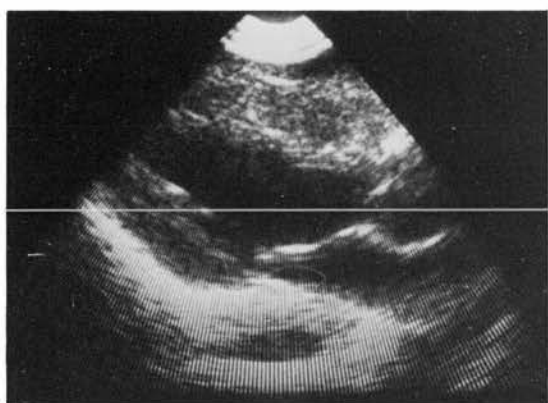
10	38	M	WR	12 S	12	++	++	++	++	++	++	++	++	++
Clinical	Pulmonary hypertension - ? primary or thromboembolic													
Echo	Large RV - normal left heart structures - thickened pulmonary valve													
Comment														
11	48	M	PC	12 S	123	++	++	++	++	++	++	++	+	++
Clinical	Pulmonary hypertension - thought to be primary													
Echo	Large RV													
Comment														
15	43	F	MW	12 S	12	++	+	o	o	+	++	+	++	+
Clinical	? Hypertrophic obstructive cardiomyopathy													
Echo	Systolic anterior movement of mitral valve - thickened septum													
Comment														
24	24	F	CT	1234S	12 4	++	++	o	++	++	++	++	++	+
Clinical	11/52 post partum - SOB ++													
Echo	Valves normal enlarged LA - enlarged diffusely hypokinetic LV													
Comment	All in keeping with congestive cardiomyopathy													

PATIENT				VIEWS		STRUCTURES								
Number	Age	Sex	Init ¹	Required	Obtained	MV	AV	TV	PV	LA	LV	EN	SP	RV
25	45	M	MB	123	123	++	++	++	o	++	++	++	++	++
Clinical	Hypertensive													
Echo	Thickening of LV wall - active LV contraction													
Comment														
43	69	M	PM	1234S	12 4S	++	++	++	o	++	++	++	++	++
Clinical	Heart block temporary pacemaker in site													
Echo	Pacing catheter visualised - no other abnormality seen													
Comment	Examined for visualisation interest													
45	68	M	JG	123 S	123 S	++	++	o	o	+	++	++	++	+
Clinical	Inferoposterolateral MI 15/7 before - pericardial friction													
Echo	Globular LV with posterior and lateral hypokinesia - pericardial effusion													
Comment	Thick chest wall													

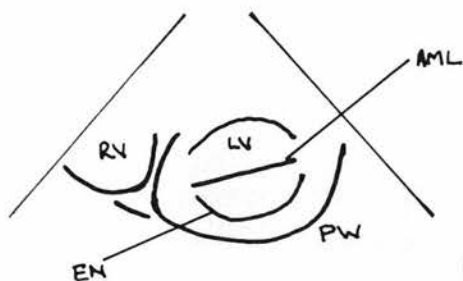
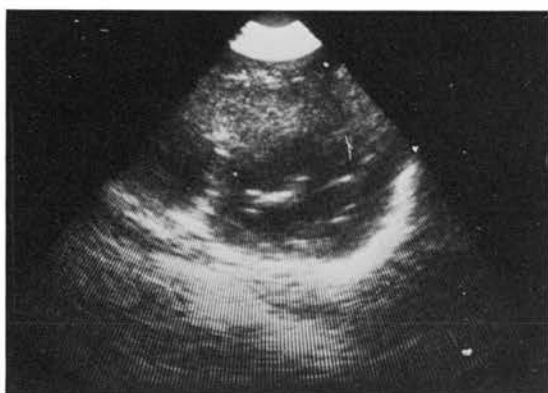
7.5 THE STANDARD VIEWS

Before discussing specific clinical conditions, a resume of how to obtain the standard views and the structures visualised in them should be helpful. Some examples are shown in figure 7.2.

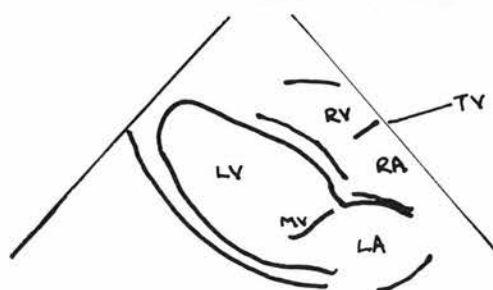
The longitudinal view gives visualisation of the anterior and posterior cusps of the mitral valve, the aortic root and valve, the left atrium, a longitudinal section through the left ventricle and occasionally visualisation of some right heart structures. The mitral valve is nearly always readily visualised although the posterior cusp is less constantly visualised than the anterior cusp. The aortic root is similarly readily visualised. The aortic valve appears within the aortic root and is most apparent during ventricular diastole when it is closed. Some minor adjustment of the scanner plane is often necessary to optimise the view of the aortic valve. The left atrium lies behind the aortic root and is again seen in most cases without difficulty. The left ventricle is difficult to visualise completely without further changes in sector angulation. With the sector in a plane optimising the aortic root, a good view of the posterior wall of the left ventricle is obtained. However in this plane the apex and anterior wall of the left ventricle are not well seen and the posterior wall endocardium cannot be distinguished



Standard longitudinal view at end systole



Transverse view of left ventricle at level of valve cusps



Subxiphoid view

FIGURE 7.2

readily. Minor angulation and usually some anti-clockwise rotation brings these structures into view while losing the optimal view of the aortic root. In some patients the apex of the left ventricle is better visualised by moving the scanner one intercostal space inferiorly, although visualisation of the endocardium at the apex proves difficult.

It has been found that right heart structures are poorly seen with this view as these lie anteriorly and to the right of the left heart and only lie partially in the scanning plane. However where there is enlargement of the right ventricle these structures may be further to the left and overlying the left heart than normal and therefore come more within the scanning plane.

The transverse view at the level of the valve cusps (view 2) allows visualisation of the atrioventricular valves. Usually a transverse section through the left ventricle is obtained with good differentiation between endocardium, myocardium and pericardium. Part of the right ventricle can often be seen and this may be improved at the expense of the left ventricular image by changes in scanner orientation. The transverse view of the distal left ventricle (view 3) shows the left ventricular wall usually in its entire circumference, again with good

differentiation between the wall layers. The view at the valve roots (view 4) shows the valve rings with surrounding ventricular walls although again the right heart structures are less well seen than the left.

Using the subxiphoid view visualisation of the complete left ventricle including the septum and apex is usually obtained. The right ventricle is also readily visualised although the optimal views lie in different planes. This approach can give foreshortened images of the ventricles but nevertheless wall motion can be assessed from these images. The tricuspid and mitral valves and also the left and right atria may be seen depending on possible scanner orientation. From a position optimising the mitral valve, further anterior movement of the sector plane brings the aortic root into view and valve cusp motion can be assessed. However visualisation of the aortic root from the subxiphoid position has proved more difficult in patients than in normal subjects, probably because this requires the scanner head to be pushed firmly under the costal margin causing discomfort and involuntary tensing of the abdominal wall muscles.

7.6 EVALUATION OF SCANNER IN CLINICAL APPLICATION

The discussion of the results begins with experience of specific clinical conditions and this is followed by a general discussion of the clinical application of the scanner and its visualisation performance on the group as a whole.

7.6.1 VALVULAR HEART DISEASE

Valvular heart disease is the name given to heart disease secondary to abnormalities of the cardiac valve. This is often due to valve damage caused by rheumatic fever, but with control of this disease by antibiotic therapy the incidence of post-rheumatic valvular heart disease is falling. Other forms of valvular heart disease are those due to congenital abnormalities of the valves or later in life disease due to degeneration and calcification of the valves. Rheumatic valvular heart disease affects in decreasing order of incidence, the mitral, aortic, tricuspid and finally the pulmonary valves. Congenital valve abnormalities may affect any valve with or without other cardiac abnormalities but in adult practice the most important lesions are those affecting the aortic and pulmonary valves. Degenerative valve disease affects mainly the aortic and mitral valves.

Visualisation of the cardiac valves is therefore important

to allow assessment of valve structure and function and the presence or absence of calcification. Mitral stenosis is the narrowing of the mitral valve orifice usually accompanied by thickening and often by calcification of the valve. Visualisation of the mitral valve is best achieved using views 1 and 2 while view 4 allows visualisation of the valve ring. The left atrium is usually enlarged in this condition and this can be assessed in view 1.

Five patients (numbers 13,14,19,22 and 29) with this condition were examined and in each satisfactory information about valve rigidity and calcification was obtained from view 1. Some information about valve motion was usually obtained in view 2. An example of this condition is shown in figure 7.3 illustrating valve cusp thickening and enlarged left atrium.

In mitral regurgitation (patient numbers, 2,3,14,17,18,21 and 39) where there is loss of competence of the mitral valve, the valve may show calcification in views 1 and 4 but can appear quite normal echocardiographically.

Examination of these patients usually reveals mitral valve thickening with normal motion or enlargement of the left atrium alone. In these patients the clinical findings allow the suspicion of this diagnosis but without any definite abnormal pattern.

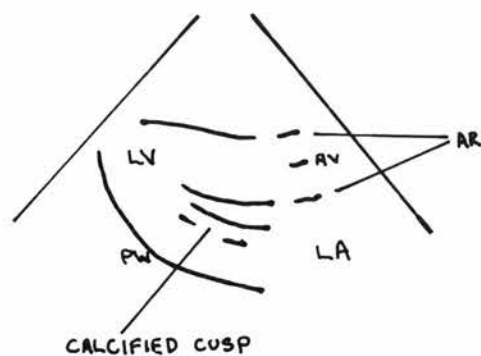


FIGURE 7.3 Patient 14 - Mitral stenosis with cusp thickening and enlarged left atrium.

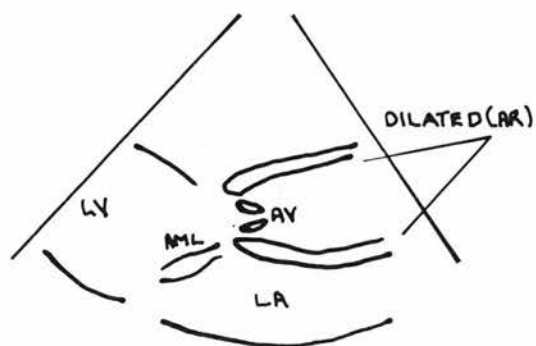
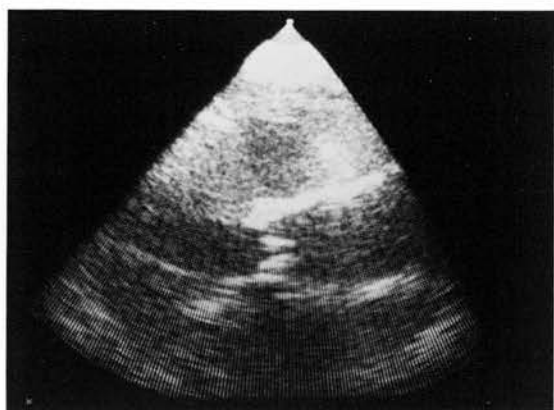


FIGURE 7.4 Patient 33 - Aortic stenosis with poststenotic dilatation of aortic root.

Aortic valve disease, whether stenosis, regurgitation or mixed, produces thickening of the aortic valve cusps. There is also often valve calcification. View 1 allows assessment of the aortic root and valve although little valve structure detail is discernible unless there is a valve abnormality. In patients number 14, 28 and 33 useful visualisation of the aortic root and valve was obtained and in patient 33, poststenotic dilatation of the aortic root could also be seen as illustrated in figure 7.4.

Disease of the tricuspid and pulmonary valves is comparatively rare without accompanying mitral or aortic valve disease. The tricuspid valve is most readily visualised in view 2 and in the subxiphoid view. The pulmonary valve is difficult to visualise and some success in this has been achieved using a modification of the longitudinal view as outlined earlier. Experience of the subxiphoid view in normal subjects has shown that both the aortic and pulmonary roots and valves may be visualised as outlined in the last chapter, but the potential of this was not realised during clinical trials. The tricuspid valve was visualised in 50% of patients and the pulmonary in 22%. In few of these patients was any abnormality of the tricuspid or pulmonary valve seen. However, in patient number 10, the pulmonary valve was found to be thickened

although this patient did not have valvular heart disease but was suffering from primary pulmonary hypertension and is discussed below.

Prosthetic heart valves may be inserted in the heart to replace any of the four valves which are severely diseased but as valve disease is commonest in the aortic and mitral valves, prosthetic valves tend to be most commonly in these positions. At present the most popular types of prosthesis fitted in Edinburgh are the Bjork-Shiley, which consists of a tilting metal disc within a low profile metal cage, and the Hancock prosthesis which is a pig aortic valve mounted on a metal frame, the commissures of the valve being supported on uprights known as stents.

Patient numbers 1, 9, 40 and 46 all had prosthesis in the aortic valve position. Patients 9 and 46 had Bjork-Shiley valves and the tilting motion of the disc could be seen in both. Patient 46 had developed endocarditis on the prosthetic valve and the valve ring was seen to be rocking within the aortic root. This suggested instability of the valve and in fact this valve had to be replaced later.

Patient 40 had a Hancock prosthesis. The valve stents and some movement of the pig valve cusps could be seen.

Patient 1 had a Starr-Edwards prosthesis, a ball in cage valve, still the most popular prosthesis although now not

often inserted in Edinburgh. In this case the motion of the ball could be seen and there was a suggestion of thickening at the root of the cage, suggesting some obstruction to valve outflow, possibly due to blood clot. Illustrative images from patients 40 and 46 are shown in figure 7.5.

7.6.2 CORONARY ARTERY DISEASE

Coronary artery disease is the name given to the disease produced by narrowing of the coronary arteries usually due to atheroma, Narrowing of the arteries causes reduction in blood flow and therefore oxygen carriage to the area of myocardium supplied by the affected vessel. The myocardium becomes ischemic and this causes pain and interference with myocardial function. The affected myocardium contracts less vigorously than normal and the resultant reduced movement is termed hypokinesis. If ischemia is so severe that contraction is absent, then akinesia is said to be present. Profound myocardial ischemia may result in cell death, termed myocardial infarction. The infarcted area may show akinesia, or even move paradoxically, termed dyskinesia. This paradoxical movement is caused by the contraction of normal myocardium forcing blood into the non contracting segment, resulting in opposite movement. Diskinesia or akinesia may also occur in ventricular aneurism where an

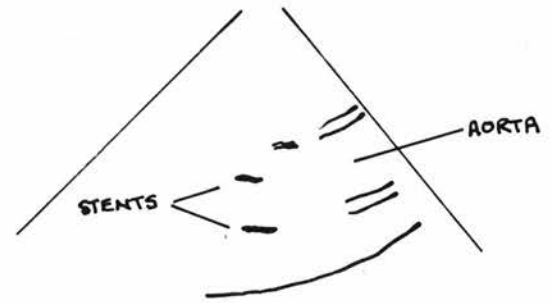
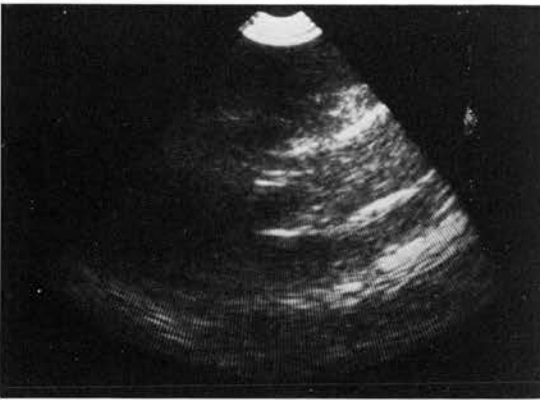
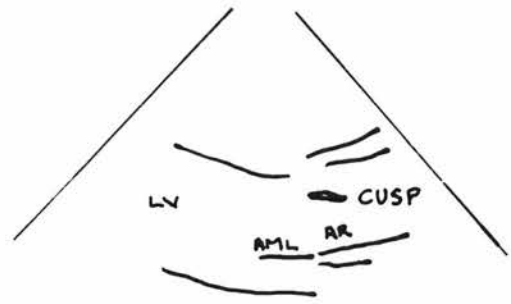
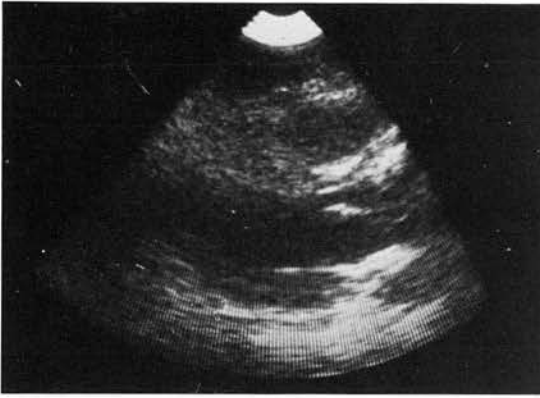


FIGURE 7.5 Patient 40 - Hancock aortic prosthesis showing pig valve cusp and stents of valve.

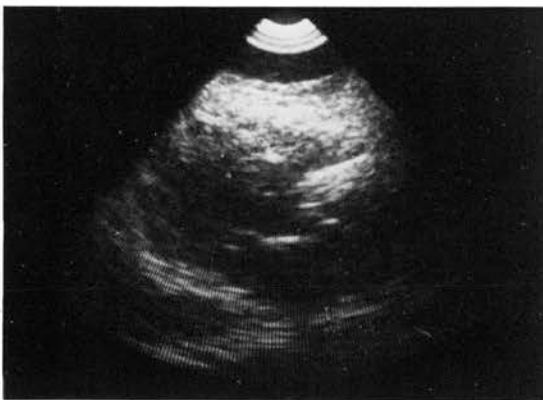


FIGURE 7.5 Patient 46 - Bjork-Shiley aortic prosthesis showing the tilting disc and aortic root.

infarcted area of heart becomes dilated to form a non contracting sac. Visualisation of the whole left ventricle is therefore desirable in this condition to help assess global function and search for local malfunctioning parts of myocardium. The differentiation of endocardium and myocardium is also important in identifying the extent and type of malfunction.

Patient numbers 4,6,7,26,27,31,32,34,35,36,37,39,41,42,47 and 50 all had coronary artery disease as detailed in table 7.1. Although some (4,6,7,31,39) showed normal left ventricular function, many (32,35,37,41,42,47,50) showed segmental hypokinesia or akinesia in the portion of ventricular wall suggested as the site of infarction by examination of the E.C.G. A further group showed diffuse hypokinesia without segmental abnormality (27,34,36).

Two patients, 26 and 47, had ventricular aneurisms, number 26 having a saccular anterior aneurism and number 47 having an apical aneurism. This is shown in figure 7.6. In five patients, (26,34,37,45,47) the findings were confirmed by nuclear angiography and there was good agreement between the two techniques in the assessment of segmental contraction abnormalities. Two patients, 35 and 36, were studied sequentially following myocardial infarction. Patient 36 was studied at seven and ten days after infarction. Both examinations showed diffuse left

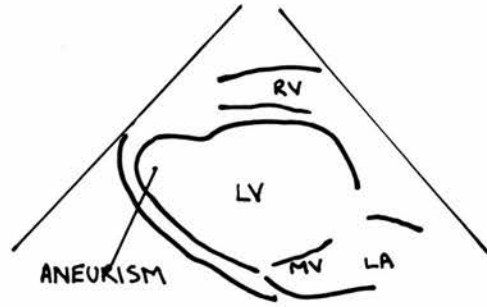
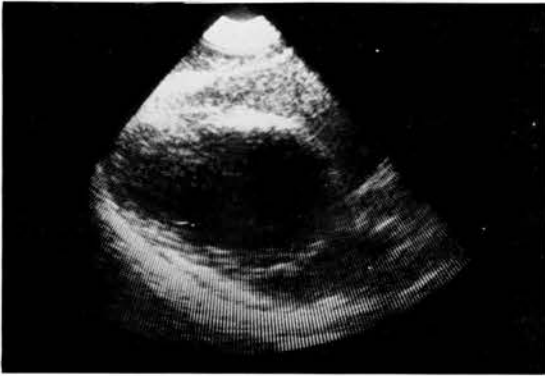


FIGURE 7.6 Patient 47 - Subxiphoid view of apical aneurism and globular left ventricle.

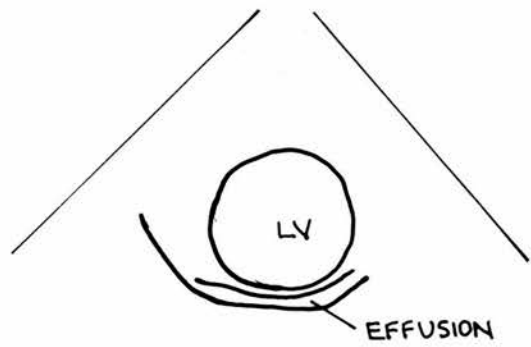


FIGURE 7.6 Patient 35 - Transverse view of posterior pericardial effusion.

ventricular hypokinesia with no difference between the two examinations. Patient 35 was studied three days after infarction. At this stage the posterior and apical left ventricular walls were akinetic. Seven days after infarction there was some improvement in the motion of these walls but they remained grossly hypokinetic. At this stage a small posterior pericardial effusion was demonstrated as shown in figure 7.6. By ten days after infarction there had been further improvement in posterior wall motion and the effusion persisted. Some of these conditions are illustrated in figures 7.6 and 7.7.

7.6.3 CHRONIC OBSTRUCTIVE LUNG DISEASE

This is a group of conditions where the airways in the lungs are narrowed. The narrowing may be intermittent in which case the condition is called bronchial asthma, or constant and accompanied by overproduction of mucus, when it is termed chronic bronchitis. These conditions, particularly chronic bronchitis cause arterial hypoxaemia which causes pulmonary arterial vasoconstriction. This causes pulmonary hypertension and increased strain on the right ventricle, sometimes leading to right ventricular failure, known as cor pulmonale. In both asthma and chronic bronchitis there is increased air trapping in the lungs causing hyperinflation of the lungs and therefore likely parasternal access problems. In any case, assessment of right ventricular function is not best made from the

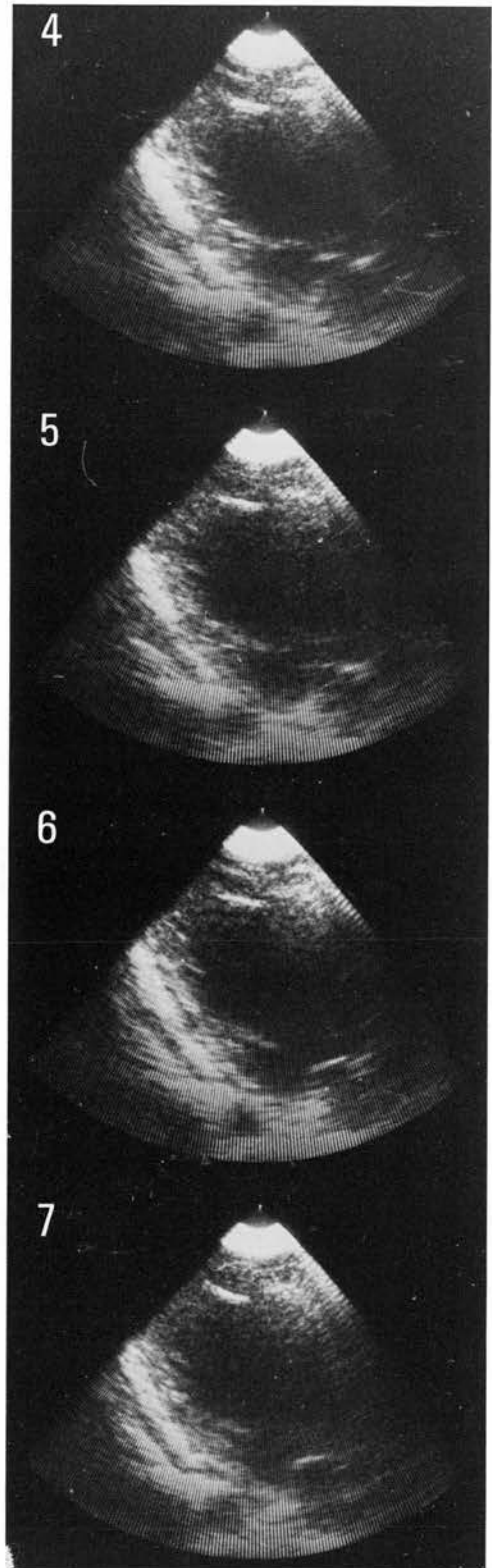
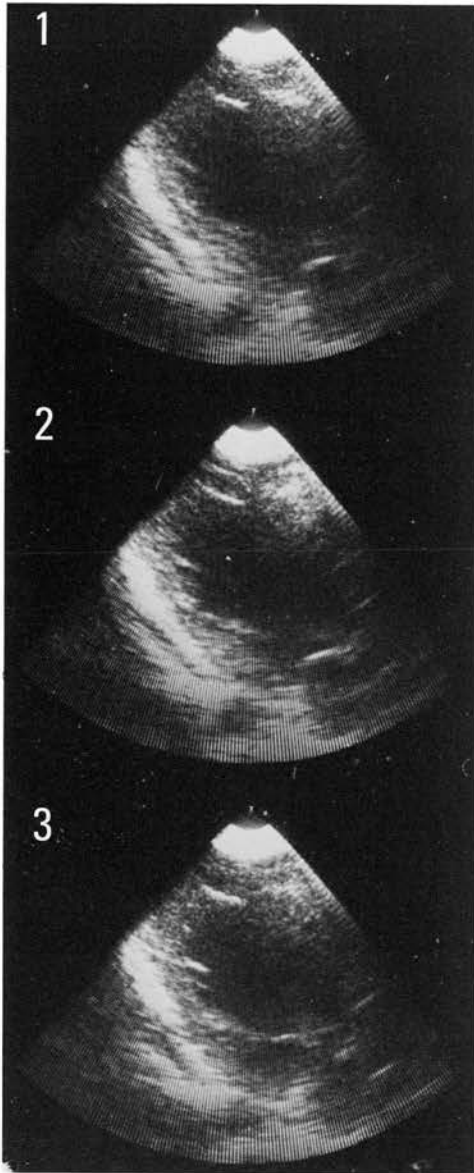
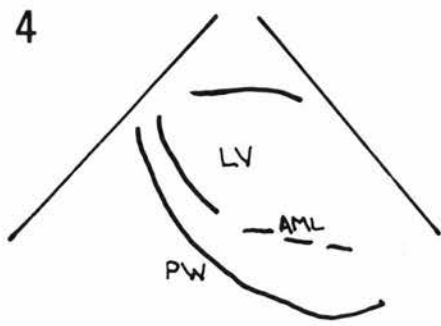


FIGURE 7.7 Patient 47 - Series of seven sequential frames at 1/10th second intervals showing the grossly hypokinetic left ventricle in the longitudinal parasternal view.

parasternal position even although it may be inflated and more easily visualised than normal and therefore the subxiphoid approach is most relevant in this disease.

Of the patients examined, patient 5 had bronchial asthma and patient numbers 8,30,38,48 and 49 had chronic bronchitis. In patients 5 and 8 no abnormality of the heart was detected. In both, parasternal views were obtained and the subxiphoid view was not attempted. In patient 30 both parasternal and subxiphoid views were obtained although the latter approach provided much better images of the heart. No abnormality was detected in this patient. Patients 38, 48 and 49 had more severe bronchitis and patient 49 had cor pulmonale. In these three patients it was impossible to obtain parasternal access due to hyperinflation of the lungs obliterating the echocardiographic window. However in all three patients the subxiphoid approach allowed good visualisation of the heart and enabled the right ventricle to be studied, as can be seen in figure 7.8. Right ventricular contraction was extremely active in all three patients, even in patient 49 who had clinical signs of right ventricular failure. This patient also had pulsus paradoxus, where the arterial pulse volume is reduced on inhalation because of complex mechanisms. It could be seen on the real-time images that the left ventricular volume was reduced during inhalation confirming the presence

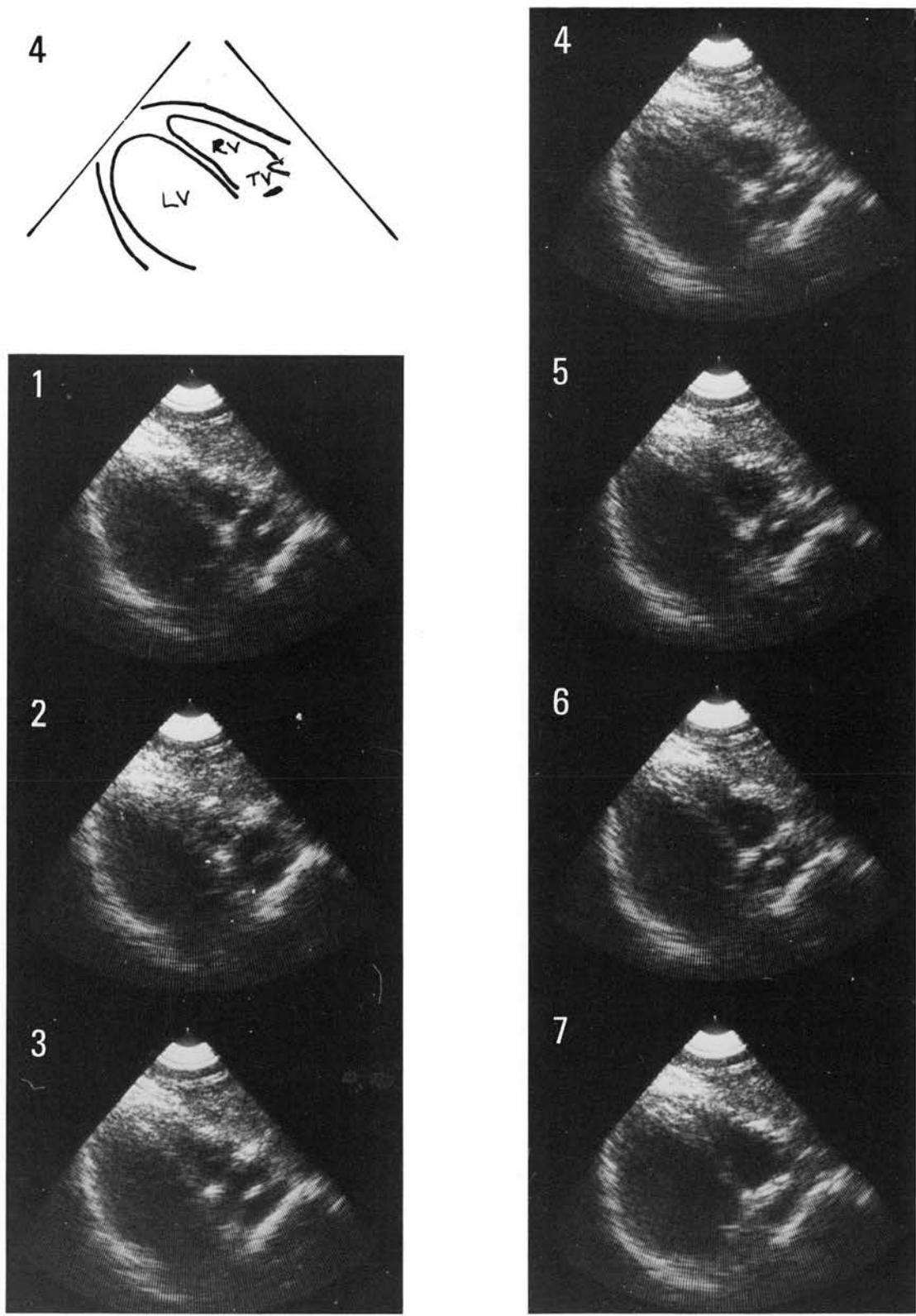


FIGURE 7.8 Patient 48 - Good right ventricular contraction illustrated from the subxiphoid view in these seven consecutive frames.

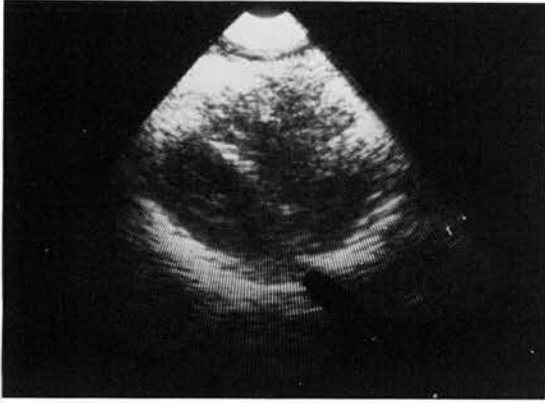
of this condition. Figure 7.9 shows this in two views, both at diastole, one on inhalation and one on exhalation. In addition septal movement was more active during exhalation when the left ventricular volume was larger.

7.6.4 PRIMARY PULMONARY HYPERTENSION

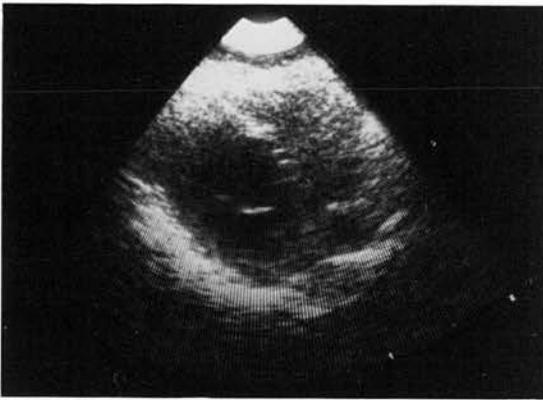
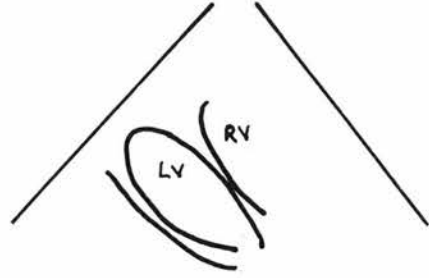
In this condition, the pulmonary arterial pressure becomes progressively elevated causing right ventricular overload and failure and ultimately reduced filling of the left ventricle with a fall in cardiac output and eventually death. No cause is known and there is at present no treatment. The condition is exceptionally rare but two patients (10 and 11) were examined with this condition as the unit referring the patients has a special interest in pulmonary hypertension. In both cases, parasternal views were obtained and both longitudinal and transverse views confirmed dilatation of the right ventricle with the right heart structures being more prominent than usual. Subxiphoid views would have been useful but were not attempted. In patient number 10 the pulmonary valve was thickened.

7.6.5 PERICARDIAL EFFUSION

Pericardial effusion is a collection of fluid lying within the pericardial sac and separating the two layers of pericardium. Many underlying conditions may cause this



DURING INHALATION



DURING EXHALATION

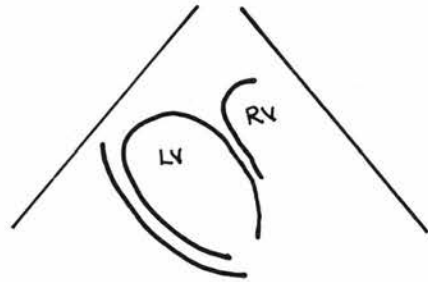
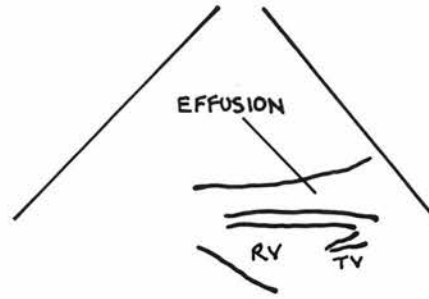
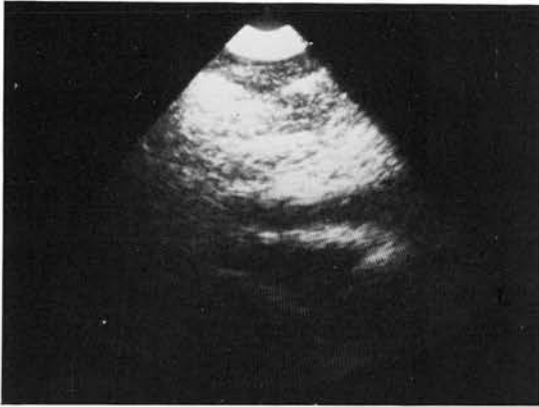


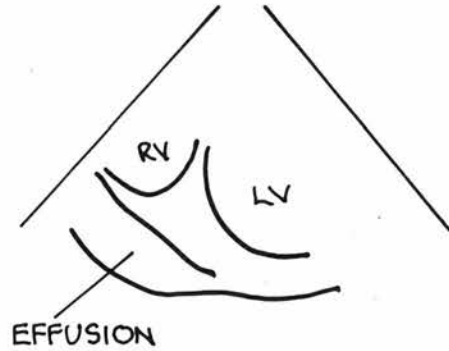
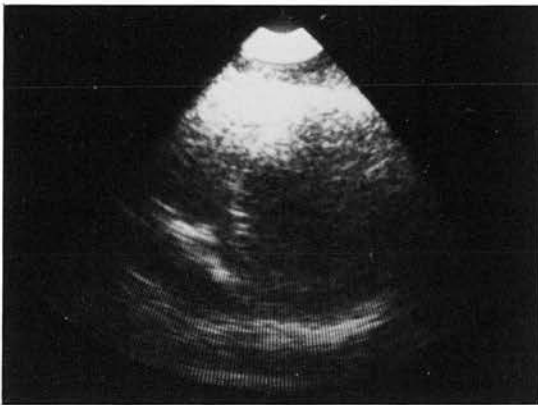
FIGURE 7.9 Patient 49 - Left ventricle at end diastole during inhalation and exhalation demonstrating the different left ventricular dimensions associated with pulsus paradoxus.

As the pericardium is inelastic, a large collection of fluid within the parietal pericardium compresses the heart causing a reduction in cardiac output. Rapid diagnosis is therefore important. Effusions can develop anywhere round the heart and therefore good overall visualisation of the heart wall and differentiation between layers is required. The visualisation of an anterior effusion is best made from the parasternal position. The transverse parasternal view and the subxiphoid view are both useful for locating effusions and especially those in the lateral areas of the heart.

Patient numbers 20, 23, 44 and 45 were referred because of suspected pericardial effusions. A pericardial effusion was demonstrated as an echo free space surrounding the heart in patients 20 and 45 but no effusion was demonstrated in patients 23 and 44. These findings were confirmed by T-M echocardiography, the diagnostic method of choice, in patients 20 and 23. In addition, a small pericardial effusion, which was not clinically suspected, developed in patient 35 who was being studied sequentially for a myocardial infarction. Figure 7.6 shows this in a transverse section. Patient 45 was suspected of having the post-myocardial infarction syndrome. A pericardial effusion was demonstrated and was best seen in the subxiphoid view. This is shown in figure 7.10, but unfortunately the heart



SUBXIPHOID



TRANSVERSE

FIGURE 7.10 Patient 45 - Pericardial effusion seen from the subxiphoid view and the parasternal transverse view.

structure beyond the effusion is not optimal in this recording.

7.6.6 CARDIOMYOPATHY

This is a disorder of cardiac muscle of unknown cause. In one type of cardiomyopathy there is poor contraction of ventricular muscle with resultant biventricular failure. This is termed congestive cardiomyopathy. In another type there is hypertrophy of cardiac muscle, particularly of the interventricular septum in the region of the left ventricular outflow tract. This mimics the effects of aortic stenosis and is termed hypertrophic obstructive cardiomyopathy (HOCM). In HOCM T-M echocardiography is a very useful diagnostic investigation. Suggestive findings are thickening of the interventricular septum and anterior movement of the mitral valve in systole. Patient 15 was suspected of having HOCM. Prominence of the interventricular septum and systolic anterior motion of the mitral valve were present supporting the diagnosis. Figure 7.11 shows this in a sequence of seven frames through systole. This was confirmed on subsequent T-M scanning. Patient 24 had developed biventricular failure shortly after delivery of her first baby. Real-time images revealed enlargement of the cardiac chambers and profound diffuse hypokinesia of the left ventricle, suggesting

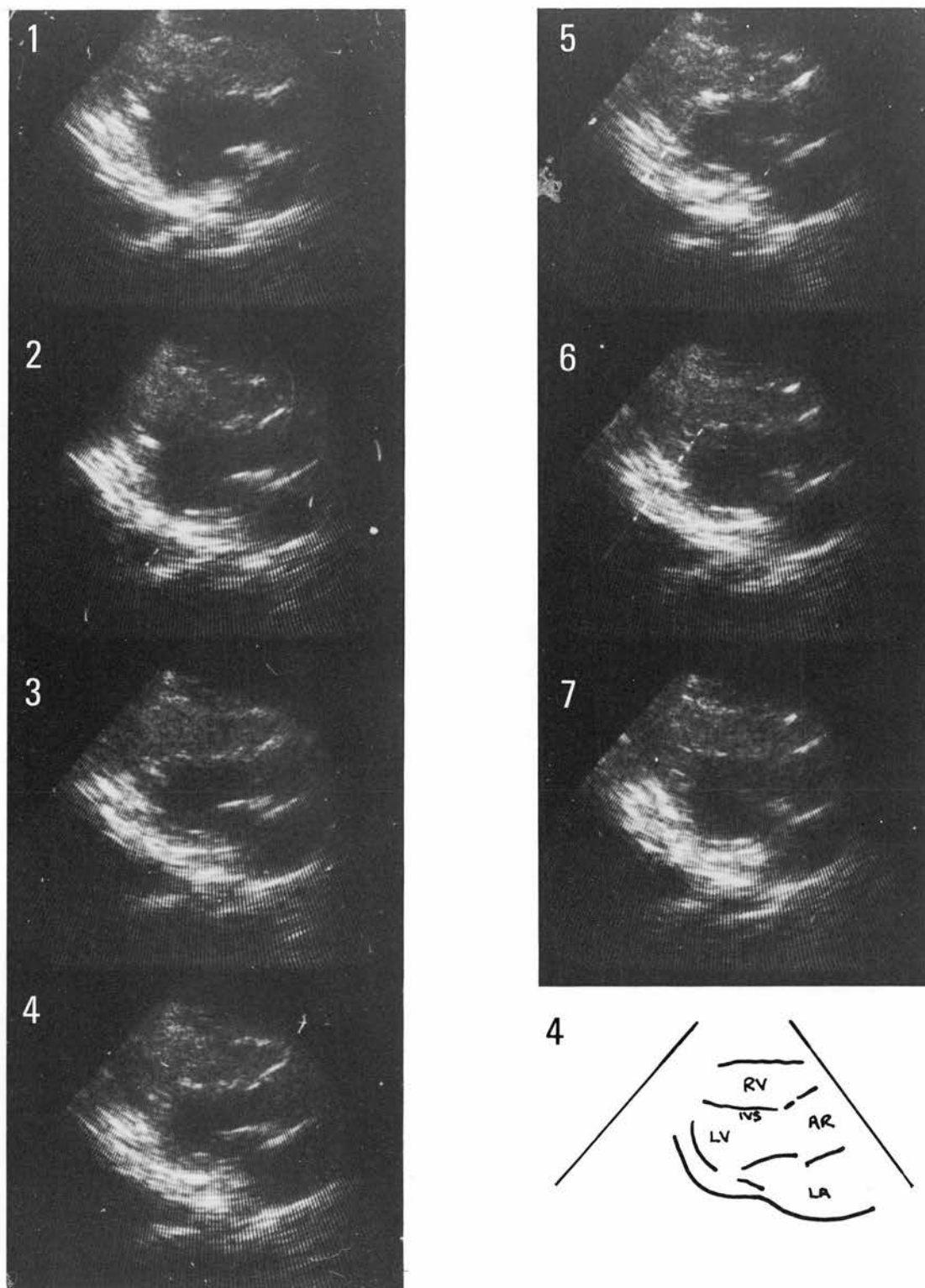


FIGURE 7.11 Patient 15 - Sequence through systole showing systolic anterior motion (SAM) of the septum in accordance with HOCM.

congestive cardiomyopathy.

7.7 GENERAL DISCUSSION

The 50 patients studied with the scanner were consecutive referrals for echocardiographic examination from a general medical unit over a 15 month period. Their clinical diagnosis covered a broad spectrum of cardio-respiratory disease, which allowing for the special interests of the unit is representative of that encountered in general medical practice. The age range of the patients was from 18 to 84 years and the sex distribution was 39 male and 11 female. The patients varied considerably in build from the thin to the grossly obese resulting in a spectrum of chest wall thicknesses, rib cage shapes and costal margin angles. Similarly, the anatomical axis of the heart varied, thinner patients tending to have a vertical heart and more obese patients having a horizontal heart.

Within this wide range of variables there are two factors which consistently reduce visualisation quality. One is lung partially overlying the heart, which can be reduced by exhalation, depending on the degree of overlap. The other is obesity which causes the scanner to be raised above the intercostal space and hence causes rib interference at the extremes of the sector. However, parasternal views were still obtainable even in the grossly

overweight. Female patients with large pendulous breasts proved more difficult to examine satisfactorily, the increase in chest wall thickness providing similar problems to simple obesity. However the small size of the scanner allows it to be applied to the chest wall immediately adjacent to the sternal border, medial to the mass of breast tissue in most cases, while still allowing alignment of the sector plane along the long axis of the heart by rotation of the scanner. Due to the point of entry aspect of the scanner factors such as thin and round chest walls, and narrow costal margin angles do not impede acoustic contact to the patient. Similarly variations in heart orientation present few difficulties.

The only consistent hindrance to subxiphoid access is a rigid abdominal wall or a distended abdomen. The view most affected by these factors is the useful four chamber view. This requires the sector section to approximate to the coronal plane and hence the semi rectangular profile of the scanner to penetrate the costal margin. The less useful sagittal section is not affected to the same extent due to the round profile of the scanner lying more naturally under the costal margin.

Using either the parasternal or subxiphoid approach the mitral valve was satisfactorily visualised in all the

patients and the aortic valve was seen in 88%. Right sided valves were visualised less well, the tricuspid valve being seen in 50% and the pulmonary valve in 22%. In 98% the left ventricle could be identified and good functional assessment could be made in 72% of cases. Although all structures may not be visualised in any one patient, this is not necessarily a diagnostic set-back. Right sided heart valves are only rarely diseased and such disease is commonly associated with right heart enlargement, a factor which improves echocardiographic accessibility to these valves. A general assessment of cardiac chamber size and function can often be made without defining the entire ventricular outline throughout the cardiac cycle. Echocardiography in the form of T-M scanning now has a wide application in the investigation of cardiac disease. It has proved useful particularly in the assessment of the severity of mitral stenosis, by direct measurement of the diastolic closing rate of the mitral valve. The high sampling rate of the T-M technique is required to record the detailed movements of fast moving cusps. It is the current diagnostic method of choice in left atrial myxoma and pericardial effusion and also provides useful information in conditions such as HOCM, COCM and aortic valve disease. Left ventricular function is often assessed by T-M scanning

but the one dimensional information limits its application. Hypokinetic or diskietic areas of left ventricular wall may be completely undetected using T-M scanning. Similarly right ventricular assessment from the subxiphoid is limited.

The real-time images obtained provide information on the overall movement and structure of cardiac valves particularly the mitral and aortic valves. Qualitative information about the valves is readily obtained from the images by an experienced observer, and this is adequate for diagnostic purposes. Thorough examination of the left ventricle allowed small areas of hypokinesia or diskinesia to be located in patients suffering from coronary artery disease. In chronic obstructive lung disease, assessment of the right ventricle has previously proved difficult due to hyperinflation of the lungs. The scanner provides good images of the right ventricle from the subxiphoid approach which have proved useful in the assessment of right ventricular function in this condition. The diagnostic information obtained in the cardiomyopathy and pericardial effusion cases was comparable with that from T-M scanning. A major advantage of real-time scanning is the comparative ease with which the required images were found. T-M scanning demands a considerable amount of training and

practice before satisfactory traces are readily produced. Using the real-time scanner cardiac anatomy was well visualised and appreciated throughout the heart and less training would be needed to obtain good images compared with good T-M traces. The nature of the information from the two techniques differs and at present they compliment each other.

7.8 CONCLUSION

Visualisation of cardiac structures and their movements on a representative group of patients suffering from cardio-respiratory disease has been very successful. The small scanner size and the point of entry sector format has allowed a flexibility in scanning action which has overcome many of the problems associated with ultrasonic access to the heart. Subxiphoid application of the scanner has proved to be possible and very useful clinically. These features along with the high quality grey scale images are a result of the physical considerations made which led to the ultrasonic, mechanical and physical design of the scanner.

8.1 INTRODUCTION

Congenital heart disease is mainly a disease which affects infants and children. The complex congenital anomalies result in major alteration to cardiac anatomy in some cases. T-M echocardiography has been, and still is used to analyse the deformed structures and the logical piecing together of the information is referred to as deductive echocardiography. However since it is visualisation of structure rather than functional assessment which is of primary importance this is an application which lends itself to real-time echocardiography. Linear arrays have been applied successfully to visualise young hearts (Sahn et al., 1974). This success over adult applications is mainly due to the absence of a bony rib cage and a thick chest wall. However linear arrays are limited to views obtained from the parasternal location. Other types of scanner have been used in the parasternal position such as mechanical oscillating scanners (Henry et al., 1975; Houston et al., 1977), and phased arrays. The design of the rotating sector scanner was not influenced by pediatric considerations and in any case, before the potential of the subxiphoid approach was appreciated,

the small field of view in the anterior region of a sector format scan was not considered ideal for visualisation of small hearts. The primary aim in the examination of a congenitally defective heart is to identify cardiac structures and to understand their spatial relationship. The identification of the four chambers, their relative size and the existence of the four heart valves is a major part of any pediatric examination. The success of the subxiphoid four chamber view in adult applications therefore led to the investigation of the acquisition of subxiphoid views on young infants and children. The results of a similar approach using a phased array at the apex of the heart suggest that in the examination of certain congenital defects this approach could give the most valuable views (Silverman and Schiller, 1978).

This chapter deals with the scanning experience on a small group of pediatric patients and discusses possible developments to the scanner design which would optimise this point of entry sector format design for the diagnosis of congenital heart disease in pediatric patients.

8.2 PATIENT GROUP

Six patients with various congenital heart defects were examined. The nature of the defects are not particularly

relevant since variation in the physical size of the subjects is the dominant factor affecting access and visualisation performance. The greatest rate of change of subject size is in the earlier months and years of development and therefore the patient group was selected with particular emphasis on the younger infants. It is with the sick newborn that the risk from cardiac catheterisation is highest and therefore when echocardiographic diagnosis is most useful. The patients selected were as representative as possible from a physical standpoint. All were taken from routine referrals for cardiac catheterisation and cineangiography. The youngest patient was a four day old, three weeks premature baby. The others were nine, ten and twenty one months, and four and nine years old.

8.3 PEDIATRIC ECHOCARDIOGRAPHIC EXAMINATION

The patients are examined in the supine position and longitudinal and transverse views are looked for from an approximate parasternal location. The optimisation of the view required is easier than with adults due to the ultrasonic window being less restricted by bone and lung. This allows both the scanner point of contact and the sector orientation to be easily varied. This view allows the septum, left ventricle and atrium, aorta and

aortic root and both the mitral and aortic valves to be visualised. The right heart structures are less well visualised depending on how anterior they lie.

The relationship between the atrioventricular valve and the semilunar valve is very important in identifying that atrioventricular valve. If the semilunar valve is close to the atrioventricular valve and its root continuous with the atrioventricular valve then it is assumed to be the mitral valve. The tricuspid valve is separated from its semilunar valve by an outflow tract and therefore the root of the semilunar valve is separated by the tissue of the outflow tract from the atrioventricular valve. Having identified the atrioventricular valve then the ventricle can be identified since invariably the left ventricle belongs to the mitral valve and the right to the tricuspid. Therefore if the tricuspid valve is identified in the normal position for the mitral valve then ventricular inversion is diagnosed.

The relationship of the interventricular septum to the aorta is important in diagnosing tetralogy of Fallot, a common congenital defect involving the dilatation and malposition of the aorta. It overrides into the right ventricular outflow tract and is accompanied by an interventricular defect below the aortic root resulting

in a right to left shunt. There are many less common congenital defects which result in a discontinuity at this point or an interatrial septal defect. Left ventricular function can be affected as a result of a congenital defect, such as a valvular defect and therefore the assessment of this contributes indirectly to the diagnosis of the defect.

A transverse view through the left ventricle and valve leaflets is mainly useful for functional assessment of both the ventricle or valve. Since ventricular function is not of primary diagnostic interest, and acquired defects of the mitral valve which affects its function such as mitral stenosis are uncommon, then this view has limited application. However visualisation of the great arteries at the base of the heart from all sector orientations is very desirable since transposition of these arteries is one of the most common anomalies in cyanotic infants. The uncoiling of the pulmonary artery and the aorta as a result of their connection to the left and right side of the heart respectively, causes them to lie parallel to each other. The relative positions of the semilunar valves changes due to this uncoiling, a feature used in T-M examination of this condition.

Visualisation of the bifurcation of the pulmonary artery

allows direct differentiation between the arteries and hence the valves. This is only possible using a two dimensional technique. Examination of these arteries and valves is the most useful of the parasternal transverse applications of the scanner.

Both a subxiphoid and a subhepatic approach are then investigated. The term subxiphoid here meaning application of the scanner anywhere along and below the left costal margin. This allows simultaneous visualisation of the atria and ventricles, the atrioventricular valves and the cardiac septa. Anterior movement of the sector plane brings the aorta and the right ventricular outflow into view while posterior movement can show the pulmonary veins attached to the left atrium. Subhepatic application of the scanner from beneath the right costal margin in a direction towards the child's left shoulder and scanning through the left lobe of the liver produced a similar section to the subxiphoid but tends to improve the visualisation of the interventricular and interatrial septum.

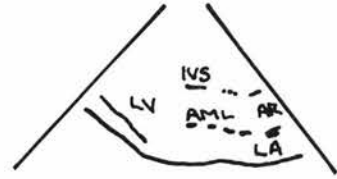
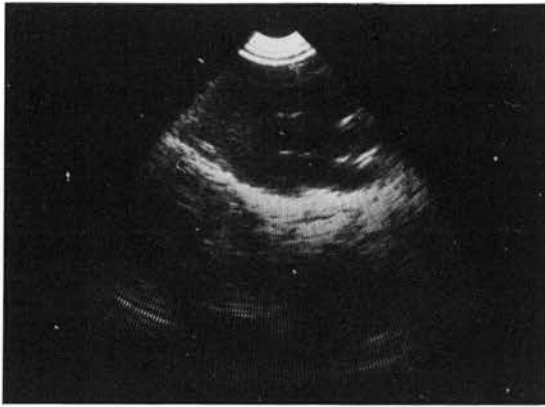
8.4 PRESENTATION OF RESULTS AND DISCUSSION

Some examples of the views described in the previous section are presented here to illustrate the overall visualisation performance achieved. It is only the

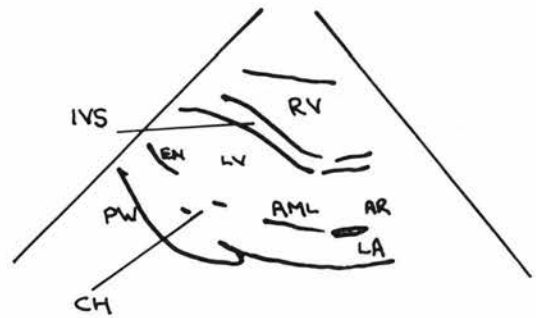
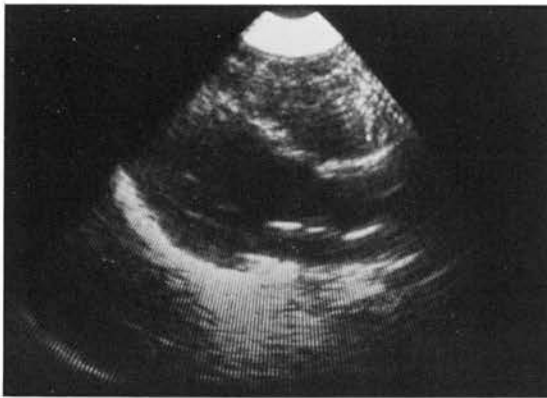
broad aspects of the possibility of pediatric application which have been assessed. The next section discusses possible developments to the scanner design based on these results.

The longitudinal view and variations of it were easily obtained in all six children. The acoustic contact was good allowing a full 90° field of view. The anatomy of the left side of the heart could be appreciated well with the anterior right structures being less well seen through the reverberation noise at the apex of the sector. The septum was seen in all except the newborn baby where visualisation was poor due to the septum being very close to the thin chest wall. However the aortic valve and root, mitral valve, left atrium and the posterior wall of the left ventricle were clearly seen in this small heart. Figure 8.1 illustrates the longitudinal section of a ten month old and a nine year old boy.

The identification of the great arteries and their relative positions from various transverse scans at the base of the heart requires a flexible and delicate scanning action. Appreciation of the anatomy of these small twisting vessels requires a skilled combination of lateral, rotational and angular movements of the



10 MONTH OLD



9 YEAR OLD

FIGURE 8.1 Longitudinal heart section of a 10 month old and a 9 year old child.

scanning plane to optimise the image while following the vessels along their length. This manipulation of scanning plane and the following of structures was executed without difficulty, apart from the lack of patient co-operation periodically in the case of young children. The images of these small anterior structures were not optimal with the scanner as it stands but allowed the field of view and applicability of scanning action to be successfully assessed. The bifurcation of the pulmonary artery was positively seen in one patient.

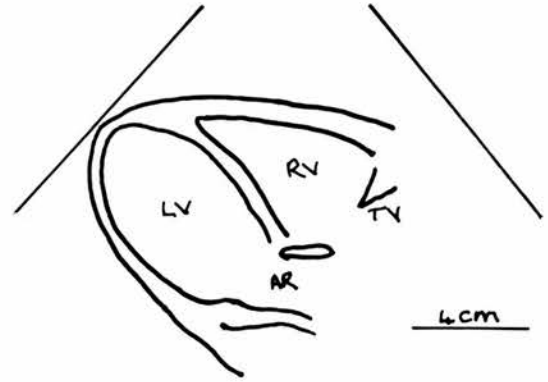
Both the subxiphoid and the subhepatic views were readily obtained in all patients. The young infant has a soft thin abdominal wall which is often slightly distended and a relatively flexible costal margin due to its cartilaginous nature. These features help to counteract the limitations to scanner access and acoustic coupling caused by the lack of fat and soft muscle and the small size of the subject. A full sector view of the complete heart was demonstrated in each case showing all four heart chambers and the atrioventricular valves. It is possible to visualise the great arteries and semilunar valves and their relationship with the atrioventricular valves. Optimal visualisation of the cardiac septa is achieved from the subhepatic approach and has the advantage of

placing the heart further from the scanner in very young infants.

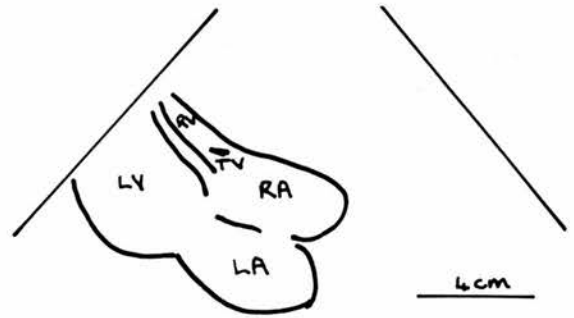
Figure 8.2 shows a subxiphoid and a subhepatic view of a patient with an atrial septal defect. A small moving structure at the centre of the interatrial septum was seen in this patient from the subhepatic approach which could have been the unsealed flap of tissue at the defect, in keeping with a patent foramen ovale. Figure 8.3 shows a subxiphoid view of a 21 month old patient with an interventricular septal defect and the same view of a 10 month old boy suffering from transposition of the great arteries and a defect in both septa.

8.5 POSSIBLE DEVELOPMENTS

Transposition of the great arteries and defects of the septum are both common congenital defects, both of which have gross secondary effects on the heart. These secondary effects such as dilated heart chambers or abnormal septal movement and shape are readily visualised but it is the visualisation of the primary defect which gives a direct diagnosis. While the present scanner has been applied successfully to visualise the heart anatomy of pediatric patients, it could be optimised for direct visualisation of congenital defects from both the parasternal and subxiphoid positions.

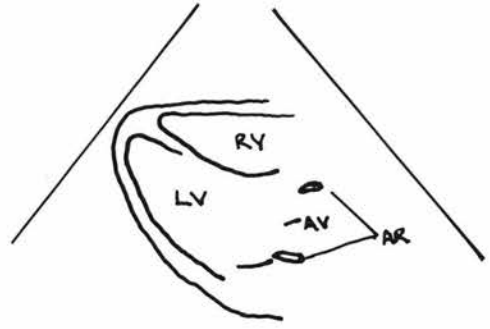


SUBXIPHOID

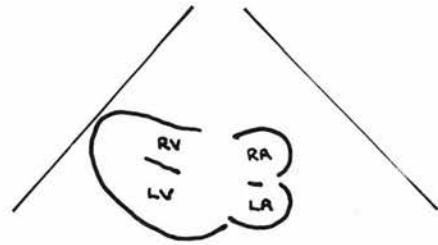
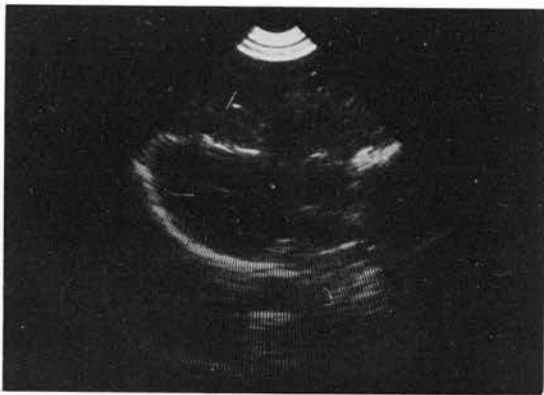


SUBHEPATIC

FIGURE 8.2 Subxiphoid and a subhepatic view of a patient with an atrial septal defect.



10 MONTH OLD



21 MONTH OLD

FIGURE 8.3 Subxiphoid view of a 21 month old patient with an interventricular septal defect and the same view of 10 month old infant suffering from transposition of the great arteries and a defect in both septa.

Due to the reduced depth of penetration required with small hearts the frequency of the transducers could be increased to about 5 MHz and the pulse repetition frequency (PRF) could be increased to between 4 and 5 KHz. The increase in frequency allows smaller diameter transducers to be used while still producing narrow well defined beam shapes which would result in better axial and lateral resolution. The increased PRF results in a proportional increase in image line density for a given frame rate. An increase in frame rate to about 30 frames per second is desirable to allow for the higher heart rate of infants. Apart from the use of different transducers the above changes are only concerned with the way the scanner is driven rather than its design.

However the use of 10mm diameter high frequency transducers would enable six transducers to fit into approximately the same diameter of scanner as four 15mm, 2.5 MHz transducers. This would result in a 60° sector and an increase of 50% in frame rate for a given line density. Alternatively excitation of every second transducer would result in a sector field of view of up to 120° at half the above frame rate or a different compromise between frame rate and line density. With

the option of operating modes, general visualisation of the heart could be performed with the wide field of view and detailed examination of particular defects could be carried out using the smaller field of view with the higher image quality. The use of weakly focussed transducers would reduce the ultrasonic beam width over a chosen working range further improving the resolution of the image.

Alternatively four of the smaller transducers could be inserted in a scanner of reduced diameter with possible acoustic contact advantages in subxiphoid and subhepatic application and in overall scanning flexibility.

However the trade off is a reduced field of view at the skin surface as the scanner diameter decreases. The only area of application where the small field of view is likely to cause concern is in the examination of anterior structures from the parasternal position. A detachable stand off device could solve this problem. At the same time it would remove the reverberation noise in the near field from the anterior parts of the heart image. However the reverberations could be reduced by using a more suitable window material.

During the pediatric trials the performance of a fluid filled stand off device was investigated attached to the

present scanner. It consisted of a water filled, perspex cone shape with a latex rubber membrane at the base of the cone which was coupled to the patient with gel. There were two serious drawbacks to this device. Firstly an inherent problem due to the high PRF causing the regular reverberations within the confined structure to be superimposed on the image. This problem was reduced by lining the cone with rubber and filling it with a suitably absorptive oil. Secondly the flexibility and precision of the scanning action is lost. An oil filled rubber surgical glove was found to be a better alternative acoustically but introduced instability and inconvenience in scanning action. It is concluded that if an increase in field of view is required while scanning anterior structures then the scanner should be raised above the chest wall by about a centimetre using a soft plastic mould which is acoustically coupled to the scanner by gel. Similar adaptors are used with some linear arrays to improve acoustic contact along the length of the array when applied to curved surfaces. Irrespective of the transducer head configuration, easier access to the coronal subxiphoid and subhepatic views could be achieved by offsetting the transducer head to one side of the scanner with the drive and slip rings

and brushes all on the same side of the scanner. This would mean less depression into the abdomen to maintain contact over the scanner window and would not affect access to the subxiphoid sagittal planes or the parasternal views.

Finally, perhaps the benefits of compound real-time imaging could be put to use in pediatric applications. For example two small transducer heads each with four high frequency transducers could be incorporated in the one scanner head and driven together. The small diameter of the two heads would result in a larger overlap of the two 90° sectors while still increasing the field of view anteriorly over a single scanner. There could be significant benefits in both overall visualisation of heart anatomy and in direct visualisation of congenital defects, especially those of the great arteries and septal defects. This design of scanner could be driven in either single or compound mode. Alternatively two scanners could be coupled together only when compound scanning thus maintaining the flexibility of scanning action when using a single scanner.

8.6 CONCLUSION

The early success of linear arrays in pediatric applications perhaps detracted from the development of sector scanners

specifically for pediatrics. However although not designed for pediatric application this design of scanner has the large field of view and flexibility of scanning action required for good visualisation. A major feature over linear arrays is its applicability in the subxiphoid and subhepatic approach. Maintaining the same design philosophy and making some of the discussed modifications would result in a scanning system capable of supplying definitive diagnostic information non-invasively.

REFERENCES

- AMERICAN INSTITUTE OF ULTRASOUND IN MEDICINE (1976)
American Institute of Ultrasound in Medicine standard presentation and labelling of ultrasound images. *Journal of Clinical Ultrasound*, 4(6), 393-398.
- ÅSBERG, A. (1967)
Ultrasonic cinematography of the living heart. *Ultrasonics*, 5, 113-117.
- ÅSBERG, A.G. and HERTZ, C.H. (1967)
Ultrasound pictures of the human heart. Digest of the 7th International Conference on Medical and Biological Engineering, Stockholm, 332.
- ASHBURN, W.L., SCHELBERT, H.R. and VERBA, J.W. (1978)
Left ventricular ejection fraction - A review of several radionuclide angiographic approaches using the scintillation camera. *Progress in Cardiovascular Diseases*, XX(4), 267-284.
- BARBER, F.E., BAKER, D.W., STRANDNESS, JR., D.E., OFSTAD, J.M., and MAHLER, G.D. (1974)
Duplex scanner II: for simultaneous imaging of artery tissues and flow. I.E.E.E. Ultrasonic Symposium Proceedings, 744-748.
- BOM, N., HUGENHOLTZ, P.G., KLOSTER, F.E., ROELANDT, J., POPP, R.L., PRIDIE, R.B. and SAHN, D.J. (1974)
Evaluation of structure recognition with the multiscan echocardiograph. *Ultrasound in Medicine and Biology*, 1, 243-252.

BOM, N., LANCEE, C.T., HONKOOP, J. and HUGENHOLTZ, P.G.
(1971)

Ultrasonic viewer for cross-sectional analysis of moving cardiac structures. Biomedical Engineering, 6, 500-508.

BOM, N., LANCEE, C.T., ZWIETEN, G. VAN., KLOSTER, F.E. and ROELANDT, J. (1973)

Multiscan echocardiography. I. Technical description. Circulation, 48, 1066-1074.

CHANG, S. 1976

M-mode echocardiographic techniques and pattern recognition. Lea and Febiger, Philadelphia.

DEPARTMENT OF HEALTH AND SOCIAL SECURITY, LONDON (1979)
Evaluation of ultrasonic linear real-time scanners.

EDLER, I., GUSTAFSON, A., KARLESFORS, T. and CHRISTENSSON, B. (1961)

Ultrasound cardiography. Acta. Med.Scand.(suppl), 370, 68.

EDLER, I. and HERTZ, C.H. (1954)

Use of ultrasonic reflectoscope for continuous recording of movements of heart walls. Kung. Fysiograf. Sällsk. Lund Förhandling., 24, 40-58

EGGLETON, R.C. and JOHNSTON, K.W. (1974)

Real-time mechanical scanning system compared with array techniques. I.E.E.E. Proceedings in Sonics and Ultrasonics, 16-18.

FEIGENBAUM, H. (1976)

Echocardiography. Lea and Febiger, Philadelphia.

- FEIGENBAUM, H. WALDHAUSEN, J.A. and HYDE, L.P. (1965)
Ultrasound diagnosis of pericardial effusion. Journal
of the American Medical Association, 191(9), 107-110.
- FEIGENBAUM, H., ZAKY, A and NASSER, W.K. (1967)
Use of ultrasound to measure left ventricular stroke
volume. Circulation, 35, 1092-1099.
- FLAHERTY, J.J., CLARK, J.W. and WALGREN, H.N. (1967)
Simultaneous fluoroscope and rapid scan ultrasonic
imaging. Digest of the 7th International Conference
on Medical and Biological Engineering, Stockholm, 321.
- GARRETT, W.J. and KOSSOFF, G. (1975)
An obstetric test for resolution by ultrasonic
echosopes. Ultrasonics, 13, 217-218.
- GEHRKE, J. (1976)
Videasonotomography of the adult heart using the
real-time B-scan technique. Electromedica, 1, 2-5.
- GRAMIAK, R., SHAH, P.H. and KRAMER, D.H. (1969)
Ultrasound cardiography: contrast studies in anatomy
and function. Radiology, 92, 939-948.
- GRAMIAK, R., WAGG, R.C. and SIMON, W. (1973)
Cine ultrasound cardiography. Radiology, 107, 175-180.
- GRIFFITH, J.M. and HENRY, W.L. (1974)
A sector scanner for real-time two-dimensional
echocardiography. Circulation, 49, 1147- 1152.
- GRIFFITH, J.M. and HENRY, W.L. (1978)
An ultrasound system for combining cardiac imaging
and Doppler blood flow measurement in man.
Circulation, 57, 925-930.

- HENRY, W.L., MARON, B.J. and GRIFFITH, M.J. (1977)
Cross-sectional echocardiography in the diagnosis of congenital heart disease: Identification of the relation of the ventricles and great arteries. *Circulation*, 56, 267-273.
- HENRY, W.L., MARON, B.J., GRIFFITH, J.M., REDWOOD, D.R. and EPSTEIN, S.E. (1975).
Differential diagnosis of anomalies of the great arteries by real-time two-dimensional echocardiography *Circulation*, 51, 283-291.
- HOLM, H.H., KRISTENSEN, J.K., PEDERSEN, J.F., HANCKE, S. and NORTHEVED, A. (1975).
A new mechanical real-time ultrasonic scanner. *Ultrasound in Medicine and Biology*, 2, 19-23.
- HOUSTON, A.B., GREGORY, N.L. and COLEMAN, E.N. (1977).
Two-dimensional sector scanner echocardiography in cyanotic congenital heart disease. *British Heart Journal*, 39, 1076-1081.
- HOUSTON, A.B., GREGORY, N.L., SHAW, A., WHEATLEY, D.J. and COLEMAN, E.N. (1977)
Two-dimensional echocardiography with a wide angle (60°) sector scanner. *British Heart Journal*, 39, 1071-75.
- KAMBE, T., NISHIMURA, K., HIBI, N., SAKAKIBARA, T., KATO, T., FUKUI, Y., ARAKAWA, T., TATEMATSU, H., MIWA, A., TADA, H. and SAKAMOTO, N. (1977)
Clinical application of high speed B mode echocardiography. *Journal of Clinical Ultrasound*, 5 (3), 202-207.

- KING, D.L. (1972)
Cardiac ultrasomography: A stop-action technique for imaging intracardiac anatomy. *Radiology*, 103, 387-392.
- KING, D.L., STEEG, C.N. and ELLIS, K. (1973)
Visualisation of ventricular septal defect by cardiac ultrasonography. *Circulation*, 48, 1215-1220.
- KINSLER, L.E. and FREY, A.R. (1962)
Fundamentals of Acoustics, second edition, 136-142, John Wiley.
- KISSLO, J.A., ROBERTSON, D., GILVERT, B.W., VON RAMM, O. and BEHER, V.S. (1977)
A comparison of real-time, two-dimensional echocardiography and cineangiography in detecting left ventricular asynergy. *Circulation* 55, 134-141.
- KISSLO, J., VON RAMM, O.T. and THURSTONE, F.L. (1976)
Cardiac imaging using a phased array ultrasound system. II Clinical technique and application. *Circulation*, 53, 263-267.
- KOSSOFF, G. (1966)
The effect of backing and matching on the performance of piezoelectric ceramic transducers. *I.E.E.E. Transactions on Sonics and Ultrasonics* SU-13(1), 20-30.
- KOTLER, M.N., SEGEL, B.L., MINTZ, G. and PARRY, W.R. (1977)
Pitfalls and limitations of M-mode echocardiography. *American Heart Journal*, 94(2), 227-249.

KRATOCHWIL, A., JANTSCH, C., MÖSSLACHEY, H., SLANY, J.
and WENGER, R. (1974)

Ultrasonic tomography of the heart, *Ultrasound in
Medicine and Biology*, 1, 275-281.

LIEPPE, W., SCALLION, R., BEHAR, V.S. and KISSLO, J.A. (1977)

Two-dimensional echocardiographic findings in atrial
septal defect. *Circulation*, 56, 447-456.

McDICKEN, W.N., ANDERSON, T., McHUGH, R., BOW, C.R.,
BODDY, K and COLE, R. (1979)

An ultrasonic real-time scanner with pulsed Doppler
and T-M facilities for fetal breathing and other
obstetrical studies. *Ultrasound in Medicine and
Biology*, (in press).

McDICKEN, W.N., BRUFF, K. and PATON, J. (1974)

An ultrasonic instrument for rapid B-scanning of the
heart. *Ultrasonics*, 12, 269-272.

McHUGH, R., McDICKEN, BOW, C.R., ANDERSON, T. and
BODDY, K. (1978)

An ultrasonic pulsed Doppler instrument for monitoring
human fetal breathing in utero. *Ultrasound in Medicine
and Biology*, 3, 381-384.

MANLEY, M.T. (1977)

The prediction and diagnosis of heart disease by non-
invasive methods. In "Physical techniques in medicine",
Vol. 1, 287-312. (ed. J.T. McMullan). John Wiley.

PEDERSEN, J.F. and NORTHEVED, A. (1977)

An ultrasonic multitransducer scanner for real-time
heart imaging. *Journal of Clinical Ultrasound*, 5(1),
11-15.

POSAKONY, G.J. (1975)

Engineering aspects of ultrasonic piezoelectric transducer design. I.E.E.E. Ultrasonic Symposium Proceedings, Cat. No., 75 CHO 994-4SU, 1-9.

REDWOOD, M. (1963)

A study of waveforms in the generation and detection of short ultrasonic pulses. Applied Materials Research, 2, 76-84.

REID, J.M. (1966)

A review of some basic limitations in ultrasonic diagnosis. In "Diagnostic Ultrasound" (ed. C.C. Grossman, J.H. Holmes, C. Joyner and E.W. Purnell) 1-12, Plenum Press, New York.

REID, J.M., SIGELMANN, R.A., NASSER, M.G. and BAKER, D.W. (1969)

The scattering of ultrasound by human blood. Abstr. 8th Int. Congr. Med. Biol. Engng., 10-17.

ROELANDT, J. KLOSTER, K.E., CATE, F.J. TEN, DORP, W.G. VAN, HONKOOP, J., BOM, N and HUGENHOLTZ, P.G. (1974)

Multidimensional echocardiography. British Heart Journal, 36, 29-43.

SAHN, D.J., HENRY, W.L., ALLEN, D.H., GRIFFITH, J.M. and GOLDBERG, S.J. (1977)

The comparative utilities of real-time cross-sectional echocardiographic imaging systems for the diagnosis of complex congenital heart disease. American Journal of Medicine, 63, 50-60.

SAHN, D.J., TERRY, R., O'ROURKE, R., LEOPOLD, G. and
FRIEDMAN, W.F. (1974)

Multiple crystal cross-sectional echocardiography in
the diagnosis of cyanotic congenital heart disease.
Circulation, 50, 230-238.

SCHILLER, N. and SILVERMAN, N.H. (1977)

Apex echocardiography: A new method of imaging the adult
heart using a phased array real-time two-dimensional
sector scanner (abstr.) American Journal of
Cardiology, 39, 279.

SILVERMAN, N.H. and SCHILLER, N.B. (1978)

Apex echocardiography: A two-dimensional technique for
evaluating congenital heart disease. Circulation, 57,
503-511.

SKOLNICK, M.L. and MATZUK, T. (1978)

A new ultrasonic real-time scanner featuring a servo-
controlled transducer displaying a sector image.
Radiology, 128, 439-445.

SOMER, J.C. (1968)

Electronic sector scanning for ultrasonic diagnosis.
Ultrasonics, 6, 153-159.

STOCKHAM, JR. T.G. (1972)

Image processing in the context of a visual model.
Proceedings of the I.E.E.E., 60(7), 828-842.

THURSTONE, F.L. and VON RAMM, O.T. (1974)

A new ultrasound imaging technique employing two-
dimensional electronic beam steering. In "Acoustical
Holography" (ed. P.S. Green) 5, 149-159, Plenum Press,
New York.

UPTON, M.T. and GIBSON, D.G. (1978)

The study of left ventricular function from digitized echocardiograms. Progress in Cardiovascular Diseases, XX(5), 359-384.

WAGG, R.C. and GRAMIAK (1974)

Computer-controlled two-dimensional cardiac motion imaging. Proceedings of the I.E.E.E. Ultrasonics Symposium, 12-15.

WELLS, P.N.T. (1974)

Ultrasonic Doppler probes. In "Cardiovascular Applications of Ultrasound" (ed. R.S. Reneman) 125-131, North Holland, Amsterdam.

WELLS, P.N.T. (1977)

Biomedical Ultrasonics. Academic Press, London, New York and San Francisco.

WEYMAN, A.E., HEGER, J.J., KRONIK, T.G., WANN, L.S., DILLON, J.C. and FEIGENBAUM, H. (1977)

Mechanism of paradoxical early diastolic septal motion in patients with mitral stenosis: A cross-sectional echocardiographic study. American Journal of Cardiology, 40(5), 691-699.

WEYMAN, A.E., WANN, S., FEIGENBAUM, H. and DILLON, J.C. (1976)

Mechanism of abnormal septal motion in patients with and without right ventricular volume overload: A cross-sectional echocardiographic study. Circulation, 54, 179-186.

VON RAMM, O.T. and THURSTONE, F.L. (1976)

Cardiac imaging using a phased array ultrasound system. I, system design. Circulation, 53, 258-262.

P U B L I S H E D P A P E R S

BOW, C.R., McDICKEN, W.N., ANDERSON, T., SCORGIE, R.E. and MUIR, A.L. (1979)

A rotating transducer real-time scanner for ultrasonic examination of the heart and abdomen. *British Journal of Radiology*, 52, 29-33.

McDICKEN, W.N., ANDERSON, T., McHUGH, R., BOW, C.R., BODDY, K., and COLE, R. (1979)

An ultrasonic real-time scanner with pulsed Doppler and T-M facilities for fetal breathing and other obstetrical studies. *Ultrasound in Medicine and Biology*, (in press).

McHUGH, R., McDICKEN, W.N., BOW, C.R., ANDERSON, T. and BODDY, K. (1978)

An ultrasonic pulsed Doppler instrument for monitoring human fetal breathing in utero. *Ultrasound in Medicine and Biology*, 3, 381-384.

A rotating transducer real-time scanner for ultrasonic examination of the heart and abdomen

By C. R. Bow, B.Sc., W. N. McDicken, B.Sc., Ph.D., and T. Anderson,

Department of Medical Physics and Medical Engineering, Royal Infirmary, Edinburgh EH3 9YW, Scotland

and R. E. Scorgie, M.B., Ch.B., M.R.C.P., and A. L. Muir, M.D., F.R.C.P.E.

Department of Medicine, Royal Infirmary, Edinburgh EH3 9YW, Scotland

(Received April, 1978 and in revised form August, 1978)

ABSTRACT

A mechanical real-time ultrasonic scanner utilizing a rotating transducer head has been successfully applied clinically to visualize the heart and abdomen. The design features of this scanner are discussed. The small dimensions and the 90° field of view of the sealed oil-filled transducer head optimize visualization of the heart avoiding bone and lung. The single point of entry aspect of this scanner results in a good field of view from any point on the abdominal surface. For example, in upper abdominal studies the liver and kidney can be readily viewed. Rapid and thorough searching of the abdomen is easily carried out and good quality selected sections can be captured by optimizing frame rate and angle of view. In obstetrical applications the complete mature fetus can be visualized using the alternative large 180° field of view.

Real-time ultrasonic imaging allows visualization of dynamic structures and removes patient movement artifacts while scanning through static structures. The ultrasonic beam is rapidly moved by mechanical or electronic means to form the real-time images. This paper describes a mechanical real-time scanner which has been designed to overcome the anatomical problems encountered in clinical applications. By rotating standard transducers through a chosen sector, images are formed using a constant well defined beam shape at all angles in that sector.

Oscillating mechanical scanners have been developed for real-time echocardiography (Griffith and Henry, 1974; Flaherty *et al.*, 1967; McDicken *et al.*, 1974). A rotating transducer scanner in which the transducers are swept across the skin surface has been developed primarily for scanning the abdomen (Holm *et al.*, 1975). A rotating transducer scanner has also found application in visualizing superficial blood vessels. In this assembly the transducers are coupled to the patient's skin via a water bath (Barber *et al.*, 1974). Electronic real-time scanners take the form of linear arrays or phased arrays (Bom *et al.*, 1971; Kisslo *et al.*, 1976; Somer, 1968; Von Ramm and Thurstone, 1976). Electronic scanners have the advantage of having no moving parts. Ultrasonic access to the patient is often limited when linear arrays are employed due to gas, bone and difficulty in coupling to curved body surfaces. At present phased arrays are expensive and have a limited field of view.

Although the scanner described here is well suited to visualization of the abdomen it was initially designed for cardiac studies. A small point of entry device was desirable to avoid ribs, sternum and lung interfering with the ultrasonic beam while giving the freedom to visualize more than one plane of view simultaneously using multiple scanners. The restricted dimensions also allow two or more scanners to be used at adjacent intercostal spaces. It also retains the flexibility of scanning of a single transducer which has been used successfully in cardiac T-M mode scanning. The rotating transducer has been used successfully in cardiology, obstetrics and general abdominal scanning.

DESCRIPTION

A mechanical real-time rotating scanner was developed after investigating the feasibility of heart visualization using oscillating and rotating transducer techniques. The rotating head consists of four 1.5 cm diameter, 2.5 MHz transducers inserted into a 3 cm diameter wheel. Similar transducers are used in static B-scanning applications and are known to produce high quality images. The crystal faces are evenly spaced round the periphery of the wheel with an angular separation of 90°. The wheel rotates within an oil filled cylindrical cavity and electrical coupling to the transducers is via gold slip rings and brushes. Acoustic coupling to the patient is maintained by gel between the thin Perspex (Plexiglass) outer wall of the cavity and the skin. This avoids any moving parts coming into direct contact with the patient. Figure 1 shows the transducer head which is driven by a d.c. motor via a gearbox and belt-drive. The scanner is presented hand-held in Fig. 2.

The transducers are pulsed while they pass through the 90° sector of the head which is in contact with the patient. A 90° sector image is produced each time a transducer sweeps through this sector and therefore the frame rate is four times the angular velocity of the transducer head. This is varied by controlling the d.c. motor speed, and frame rates up to approximately 40 frames per second are possible. The pulse repetition frequency (PRF) of the A-scan

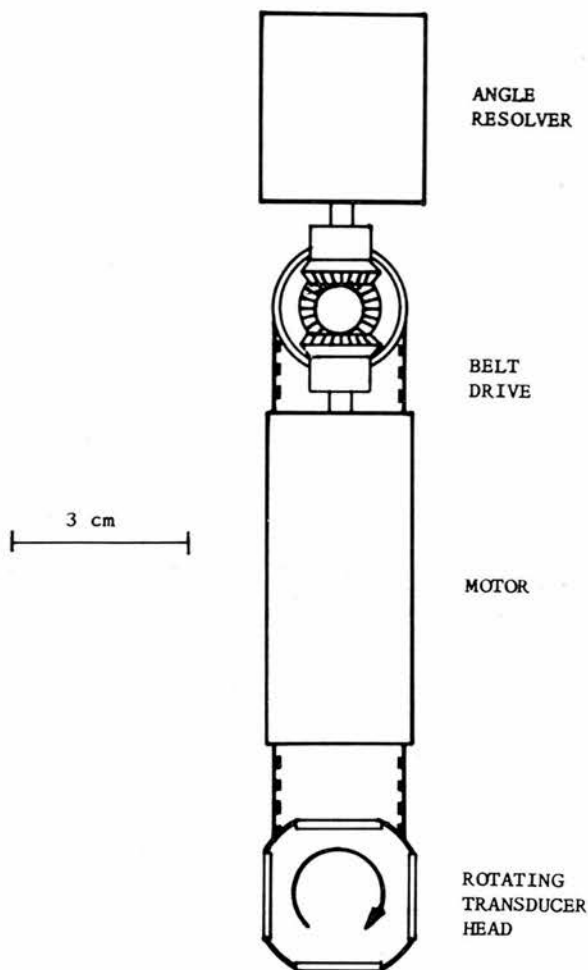


FIG. 1.

Schematic diagram of scanner components.

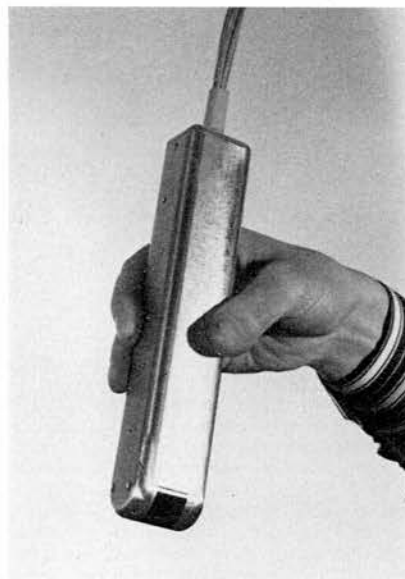


FIG. 2.
Scanner hand held.

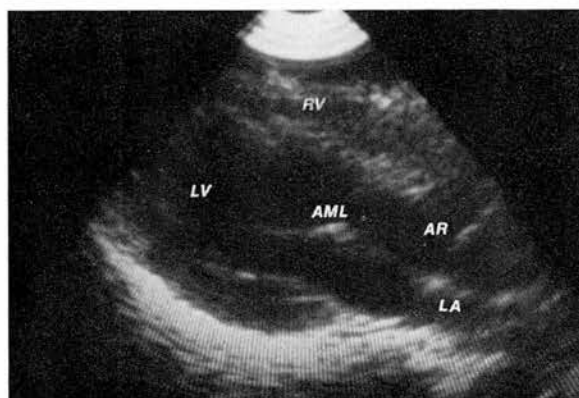


FIG. 3.

Longitudinal section of the heart corresponding to frame eight of Fig. 4 showing left ventricle (LV), right ventricle (RV), left atrium (LA), aortic root (AR), anterior mitral leaflet (AML), aortic valve, septum and endocardium in the left ventricle.

transmitter is 3000 Hz and therefore at 20 frames per second a 90° sector image contains 150 evenly spaced lines.

The angular position of the ultrasound beam is measured by a resolver which is driven in phase with the transducer head. This angular information is used to locate the individual lines of the image. Synchronization pulses are obtained from an optoelectronic timing device. The individual lines are written at the pulse repetition frequency on a gray scale display to generate a single sector image. These sectors are then refreshed at the frame rate and yield real-time gray scale images.

DISCUSSION

A 3 cm diameter wheel allows two scanners to operate at adjacent intercostal spaces. Preliminary

tests simulating a 1.5 cm diameter transducer rotating within these dimensions showed that 50° to 80° sector images of the heart were feasible without rib interference. However, although sector angle is limited in heart visualization it need not be in other areas of application. If two opposing transducers are excited instead of four then a 180° sector is possible, the actual angle of view being determined by the acoustic contact made with the patient. Because of

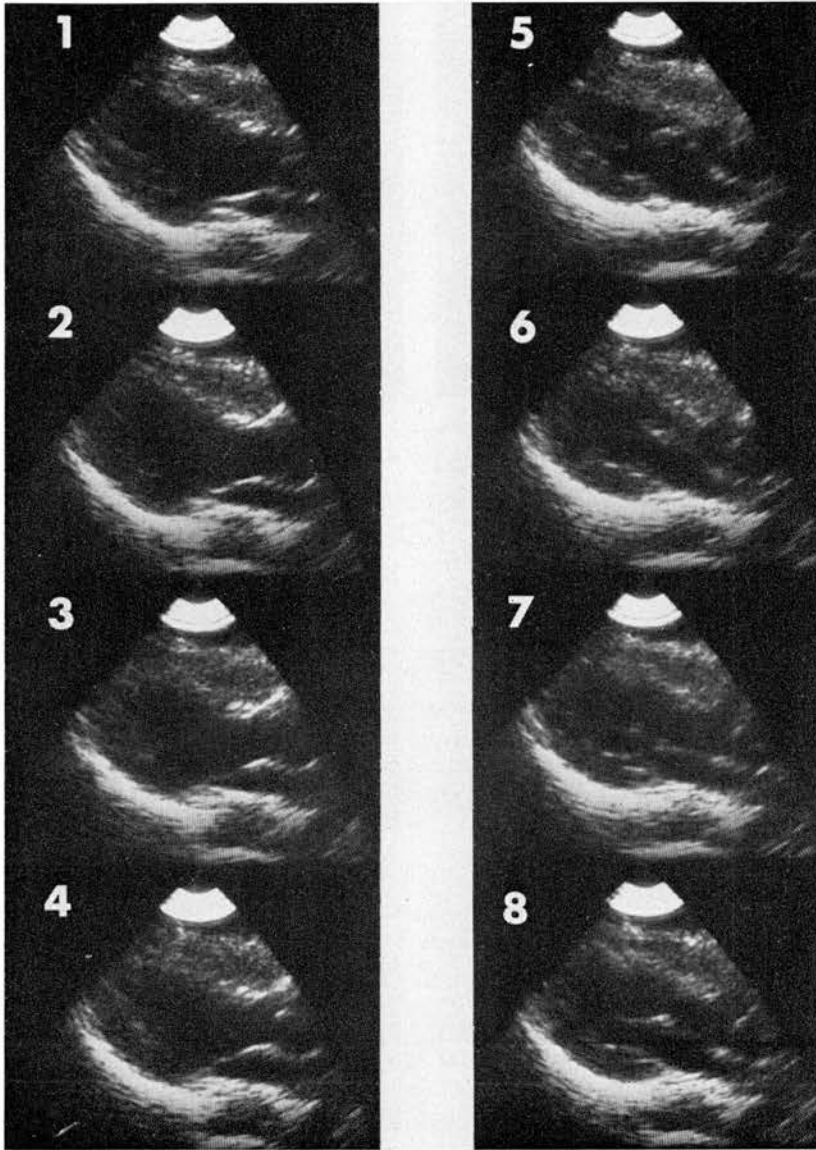
A rotating transducer real-time scanner for ultrasonic examination of the heart and abdomen

FIG. 4.

Series of eight successive cine frames at 1/10th second intervals showing the action of the longitudinal section of the heart.

the small diameter of the sealed head this can be in the range 120° to 150° for abdominal scans. Depression into the abdomen to increase contact angle does not mechanically load the rotating head and gel is not removed by any moving parts.

Used in this mode on the abdomen a wide angle of view can be used to search for a specific section of interest with the scanning device either hand held or connected to the scanning arm of a conventional

B-scan unit. The rotation speed of the transducer head can be adjusted to optimize frame rate and line density while searching. Having found a section of interest the operator then has the choice of the two or four transducer mode to optimize angle of view or frame rate and line density. Alternatively using a single slow sweep of the ultrasonic beam the scanner can produce a high line density image of quality similar to that of a conventional B-scan unit.

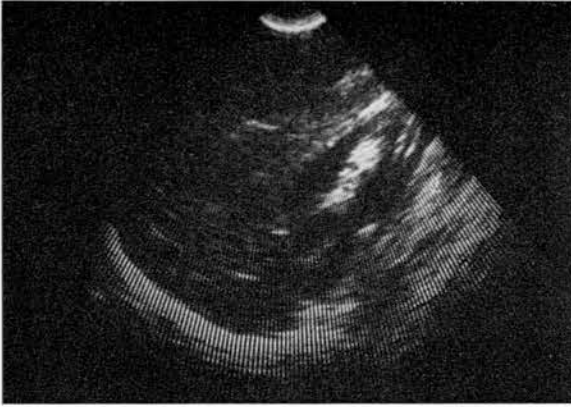


FIG. 5.

Longitudinal scan of upper abdomen showing liver and kidney.

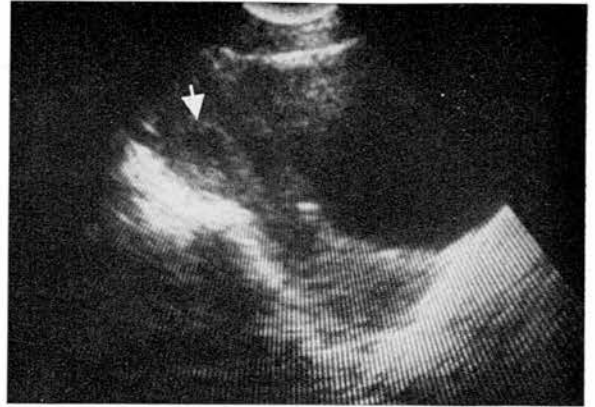


FIG. 6.

Early pregnancy. Arrow indicates gestation sac containing fetus.

A T-M trace can be generated from any one line in the section being imaged by gating this line out of every frame and brightness modulating a fibre optic chart recorder with the echo signals. The sampling rate (effective PRF) of this trace is that of the frame rate which can be increased having selected the line of interest in the section of high line density. Alternatively the scanner can be stopped with one transducer in a selected direction and a conventional T-M record made. This provides a high quality T-M record due to the high pulse repetition frequency and resolution of the ultrasonic signals.

Recording of real-time images can be achieved using a TV camera and video tape recorder. Instant playback of real-time images on a TV display is therefore possible and the recording material is reusable. For cardiac work good quality still frames are required at specific parts of the cardiac cycle for quantitative analysis. A stop action facility which provides distortion free single frames is available on the more expensive TV systems. Real-time scan converters also offer this facility and are being developed at present. A less expensive alternative is to use a cine camera synchronized with the scanner frame rate and to record every second ultrasonic frame. Alternate frames are not recorded during the cine film pull down time. The film is not instantly replayable but renders good quality still frames for analysis.

The mechanical scanner described makes use of standard transducers which can be driven by a conventional ultrasonic unit. Therefore when interfaced to such a unit it can be regarded as an accessory with obvious cost advantages over electronic scanners which require a unique electronic drive.

Due to its compact sealed design the scanner is suitable for visualization of the heart and abdomen as a hand held device. Figure 3 shows a longitudinal section of the heart which is a single frame from the series of successive frames illustrated in Fig. 4. A view of liver and kidney is shown in Fig. 5. In obstetrical applications maintenance of acoustic contact with the distended abdomen presents no problem due to the head size and therefore good large views are always possible. An example of a scan in early pregnancy is shown in Fig. 6.

A horizontal tubular version containing a similar sealed transducer head has been used to monitor fetal heart and breathing movements (McHugh *et al.*, 1978). This compact device can be strapped on to the abdomen once the appropriate section has been selected. A possible development of this format of device is to reduce its overall diameter and, using a single transducer head, achieve a 360° field of view for internal PPI scanning.

CONCLUSION

The rotating transducer scanner described has been successfully used in routine clinical applications. In initial trials 50 cardiac patients have been thoroughly examined. The device has also been used on approximately 300 obstetrics cases.

At present the large majority of real-time scanners commercially available are of the electronic type. The performance of the hand-held mechanical scanner described in this paper has been very acceptable in a range of clinical applications. This performance has resulted from the combination of the following design features. The use of modern standard transducers produces high resolution images

A rotating transducer real-time scanner for ultrasonic examination of the heart and abdomen

and allows the device to be easily interfaced with conventional B-scan equipment. Rotation of the transducers in an oil filled chamber provides vibration-free coupling to the patient. The small size of the scanning head results in large fields of view from single points of entry on the skin surface.

ACKNOWLEDGMENTS

We wish to acknowledge the support and encouragement of Professor J. R. Greening throughout this project. We are also indebted to Mr. R. Borthwick for his expertise during the mechanical construction. One of us, C. R. Bow, is grateful for a Scholarship provided by the Faculty of Medicine of the University of Edinburgh.

REFERENCES

- BARBER, F. E., BAKER, D. W., STRANDNESS, JR., D. E., OFSTAD, J. M., and MAHLER, G. D., 1974. Duplex Scanner II: for simultaneous imaging of artery tissues and flow. *I.E.E.E. Ultrasonic Symposium Proceedings*, 744-748.
- BOM, N., LANCEE, C. T., HONKOOP, J., and HUGENHOLTZ, P. G., 1971. Ultrasonic viewer for cross-sectional analysis of moving cardiac structures. *Biomedical Engineering*, 6, 500-508.
- FLAHERTY, J. J., CLARK, J. W., and WALGREN, H. N., 1967. Simultaneous fluoroscopic and rapid scan ultrasonic imaging. Digest of the 7th International Conference on Medical and Biological Engineering, Stockholm, 321.
- GRIFFITH, J. M. and HENRY, W. L., 1974. A sector scanner for real-time two-dimensional echocardiography. *Circulation*, 49, 1147-1152.
- HOLM, H. H., KRISTENSEN, J. K., PEDERSEN, J. F., HANCKE, S., and NORTHEVED, A., 1975. A new mechanical real-time ultrasonic scanner. *Ultrasound in Medicine and Biology*, 2, 19-23.
- KISSLO, J., VON RAMM, O. T., and THURSTONE, F. L., 1976. Cardiac imaging using a phased array ultrasound system. II. Clinical techniques and application. *Circulation*, 53, 262-267.
- MCDICKEN, W. N., BRUFF, K., and PATON, J., 1974. An ultrasonic instrument for rapid B-scanning of the heart. *Ultrasonics*, 12, 269-272.
- MCHUGH, R., MCDICKEN, W. N., BOW, C. R., ANDERSON, T., and BODDY, K., 1978. An ultrasonic pulsed Doppler instrument for monitoring humal fetal breathing in utero. *Ultrasound in Medicine and Biology*, 3, 381-384.
- SOMER, J. C., 1968. Electronic sector scanning for ultrasonic diagnosis. *Ultrasonics*, 6, 153-159.
- VON RAMM, O. T., and THURSTONE, F. L., 1976. Cardiac imaging using a phased array ultrasound system. I. System design. *Circulation*, 53, 258-262.

AN ULTRASONIC PULSED DOPPLER INSTRUMENT FOR MONITORING HUMAN FETAL BREATHING IN UTERO

R. MCHUGH, W. N. MCDICKEN, C. R. BOW and T. ANDERSON
Department of Medical Physics, Royal Infirmary, Edinburgh EH3 9YW, Scotland
and

K. BODDY
Department of Obstetrics and Gynaecology, University of Edinburgh, Edinburgh, Scotland

(First received 30 May 1977; and in final form 27 July 1977)

Abstract—Fetal breathing movements in human pregnancy are being studied extensively at present, since preliminary results suggest they may be a valuable indicator of fetal welfare.

An ultrasonic pulsed Doppler instrument designed to monitor such fetal movements over long periods of time has been developed. This instrument operates with a single 2.5 MHz transducer strapped onto the maternal abdomen and monitors the velocity of movement within the fetal chest or abdomen. The system incorporates a Real-Time *B*-scanner mechanism to enable an initial search and identification of the fetal structure.

This instrument is simpler to operate and demands less skill of the operator than the *A*-scan plus *T-M* scan technique. A comparison of simultaneous recordings obtained with an *A*-scan plus *T-M* scan instrument and with the pulsed Doppler instrument is presented.

Key words: Ultrasonic, Fetus, Breathing, Pulsed Doppler, Real-Time *B*-scan, Monitoring.

INTRODUCTION

Initially, fetal breathing was detected using the *A*-scan technique (Boddy and Robinson, 1971) employing an *A*-scan instrument with a gated *T-M* scan facility. More recently Real-Time *B*-scan machines have been used to observe the actions of fetal breathing movements and to assist in the location of the fetal anatomy (Marshal *et al.*, 1976). Neither of these instruments is very suitable for long term recordings. The *A*-scan plus gated *T-M* trace method has the disadvantage in that it relies on there always being a distinct chest or abdominal wall echo lying within its gated range (Farman *et al.*, 1975). To obtain an uninterrupted and meaningful recording of fetal breathing movements using this technique requires an experienced operator who will have to monitor the *A*-scope continuously. With Real-Time *B*-scan machines the larger ranges of movement can be recorded using the *M*-mode with a fibre optic chart recorder. Small movements of range of less than 1 mm will require electronic gating of specific echoes to produce a chart recorder output. A pulsed Doppler system has been added to a *B*-scan machine (Tremewan *et al.*, 1977) allowing structure location and velocity measurements to be made using the same attached probe. A probe not secured to the maternal abdomen makes long term record-

ings difficult. There is, therefore, a need for a machine which is simple to operate and capable of producing a continuous recording of fetal breathing movements for long periods of time, typically 15-30 min as required.

Other investigators (Boyce *et al.*, 1976) have used a continuous wave Doppler to monitor fetal activity. The continuous wave device has the disadvantage in that it does not separate out the Doppler activity according to range within the patient. This difficulty is overcome by the use of a pulsed Doppler instrument. This is a pulse-echo device similar to the *T-M* scan instrument but instead of monitoring echo position with time it measures the velocity of movement which occurs at a specific depth from the transducer. It is thus possible to examine the velocities of structures lying at a known depth. By placing the depth selective range gate of the instrument to lie within the fetal chest or abdomen, the velocities of movement of the interfaces lying within the range gate can be obtained. The instrument has a conventional *A*-scope echo presentation to aid in the positioning of the range gate. The audio Doppler shift signals are fed into an audio amplifier and hence to a loudspeaker and also into a frequency to voltage converter to output onto a chart recorder.

The probe used with the pulsed Doppler

instrument is belt mounted onto the maternal abdomen and can be rotated within its sealed barrel housing to produce a Real-Time *B*-scan display (C. R. Bow *et al.*, 1977). In this mode it enables identification and location of fetal anatomy and movements which assist in the positioning of the range gate for the pulsed Doppler recording. This Real-Time *B*-scan facility is a valuable method for studying the characteristics of fetal breathing movements (Bots *et al.*, 1976). Figure 1 shows a diagram of the rotating probe arrangement.

PULSED DOPPLER INSTRUMENT

A block diagram of the instrument is shown in Fig. 2. A 2.5 MHz oscillator is gated by the pulse repetition frequency (p.r.f.) generator to produce fifteen cycle pulses at regular intervals. The p.r.f. can be varied in the range of 300 Hz to 3 kHz. The gated oscillation is amplified to produce an 80 V peak to peak drive to the single unfocused 2.5 MHz transducer.

The ultrasound echoes reflected from tissue interfaces lying along the beam are amplified in a three stage r.f. amplifier, the initial stage of which has swept gain. The output of the r.f. amplifier is fed into a phase

sensitive detector. The instantaneous difference in phase between the r.f. echoes and the reference oscillator is presented as a voltage signal at the output of the phase detector. This output is sampled at the pulse repetition frequency by a sample and hold network. The sampling period is $4 \mu\text{sec}$ and the point at which sampling occurs can be varied in the range 1 to 25 cm from the transducer. The sample and hold network holds the sampled value of the phase detector output until the next sampling time. This stepped waveform is low pass filtered to remove the sampling frequency and its harmonics. If the tissue interface lying within the range gate is in motion then the output of the filtered sample and hold network will vary with a frequency equal to the Doppler shift, which is proportional to the component of velocity of the interface motion along the ultrasound beam. As a result of the sampling theorem the maximum detectable Doppler shift is dependent on the p.r.f. of the instrument. With a p.r.f. of 3 kHz it should be possible to measure velocities up to 40 cm/sec. The expected fetal respiratory velocities for movement of chest wall or abdominal structures should only be about 2 to 4 cm/sec. High velocity fluid movements such as those reported by Boyce *et al.* have not been studied

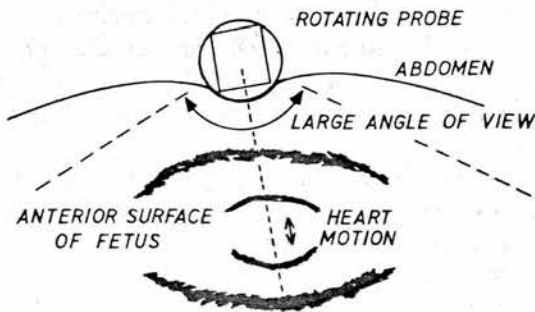


Fig. 1. Diagram of the rotating probe arrangement used with the pulsed Doppler instrument.

RESULTS

The performance of the system was tested by observing the Doppler shift frequencies from a test phantom and from the adult heart. The phantom consisted of a perspex disc rotating off-centre in a water tank. The output pitch of the Doppler signal was observed to be directly related to the velocity of movement of the outside surface of the disc. These

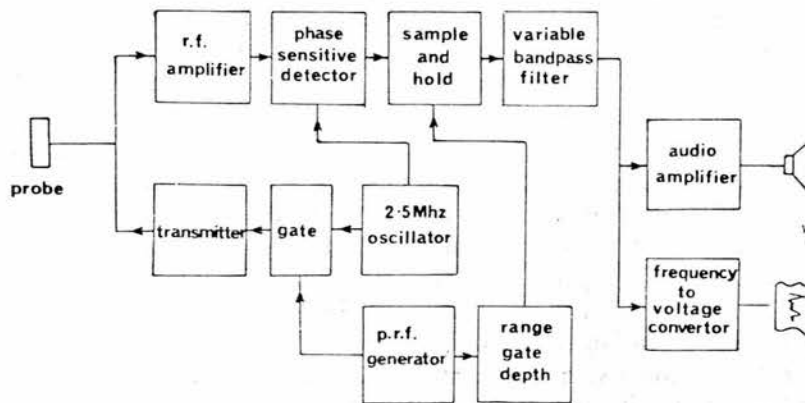


Fig. 2. Block diagram of the pulsed Doppler instrument.

Doppler shifts were in agreement with those obtained using a continuous wave Doppler. In the adult heart the depth selective range gate aids in identifying the sources of the differing velocities of motion within the heart. Slow ventricle wall movements, the flapping of the mitral cusps and fast moving blood flow can all be identified.

To establish the validity of using this instrument to monitor fetal breathing the pulsed Doppler instrument and an A-scan instrument with a gated $T-M$ trace facility were linked together to run simultaneously using a single 2.5 MHz transducer. The pulsed Doppler transmitter excited the transducer and the return echoes were fed into both receivers. A pulse repetition rate of 680 Hz was used. The output from each machine was recorded on a dual trace chart recorder.

Figure 3 shows a section of a $T-M$ trace and a pulsed Doppler recording from an adult heart with the range gate located on the posterior chest wall. The $T-M$ trace is a measure of the change of position with time and the Doppler trace measures the velocity of movement at the selected depth. As can be seen there are two peaks of pulsed Doppler trace for every one peak of the $T-M$ scan. This pattern is often obtained and is a result of tissue movement towards the transducer and away from the transducer.

In human pregnancy fetal breathing movements *in utero* have been examined with the dual machine link up in 40 patients. In most of the patients, a correlation between the two traces was observed. An exact com-

parison of A-scan plus gated $T-M$ trace to pulsed Doppler trace is obviously difficult as the two machines are not measuring the same parameters at identical locations. The A-scan records the action of the leading edge of one particular echo whereas the pulsed Doppler records the mean velocity of tissues lying within a selected range. Both traces indicated a similar incidence of breathing movements. Periods of apnoea correlated well with both machines.

Figure 4 shows a section of $T-M$ trace and pulsed Doppler recording of fetal breathing activity. The $T-M$ trace shows the change of position of anterior chest wall with time and the pulsed Doppler indicates the changing velocity of motion of tissues with the range gate set just inside the anterior chest wall. As with the adult heart recordings, there are two peaks of pulsed Doppler trace to each of the $T-M$ trace. The Doppler shift frequencies associated with the fetal chest wall were less than 150 Hz giving a typical figure of 4 cm/sec for the maximum velocity.

DISCUSSION

Preliminary results indicate that human fetal breathing movements *in utero* can be recorded using an ultrasonic pulsed Doppler instrument. It will produce a continuous output of Doppler information to a chart recorder for long periods of time. It is essentially simple to operate having only one major control namely the range selective gate. It has the advantage over the A-scan echo gating technique in that the range gate can be set on either the fetal chest or within the fetal

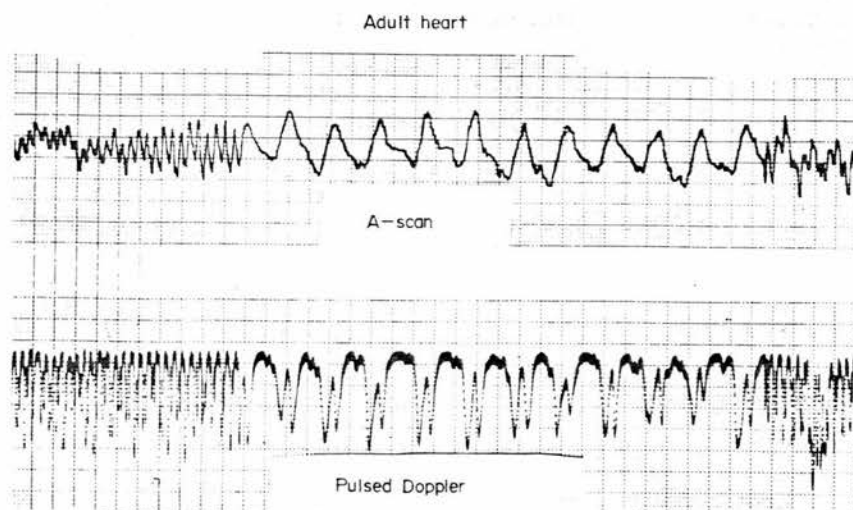


Fig. 3. A section of an A-scan plus $T-M$ trace and a pulsed Doppler recording of posterior chest wall movement of an adult heart. The time base has been expanded at the centre of the trace.

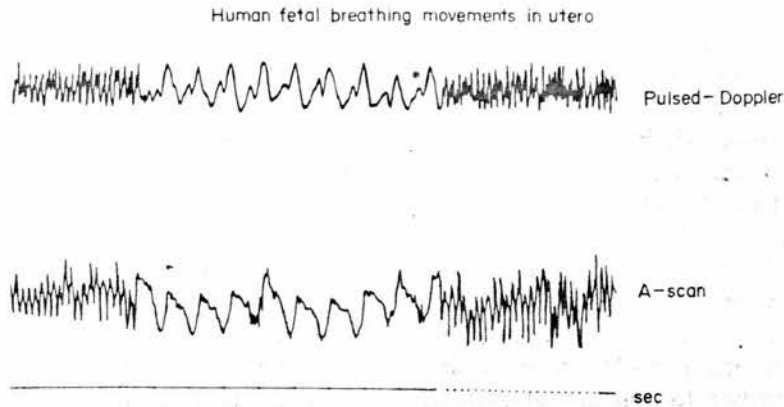


Fig. 4. A section of an A-scan plus T-M trace and a pulsed Doppler recording of fetal breathing activity. The time base has been expanded at the centre of the trace.

abdomen. No detailed selection of echoes corresponding to a specific structure is required. To date the instrument has been used to give an indication of fetal respiratory activity or apnoea. The possibility of making more accurate quantitative measurements such as the velocity of tissue or fluid movements are being studied at present. For long recordings the fetus may not remain stationary and gross fetal movements may require the range gate depth to be altered.

The Doppler shift frequencies obtained from fetal wall movements indicate that the instrument could be run at a low pulse repetition rate not much in excess of 350 Hz. The sensitivity of the present device is also higher than is required for this application and for long term recording the transmitter power could be reduced by 10 to 15 dB. The reduction of both these parameters will help to minimize the ultrasonic dose given to the fetus. Only one range gate is used on this instrument. A number of independent gates could easily be incorporated to give simultaneous recordings of anterior and posterior chest wall movements along with fetal heart.

Acknowledgements—This instrument is part of a project for the development of a pulsed Doppler instrument for examining the pregnant uterus. We would like to thank

the Scottish Home and Health Department for their support in the project.

REFERENCES

- Boddy, K. and Dawes, G. S. (1975) Fetal breathing. *Brit. Med. Bull.* **31**, 3-6.
- Boddy, K. and Mantell, C. D. (1972) Observations of fetal breathing movements transmitted through maternal abdominal wall. *Lancet* **2**, 1219-1220.
- Boddy, K. and Robinson, J. S. (1971) External method for detection of fetal breathing *in utero*. *Lancet* **2**, 1231-1233.
- Boddy, K., Dawes, G. S. and Robinson, J. (1974) Intrauterine fetal breathing movements. In *Modern Perinatal Medicine* (Edited by L. Gluck) pp. 381-383. Year Book Medical Publishers, Chicago.
- Bots, R. S. G. M., Farman, D. T. and Broeders, G. H. B. (1976) Multiscan echofetography: application to the study of fetal breathing movements. *Europ. J. Obstet. Gynec. Reprod. Biol.* **6**(5), 271-275.
- Bow, C. R. *et al.* (1977) In press.
- Boyce, E. S., Dawes, G. S., Gough, J. D. and Poore, E. R. (1976) Doppler ultrasound method for detecting human fetal breathing *in utero*. *Brit. Med. J.* **2**, 17-18.
- Farman, D. J., Thomas, G., and Blackwell, R. T. (1975) Errors and artefacts encountered in the monitoring of fetal respiratory movements using ultrasound. *Ultrasound Med. Biol.* **2**, 31-36.
- McDicken, W. N. (1976) *Diagnostic Ultrasonics Principles and Use of Instruments*. Crosby Lockwood Staples, London.
- Marshall, K., Gennser, G. and Lindström, K. (1976) Real-time Ultrasonograph for quantified analysis of fetal breathing movements. *Lancet* **2**, 718-719.
- Tremewan, R. N., Tait, J. J. and Aickin, D. R. (1977) A pulsed Doppler system incorporated into a Diasonograph. *Ultrasound Med. Biol.* **2**, 327-330.
- Wells, P. N. T. (1969) A range-gated ultrasonic Doppler system. *Med. Biol. Engng.* **7**, 641-652.